Precise Polymer Networks: An Investigation Encompassing Hydrogels, Proteins, and Nanoparticles

By

Benjamin Russell Spears

Dissertation

Submitted to the Faculty of the

Graduate School of Vanderbilt University

in partial fulfillment of the requirements

for the degree of

DOCTOR OF PHILOSOPHY

in

Chemistry

December, 2015

Nashville, Tennessee

Approved

Eva M. Harth, Ph.D.

David W. Wright, Ph.D.

Timothy P. Hanusa, Ph.D.

Scott A. Guelcher, Ph.D.

To Jeff, Dianne, and Kay Ann

ACKNOWLEDGEMENTS

This research was made possible through financial support from the National Institute of Health, the Junior Diabetes Research Foundation, and funding from the Vanderbilt Department of Chemistry.

Most notably, I must express my most sincere thanks to Dr. Eva Harth. She welcomed me into her lab when I was a synthetic inorganic scientist and helped me grow into the successful polymer materials chemist I am today. I will never be able to repay her for all of the guidance, patience, advice, and mentorship she provided over the years but know that all I have learned from her will be the basis for my success.

Furthermore, I must thank my committee members for giving their time and energy to provide personal and professional guidance during my graduate career. They were always willing to bear the brunt of an endless litany of questions and have been responsible for aiding in my scientific growth throughout my time at Vanderbilt.

I would also like to extend my thanks to all of the members of the Harth lab, who have played a significant role in my growth over the years. They have been a constant source of feedback and have helped me to grow as a scientist and researcher. I have forged many friendships within the group that will continue throughout the years.

My success at Vanderbilt would not have been possible without the unwavering support of my family. I would like to thank my parents for always supporting me through my numerous changes in major and always encouraging me to work hard at whatever endeavors I chose to pursue. They were always there for me and provided more support than I could ever deserve. I would also like to thank my younger brother for being a constant source of encouragement throughout my years in graduate school. Finally, I must thank my wife Kay Ann for standing by

me for over eight years of school and providing an unwavering source of love and support that I can only hope to repay throughout our remaining years together.

Lastly, I would like to extend my thanks to all those who provided guidance and support to me throughout the completion of my graduate degree and all who aided in my scientific research.

LIST OF FIGURES

TABLE OF CONTENTS

Page

CHAPTER I

INTRODUCTION

The quest for a single novel idea that may somehow shape the way future generations relate to the diseases that plague the human race is a noble one. However, it has been seen time and again that nature has a way of creating therapeutics so robust and efficacious that they easily outstrip most synthetic medical remedies[1]. Unfortunately, many of the most effective synthetic and natural product molecules are exceedingly hydrophobic[2-5]. The underlying issue which prevents these cures from being readily utilized today lies in the inherent desire of the human immune system to destroy any entity deemed foreign to the body. This simple fact, which has evolved as a defense mechanism against disease, can wreak havoc on the therapeutics which have been found advantageous as remedies for many serious ailments that attack one's health. Whether this limitation arises from the rapid removal of the therapeutics, or an inability to remain in solution in physiological conditions, the solution is the same: alternative methods of delivery must be created.

Though methods have been developed to overcome these shortcomings, none has come so far as the field of polymer science, which continues to diversify into many fields of research from materials and packaging[6] to drug delivery[2-4, 7-29] and protein therapeutic formation[18, 30-36]. Throughout the years, numerous polymerization methods have been developed capable of utilizing an increasingly broad range of monomers to impart moieties of desired functionality to the synthesized polymer products. From these libraries of polymer possibilities, an ever expanding list of uses can be formed, tailored for a range of desired purposes. These varied polymerization techniques, including reversible addition-fragmentation chain-transfer (RAFT), atom-transfer radical polymerization (ATRP), and ring-opening polymerization (ROP), afford a range of reaction

possibilities which allow researchers to tailor the characteristics and functionality of their polymer products for the desired applications. RAFT based systems afford polymers with high functionality potential but drastically low biodegradability due to the acrylate based backbone, an issue that also plagues polymers formed through ATRP pathways. Furthermore, many RAFT and ATRP reactions require the utilization of metal or organic based catalysts that must be kept in environments without air or water to ensure their continued viability and efficacy. Conversely, ROP, which is capable of turning almost any non-aromatic cyclic species into a polymer product, has been exploited with great success to form polymers with diverse backbones and functionalities. This mechanistic pathway is responsible for the formation of many polymers that are investigated for their drug delivery potential, such as poly(ester)s, one of the most studied drug delivery polymers, as well as poly(carbonate)s, which have gained more popularity in recent years due to their enzymatic degradability. Both of these polymer systems can be employed in the formation of drug delivery platforms, and researchers have shown these systems to be advantageous for the delivery of poorly soluble drug molecules. With the varied degradation profiles of these polymers, poly(ester)s experiencing hydrolytic degradation and poly(carbonate)s undergoing enzymatic degradation, delivery systems can be tailored based on the desired route of administration, while the ability to incorporate functionalized monomer species broadens the scope of potential applications. Unfortunately, as with RAFT and ATRP, the methods employed in the formation of these polymers often require the utilization of inert atmospheric environments, leading to prolonged preparation and reaction times.

One system that has been developed to address these stringent reaction conditions is the use of tin octanoate, a metal based catalyst that is sufficiently resistant to atmospheric conditions, allowing for benchtop synthesis of polymers through ROP[12, 16, 20, 37]. However, tin octanoate

requires the use of high temperatures to ensure the best catalytic potential, which can be problematic for some monomer species, and adds a level of complexity to the overall reaction conditions. Tin triflate is another tin based catalyst that has been studied for its catalytic potential, though to a lesser degree than tin octanoate. Research with this triflate derivative shows the ability to perform ROP based processes at room temperature, or slightly elevated temperatures, with great success, yielding poly(ester) and poly(carbonate) systems with well controlled molecular and polydispersities[5, 38]. The systems formed from polymers synthesized with tin triflate as the catalyst have been employed as drug delivery platforms for hydrophobic drug molecules and show true promise as targeted drug delivery vehicles[39]. The ability to marry these two worlds in order to form poly(ester) and poly(carbonate) systems with well-defined structures, from reactions at or slightly above room temperature, is truly a significant research discovery. This advance can be exploited to form poly(ester) and poly(carbonate) building blocks that can be utilized in the formation of polymer based structures for varied applications.

Polymer based nanoparticles are a well-established class of drug delivery systems with many researchers endeavoring to formulate synthesis routes that will afford the largest amount of cargo loading while maintaining linear release profiles. These two goals are of utmost importance as they allow for the least stressful doctor schedule and accurate dosage amounts. Many drug delivery platforms have been developed to address one or both of these goals, but few are able to successfully form nanoparticle species with viable drug delivery applications. However, there has been impressive work done utilizing poly(ester) species to form degradable nanoparticles capable of high drug loading and linear release of the encapsulated cargo. Furthermore, these systems have shown application for the delivery of highly hydrophobic drug molecules, a realm that is populated by many of the most efficacious therapeutics. While these systems have been successful, their

relative hydrophobicity necessitates the utilization of a PEG surfactant for increased solubility, and a similar system formed from more hydrophilic polymer structures has the potential to maintain the high loading and release profile while decreasing the need for the presence of this PEG species.

Another field that has continued to increase its utilization of polymer structures is that of protein therapeutics. The utilization of proteins as therapeutics has been a continuous growth sector since its advent in the 1980s when the first crude protein-polymer conjugates were formed by covalently binding a poly(ethylene glycol) (PEG) polymer to the surface of proteins to test its effect on the blood life of the formed conjugates. This straightforward approach to the formation of bioconjugates yields proteins with large decreases in reactivity, but disproportionately higher levels of efficacy and decreased immunogenicity. This increase in therapeutic ability arises from the cloaking function the polymer structures perform, allowing the proteins to survive and circulate for longer periods in the body[33, 36, 40, 41]. Though PEG is still the most widely utilized polymer for the formation of these protein-polymer conjugates, with fourteen PEGylated species on the market, the prolonged administration necessary for the treatment of many of the diseases applicable for protein therapy has shown that large linear species can lead to polymer aggregation. For this reason, the use of branched PEG species has begun to be investigated, with results showing branched species of lower molecular weight are capable of yielding protein-polymer conjugates with the same, and in some cases improved, therapeutic activity. However, this method adds complexity to the polymerization reaction, as many of the branched species are accomplished through the secondary functionalization of other types of polymers, such as poly(acrylate)s[30]. Polymers can be chosen that lead to decreased immunogenicity as well as increased plasma half-life, allowing the proteins to not only be more effective, but administered less often. Though not a

disqualifying factor, the ability to form polymers of similar architecture and shielding ability to PEG through a single step reaction mechanism would be an exciting advancement within the field of protein therapeutics.

The field of hydrogel formation is one that, since its inception, has been dominated by polymers[19, 22, 28, 42]. The ability to form a hypercrosslinked network, affording a product that is insoluble and, dependent upon the polymer building blocks chosen, rigid, has led to the use of hydrogel structures in diverse fields from tissue scaffolds to drug delivery vehicles. Furthermore, the myriad of gelation reactions that are available for hydrogel formation have opened the field to almost every conceivable fabrication method, as gels of the desired size and morphology can be formed either before or after the gelation step, allowing researchers to work in both the solid and liquid phases during formulation. Not only does this allow for an enormous range of formation potential, it also affords researchers unparalleled creative license in the choice of polymer building blocks as well as the cargo that is to be delivered. The most studied polymer scaffold is formed from poly(lactic-glycolic acid), a hydrolytically degradable polymer that affords some degree of rigidity and a surface well suited for cell growth and tissue regeneration[28, 29, 43, 44]. However, the degradation of PLGA leads to localized acidity issues and the rigidity of the system limits the potential applications for systems formed from this polymer species[29]. The ability to form gel systems which can degrade into inert products and harness the linear release profiles seen with other gel systems is another exciting avenue for research.

Dissertation Overview

Polymerization methods have been developed and characterized for the synthesis of numerous polymer products including poly(glycidol), poly(carbonate), and poly(ester) systems. These polymer building blocks were then employed in the formation of novel nano- and micro-

polymer networks with the purpose of sustained drug delivery. Through the course of this work, tin triflate was used as a readily active catalyst capable of driving benchtop reactions with good control of polymer size and polydispersity. Furthermore, the nature of the research allowed alternate avenues for the polymerization and utilization of poly(glycidol) to be pursued.

Using tin triflate, poly(glycidol) structures with hitherto unseen degrees of branching were formed. The control over this branching was seen achieved through depression or increase of the reaction temperature, with reaction temperature having a direct relationship with polymer branching. Functionalized glycidol monomers were easily incorporated into the growing polymer structures through the same polymerization methods and afforded systems with further decrease in overall polymer branching. By exploiting the inherent interaction between glycidol and water a secondary reaction pathway was discovered in which poly(glycidol) systems were formed in the presence of slightly acidic phosphate buffer solution. In order to fully understand this novel pathway a number of parameters, including pH, concentration, and reaction temperature were investigated. It was also discovered that functionalized monomer units could be successfully incorporated into the system though to a slightly lesser degree than with the tin systems. Most importantly, this new method yielded products with even lower branching and represents an entirely new polymerization technique called aqueous epoxide ring-opening polymerization (AEROP).

Taking what was learned from the discovery of AEROP, in conjunction with the fact that poly(glycidol) very nearly mirrors the structure of PEG, research focused on the implementation of poly(glycidol) as a cloaking polymer for the formation of protein-polymer conjugates. Through a graft-from method in water, protein-polymer conjugates of bovine serum albumin (BSA) and lysozyme (LYZ) were successfully formed and characterized. Furthermore, through the

adjustment of reaction time and concentration, polymer species of increased length were successfully attached to the protein surfaces. These proteins were investigated for their retained bioactivity and proved comparable to PEG counterparts.

Using the synthesized, allyl-functionalized poly(glycidol)s, and, separately, allyl-functionalized poly(ester)s, nanonetwork structures were successfully formed through thiolene-click reactions with 3,6-dioxa-1,8-octanedithiol to form nanoparticles with distinctly variable hydrophilicity. Particle crosslinking was varied through this thiolene-click reaction to yield products with variable crosslinking density, which will allow for control over the release rate of the cargo that will be loaded. These systems stand poised to be employed as drug delivery vehicles that, with their diverse chemical characteristics, can be utilized for a broad range of potential therapeutic cargo.

Thiolene-click chemistry was also employed in the formation hydrogel systems through the use of highly concentrated conditions. 3,6-dioxa-1,8-octanedithiol was used to covalently attach allyl poly(carbonate) and/or allyl poly(glycidol) polymer species together with sufficiently high crosslinking to yield insoluble hydrogel structures with varied chemical and structural properties. These gel structures were first formed on the macroscale before utilizing the gel solution as an ink that was printed, using a piezoelectric printing cartridge, to give micron size hydrogel structures loaded with dye molecules which served as fluorescent drug cargo. Through this method, microparticles of 2-15μm were successfully fabricated in a highly reproducible and monodisperse manner.

References

1. Newmann, D. J., Cragg, G. M., and Snader, K. M. (2003) Natural Products as Sources of New Drugs over the Period 1981-2002, *Journal of Natural Products 66*, 1022-1037.

2. Georgiadis, M., Russell, E., Gazdar, A., and Johnson, B. (1997) Paclitaxel cytotoxicity against human lung cancer cell lines increases with prolonged exposure durations, *Clinical Cancer Research 3*, 449-454.

3. Mu, L., and Feng, S. (2003) A novel controlled release formulation for the anticancer drug paclitaxel (Taxol (R)): PLGA nanoparticles containing vitamin E TPGS, *Journal of Controlled Release 86*, 33-48.

4. Zhang, Z., and Feng, S. (2006) The drug encapsulation efficiency, in vitro drug release, cellular uptake and cytotoxicity of paclitaxel-loaded poly(lactide)-tocopheryl polyethylene glycol succinate nanoparticles, *Biomaterials 27*, 4025-4033.

5. Stevens, D., Rahalkar, A., Spears, B., Gilmore, K., Douglas, E., Muthukumar, M., and Harth, E. (2015) Semibranched polyglycidols as "fillers" in polycarbonate hydrogels to tune hydrophobic drug release, *Polymer Chemistry 6*, 1096-1102.

6. Vasilache, V., Popa, C., Filote, C., Cretu, M.-A., and Benta, M. (2011) NANOPARTICLES APPLICATIONS FOR IMPROVING THE FOOD SAFETY AND FOOD PROCESSING, 7th International Conference on Materials Science and Engineering, Conference Paper.

7. Potineni, A., Lynn, D., Langer, R., and Amiji, M. (2003) Poly(ethylene oxide)-modified poly(beta-amino ester) nanoparticles as a pH-sensitive biodegradable system for paclitaxel delivery, *Journal of Controlled Release 86*, 223-234.

8. Win, K., and Feng, S. (2005) Effects of particle size and surface coating on cellular uptake of polymeric nanoparticles for oral delivery of anticancer drugs, *Biomaterials 26*, 2713-2722.

9. Elkharraz, K., Faisant, N., Guse, C., Siepmann, F., Arica-Yegin, B., Oger, J., Gust, R., Goepferich, A., Benoit, J., and Siepmann, J. (2006) Paclitaxel-loaded microparticles and

implants for the treatment of brain cancer: Preparation and physicochemical characterization, *International Journal of Pharmaceutics 314*, 127-136.

10. Fukushima, K., Pratt, R., Nederberg, F., Tan, J., Yang, Y., Waymouth, R., and Hedrick, J. (2008) Organocatalytic Approach to Amphiphilic Comb-Block Copolymers Capable of Stereocomplexation and Self-Assembly, *Biomacromolecules 9*, 3051-3056.
11. Hamoudeh, M., Diab, R., Fessi, H., Dumontet, C., and Cuchet, D. (2008) Paclitaxel-loaded microparticles for intratumoral administration via the TMT technique: Preparation, characterization, and preliminary antitumoral evaluation, *Drug Development and Industrial Pharmacy 34*, 698-707.
12. van der Ende, A. E., Kravitz, E. J., and Harth, E. (2008) Approach to formation of multifunctional polyester particles in controlled nanoscopic dimensions, *Journal of the American Chemical Society 130*, 8706-8713.
13. Vicari, L., Musumeci, T., Giannone, I., Adamo, L., Conticello, C., De Maria, R., Pignatello, R., Puglisi, G., and Gulisano, M. (2008) Paclitaxel loading in PLGA nanospheres affected the in vitro drug cell accumulation and antiproliferative activity, *Bmc Cancer 8*.
14. Mugabe, C., Hadaschik, B. A., Kainthan, R. K., Brooks, D. E., So, A. I., Gleave, M. E., and Burt, H. M. (2009) Paclitaxel incorporated in hydrophobically derivatized hyperbranched polyglycerols for intravesical bladder cancer therapy, *Bju International 103*, 978-986.
15. Ungaro, F., Bianca, R., Giovino, C., Miro, A., Sorrentino, R., Quaglia, F., and La Rotonda, M. (2009) Insulin-loaded PLGA/cyclodextrin large porous particles with improved aerosolization properties: In vivo deposition and hypoglycaemic activity after delivery to rat lungs, *Journal of Controlled Release 135*, 25-34.

16. van der Ende, A., Croce, T., Hamilton, S., Sathiyakumar, V., and Harth, E. (2009) Tailored polyester nanoparticles: post-modification with dendritic transporter and targeting units via reductive amination and thiol-ene chemistry, *Soft Matter 5*, 1417-1425.

17. Kim, M., and Lee, D. (2010) In Vitro Degradability and Stability of Hydrophobically Modified pH-Sensitive Micelles Using MPEG-Grafted Poly(beta-amino ester) for Efficient Encapsulation of Paclitaxel, *Journal of Applied Polymer Science*, 3431-3438.

18. Liechty, W., Kryscio, D., Slaughter, B., and Peppas, N. (2010) Polymers for Drug Delivery Systems, *Annual Review of Chemical and Biomolecular Engineering, Vol 1*, 149-173.

19. Shah, S., Pal, A., Gude, R., and Devi, S. (2010) Synthesis and characterization of thermo-responsive copolymeric nanoparticles of poly(methyl methacrylate-co-N-vinylcaprolactam), *European Polymer Journal*, 958-967.

20. van der Ende, A. E., Sathiyakumar, V., Diaz, R., Hallahan, D. E., and Harth, E. (2010) Linear release nanoparticle devices for advanced targeted cancer therapies with increased efficacy, *Polymer Chemistry 1*, 93-96.

21. Wilms, D., Stiriba, S. E., and Frey, H. (2010) Hyperbranched Polyglycerols: From the Controlled Synthesis of Biocompatible Polyether Polyols to Multipurpose Applications, *Accounts of Chemical Research 43*, 129-141.

22. Wu, W., Aiello, M., Zhou, T., Berliner, A., Banerjee, P., and Zhou, S. (2010) In-situ immobilization of quantum dots in polysaccharide-based nanogels for integration of optical pH-sensing, tumor cell imaging, and drug delivery, *Biomaterials 31*, 3023-3031.

23. Mugabe, C., Liggins, R. T., Guan, D., Manisali, I., Chafeeva, I., Brooks, D. E., Heller, M., Jackson, J. K., and Burt, H. M. (2011) Development and in vitro characterization of

paclitaxel and docetaxel loaded into hydrophobically derivatized hyperbranched polyglycerols, *International Journal of Pharmaceutics 404*, 238-249.

24. Mugabe, C., Matsui, Y., So, A. I., Gleave, M. E., Heller, M., Zeisser-Labouebe, M., Heller, L., Chafeeva, I., Brooks, D. E., and Burt, H. M. (2011) In Vitro and In Vivo Evaluation of Intravesical Docetaxel Loaded Hydrophobically Derivatized Hyperbranched Polyglycerols in an Orthotopic Model of Bladder Cancer, *Biomacromolecules 12*, 949-960.
25. Scoutaris, N., Alexander, M., Gellert, P., and Roberts, C. (2011) Inkjet printing as a novel medicine formulation technique, *Journal of Controlled Release 156*, 179-185.
26. Ye, L., Letchford, K., Heller, M., Liggins, R., Guan, D., Kizhakkedathu, J. N., Brooks, D. E., Jackson, J. K., and Burt, H. M. (2011) Synthesis and Characterization of Carboxylic Acid Conjugated, Hydrophobically Derivatized, Hyperbranched Polyglycerols as Nanoparticulate Drug Carriers for Cisplatin, *Biomacromolecules 12*, 145-155.
27. Gong, C., Xie, Y., Wu, Q., Wang, Y., Deng, S., Xiong, D., Liu, L., Xiang, M., Qian, Z., and Wei, Y. (2012) Improving anti-tumor activity with polymeric micelles entrapping paclitaxel in pulmonary carcinoma, *Nanoscale 4*, 6004-6017.
28. Hu, C., Feng, H., and Zhu, C. (2012) Preparation and characterization of rifampicin-PLGA microspheres/sodium alginate in situ gel combination delivery system, *Colloids and Surfaces B-Biointerfaces 95*, 162-169.
29. Kim, I., Byeon, H., Kim, T., Lee, E., Oh, K., Shin, B., Lee, K., and Youn, Y. (2012) Doxorubicin-loaded highly porous large PLGA microparticles as a sustained-release inhalation system for the treatment of metastatic lung cancer, *Biomaterials 33*, 5574-5583.

30. Li, M., De, P., Gondi, S., and Sumerlin, B. (2008) Responsive polymer-protein bioconjugates prepared by RAFT polymerization and copper-catalyzed azide-alkyne click chemistry, *Macromolecular Rapid Communications 29*, 1172-1176.

31. Mero, A., Pasut, G., Via, L., Fijten, M., Schubert, U., Hoogenboom, R., and Veronese, F. (2008) Synthesis and characterization of poly(2-ethyl 2-oxazoline)-conjugates with proteins and drugs: Suitable alternatives to PEG-conjugates?, *Journal of Controlled Release 125*, 87-95.

32. Shakya, A., Sami, H., Srivastava, A., and Kumar, A. (2010) Stability of responsive polymer-protein bioconjugates, *Progress in Polymer Science 35*, 459-486.

33. Alconcel, S. N. S., Baas, A. S., and Maynard, H. D. (2011) FDA-approved poly(ethylene glycol)-protein conjugate drugs, *Polymer Chemistry 2*, 1442-1448.

34. Wurm, F., Dingels, C., Frey, H., and Klok, H.-A. (2012) Squaric Acid Mediated Synthesis and Biological Activity of a Library of Linear and Hyperbranched Poly(Glycerol)-Protein Conjugates, *Biomacromolecules 13*, 1161-1171.

35. Spears, B. R., Waksal, J., McQuade, C., Lanier, L., and Harth, E. (2013) Controlled branching of polyglycidol and formation of protein-glycidol bioconjugates *via* a graft-from approach with "PEG-like" arms, *Chemical Communications 49*, 2394-2396.

36. Fam, C., Eisenberg, S., Carlson, S., Chlipala, E., Cox, G., and Rosendahl, M. (2014) PEGylation Improves the Pharmacokinetic Properties and Ability of Interferon Gamma to Inhibit Growth of a Human Tumor Xenograft in Athymic Mice, *Journal of Interferon and Cytokine Research 34*, 759-768.

37. van der Ende, A. E., Harrell, J., Sathiyakumar, V., Meschievitz, M., Katz, J., Adcock, K., and Harth, E. (2010) "Click" Reactions: Novel Chemistries for Forming Well-defined Polyester Nanoparticles, *Macromolecules 43*, 5665-5671.

38. Stevens, D., Watson, H., LeBlanc, M., Wang, R., Chou, J., Bauer, W., and Harth, E. (2013) Practical polymerization of functionalized lactones and carbonates with Sn(OTf)(2) in metal catalysed ring-opening polymerization methods, *Polymer Chemistry 4*, 2470-2474.

39. Ndong, J., Stevens, D., Vignaux, G., Uppuganti, S., Perrien, D., Yang, X., Nyman, J., Harth, E., and Elefteriou, F. (2015) Combined MEK Inhibition and BMP2 Treatment Promotes Osteoblast Differentiation and Bone Healing in Nf1(Osx)(-/-) Mice (vol 30, pg 55, 2015), *Journal of Bone and Mineral Research 30*, 1118-1118.

40. Pelegri-O'Day, E., Lin, E., and Maynard, H. (2014) Therapeutic Protein-Polymer Conjugates: Advancing Beyond PEGylation, *Journal of the American Chemical Society 136*, 14323-14332.

41. Vine, K., Lobov, S., Chandran, V., Harris, N., and Ranson, M. (2015) Improved Pharmacokinetic and Biodistribution Properties of the Selective Urokinase Inhibitor PAI-2 (SerpinB2) by Site-Specific PEGylation: Implications for Drug Delivery, *Pharmaceutical Research 32*, 1045-1054.

42. Raafat, A. (2010) Gelatin Based pH-Sensitive Hydrogels for Colon-Specific Oral Drug Delivery: Synthesis, Characterization, and In Vitro Release Study, *Journal of Applied Polymer Science*, 2642-2649.

43. Lee, B., Yun, Y., Choi, J., Choi, Y., Kim, J., and Cho, Y. (2012) Fabrication of drug-loaded polymer microparticles with arbitrary geometries using a piezoelectric inkjet printing system, *International Journal of Pharmaceutics 427*, 305-310.

44. Dhanda, D., Tyagi, P., Mirvish, S., and Kompella, U. (2013) Supercritical fluid technology based large porous celecoxib-PLGA microparticles do not induce pulmonary fibrosis and sustain drug delivery and efficacy for several weeks following a single dose, *Journal of Controlled Release 168*, 239-250.

CHAPTER II

SYNTHESIS OF POLY(GLYCIDOL) WITH TAILORED BRANCHING AND FUNCTIONALITY

Introduction

The emergence of poly(ethylene glycol) (PEG) as a highly versatile and biocompatible polymer system has afforded some of the most profound advances in such diverse fields as drug delivery[1-3], protein therapeutics[4-6], diagnostic development[7], and even food and hygiene additives[8]. As the years progressed, it was shown time and again that branched PEG structures, when compared to the historically utilized linear species, were capable of achieving greater results with lower molecular weights, eliminating waste and leading to more stable systems. While numerous methods are available for the formation of these branched PEG species, there is no direct synthesis route that will afford the desired branched species in a one-step reaction. Thus, the door has been left open for the discovery of a synthesis route capable of preparing branched polymers with similar capabilities while maintaining the advantageous characteristics of PEG.

Glycidol is an interesting monomer, consisting of an epoxide ring with a pendant hydroxymethyl group. The monomer can readily undergo polymerization through a number of pathways, both anionic and cationic, to yield polymer species with hyperbranched, dendrimer like architectures or, with the use of protected monomer species, polymers that are completely linear[9-26]. Hitherto, research has focused on these two extremes, or on systems where linear species are tethered to hyperbranched structures[27]. However, little attention has been paid to the intermediate area where neither linearity nor branching dominates. For this reason, we endeavored to formulate polymerization reactions capable of studying this broad region of unknown potential.

The formation of single-step dendrimer like macromolecules that provide the abilities of dendrimers without the painstaking process of dendrimer growth have garnered the most attention from those interested in the formation of poly(glycidol). The latent AB_2 monomer characteristic of glycidol allows for additional control through a step-wise polymerization rather than a rampant polycondensation, which is the usual reaction mechanism seen with other AB_2 type monomers (See Figure II-1). The capability of the glycidol monomer to suppress this AB_2 characteristic until

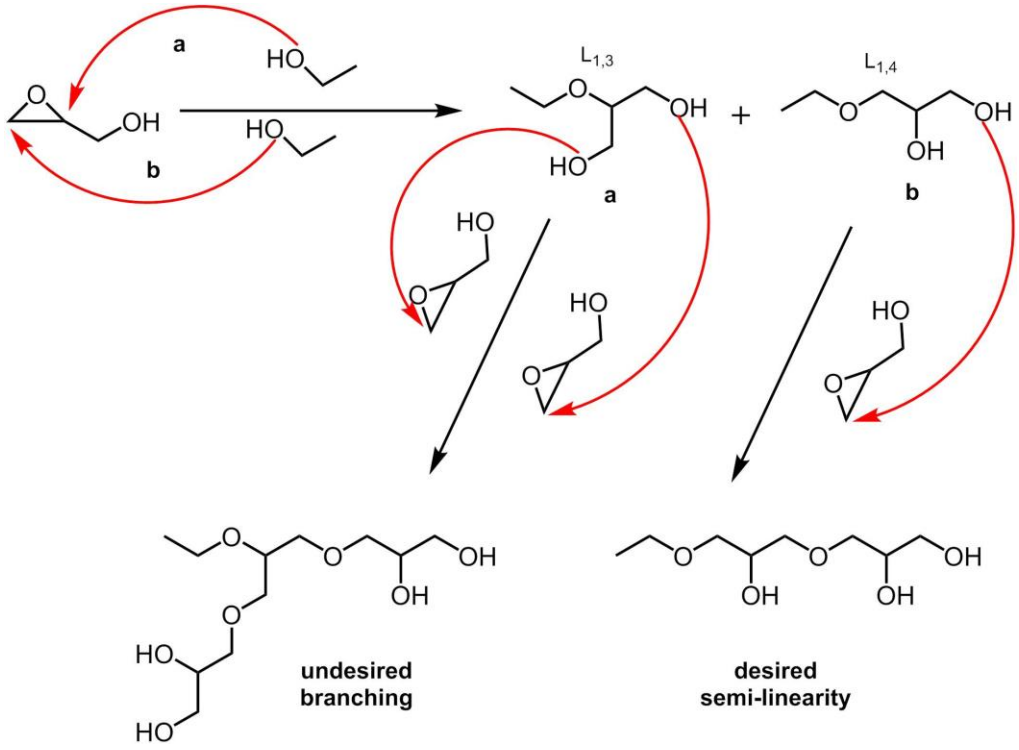

Figure II-1: Ring opening possibilities for the formation of poly(glycidol)

after the ring opens has contributed to the success of glycidol based polymers. This added control allows the synthesized poly(glycidol)s to maintain the benefits of other hyperbranched systems while affording macromolecules with polydispersity indices (PDIs) of 1.5 and lower, much more manageable than the PDIs of 5 or greater observed with other AB_2 type monomers[10, 11, 14, 15, 22]. Work in this field has been successful in forming hyperbranched poly(glycidol) systems, in varying sizes, with low polydispersity indices (PDIs) and controlled degrees of polymerization

(DP). These systems could very well become advantageous as alternatives to multistep dendrimer species.

The polymer systems that have been formed from these methods have found use in numerous applications ranging from potential vaccine models and selective drug delivery vehicles to biomineralization control and soluble catalyst supports in organic synthesis[12, 28-30]. Much of the success seen in these applications arises from the inherent characteristics of the poly(glycidol)'s branched structure. Conversely, limiting the degree of branching (DB), if possible with little change to the PDI, could prove beneficial in the formation of new, and possibly more robust, poly(glycidol) architectures[24].

The current methods for the formation of completely linear poly(glycidol)s rely on the use of protected glycidol derivatives polymerized under stringent anionic polymerization conditions. The protected polymers must then be subjected to a deprotection step that removes the protecting group, leaving a linear poly(glycidol) structure. This is a highly effective method for the formation of linear poly(glycidol) species; however, this synthetic route is far from what one might consider a facile synthesis method[26, 27, 31, 32].

The utilization of glycidol based polymers presents many advantages over the previously utilized PEG system. The preferential branching of poly(glycidol) during the polymerization process affords a final structure similar to the branched PEG species which must be formed through a multistep synthesis process. Furthermore, the backbone of the poly(glycidol) structures exhibits a high degree of similarity to PEG with repeating ether units, similar to polyethylene oxide and polyvinyl alcohol that, along with the pendant hydroxyls, add to the extreme hydrophilicity of the polymers[22, 26, 27, 31-33].

The research described herein is aimed at combating the problems associated with GLY based polymers, while still maintaining a high degree of water solubility and low PDI values[24]. Research focused on the inclusion of increased physiological degradability, through the incorporation of esters, as well as the introduction of more viable post modification units, such as thiols and allyl groups. Furthermore, two distinct polymerization methods will be discussed. The first involves stannous triflate, which has been chosen as the desired catalysis method based on its ability to allow for low reaction temperatures while maintaining high polymerization rates and low PDI values. The second method involves a newly formulated catalysis method that harnesses the glycidol monomer's known homopolymerization in water by introducing slightly acidic phosphate buffer to the glycidol monomer[9]. The chemical characteristics of the synthesized polymers will be investigated through both ^{1}HNMR and ^{13}CNMR techniques, while the biological conjugates will be characterized using a number of other techniques. By employing the stannous triflate catalyst at low temperatures, the DB of the resulting polymers can be restricted to well below the currently published values of 0.56 and higher[12, 22]. The ability of comonomers to copolymerize with glycidol to form an array of new and exciting polymer architectures, is also discussed. These polymers are proving to have interesting structural features and will foster in a new regime of polymers with high functionality, solubility and tunable biodegradability, thus imbuing all the benefits of poly(glycidol) based structures to systems that are more tailored for delivery of a range of cargo. Once these systems have been formed they will be utilized for the purposes of protein-polymer conjugate formation, and the development of precise polymer networks on the nano and micron scale for delivery of therapeutics.

Results and Discussion

Development of a Novel Benchtop Polymerization Synthesis of Poly(glycidol)

Poly(glycidol) has long been studied for its interesting characteristics and relative ease of secondary functionalization. The latent AB_2 type monomer gives rise to one-pot reactions yielding hyperbranched, dendrimer-like structures, in a much faster and more facile manner[12-16, 18, 22]. Furthermore, the utilization of protected monomer units can give rise, after subsequent deprotection, to completely linear structures that can be post modified via hydroxyl based modification reactions[13, 23, 25]. Unfortunately, the synthesis methods utilized thus far have major pitfalls for those looking for a facile synthesis route. For these reasons, a synthesis method was sought that would facilitate the formation of poly(glycidol) based structures of tunable branching characteristic through reaction mechanisms capable of yielding products in a benchtop synthesis.

The use of stannous triflate ($Sn(OTf)_2$) as a benchtop ring opening polymerization catalyst has been studied previously in the lab for the formation of poly(ester) based polymer systems as building blocks for nanoparticle structures. In this work, allyl functionalized monomers are used to form random copolymers with pendant allyl groups. These groups are then oxidized to epoxides for use in amine-epoxide crosslinking reactions. It was observed that, after epoxidation, the presence of $Sn(OTf)_2$ would facilitate a rapid ring opening of the newly formed epoxide, rendering them unviable as crosslinking units. It was therefore hypothesized that $Sn(OTf)_2$ could be used as a catalyst for the ring opening polymerization of glycidol to form poly(glycidol) based structures in a benchtop synthesis.

Determination of Kinetic Control over Degree of Branching

Initial polymerizations were performed using glycidol as the only monomer unit. Work has been done suggesting that the opening of epoxide rings can be controlled kinetically[10], and so a

Region	Shift (ppm)	40°C	20°C	0°C	-20°C
$L_{1,3}$	81.0-82.0	1.00	1.00	1.00	1.00
D	79.5-80.5	0.79	0.62	0.60	0.48
2 $L_{1,4}$	73.5-74.5	3.69	3.65	3.98	4.80
2D, 2T	72.0-73.5	7.05	7.52	7.62	8.44
$L_{1,3}$, $L_{1,4}$	70.5-72.0	3.14	3.01	3.17	2.93
T	64.0-65.0	1.74	2.13	2.17	3.53
$L_{1,3}$	62.0-63.5	3.15	2.97	2.76	2.87
Degree of Branching		0.24	0.21	0.20	0.15
Relative Abundance of Dendritic Carbons		10.5%	8.2%	8.0%	5.2

Figure II-2: Degree of branching and relative abundance of dendritic carbons for the four chosen temperatures for polymerization with $Sn(OTf)_2$

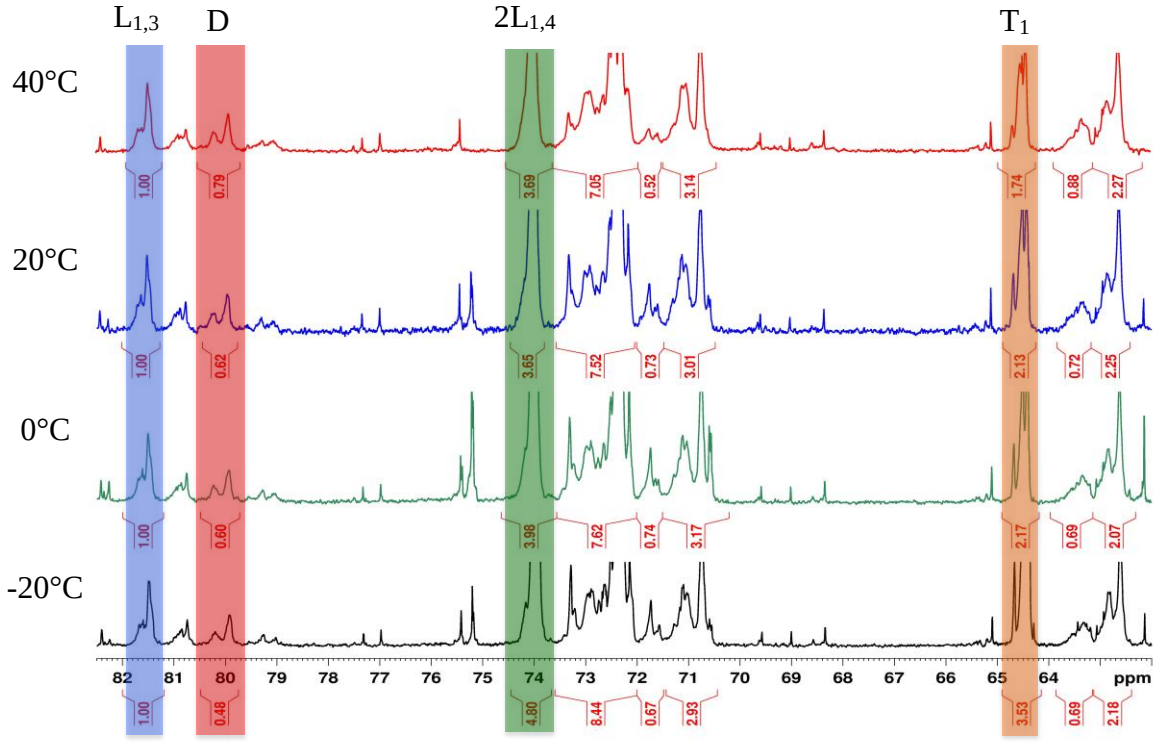

Figure II-3: ^{13}C-NMR showing decrease in dendritic character with decreasing temperature

kinetic study was performed to fully investigate the extent of this control. For the study four temperatures were chosen; -20°C, 0°C, 20°C, and 40°C (See Figure II-3). In order to maintain constant reaction temperatures, a solvent circulator was employed along with specialized glassware that allowed a constant flow of temperature stabilized solution to completely surround the polymerization reaction vessel. The $Sn(OTf)_2$ catalyst and isoamyl alcohol initiator were added to the flask and allowed to stir for 30 minutes to facilitate alcohol catalyst conjugation. The glycidol monomer was then added dropwise via syringe and the reaction was allowed to run until stirring was fully impeded. As expected, reaction times were inversely correlated to reaction temperature, and, interestingly, the degree of branching observed for each reaction varied directly with temperature, showing that the catalyzed reactions were in fact influenced by the temperature of the reaction. This exciting point yielded polymers with branching lower than that seen previously in the literature (See Figure II-2), thus allowing for a new classification of semibranched poly(glycidol).

The Formation of Stretchable Gas Barriers

In order to test the versatility of the newly synthesized poly(glycidol) systems, we worked with the Grunlan lab at Texas A&M to incorporate the poly(glycidol) into their work towards the formation of better, more flexible gas barriers. Using a Layer-by-Layer (LbL) deposition technique, the lab created tri-layers of polyethylenimine (PEI), montmorillonite (MMT) clay, and poly(glycidol). The newly formed coatings were tested for their oxygen barrier ability before and after a 10% stretching was performed, and it was determined that the barriers containing poly(glycidol) had a 17% barrier loss after stretching. However, those films without poly(glycidol) experienced a barrier loss of 4350%. This was an astonishing difference and represents the first reported stretchable thin film gas barrier. Furthermore, this proof of concept investigation points

to these poly(glycidol) containing thin films as method for the production of pressurized elastomer systems, stretchable electronic applications, or even food packaging[34].

Introduction of Comonomers for Added Functionality

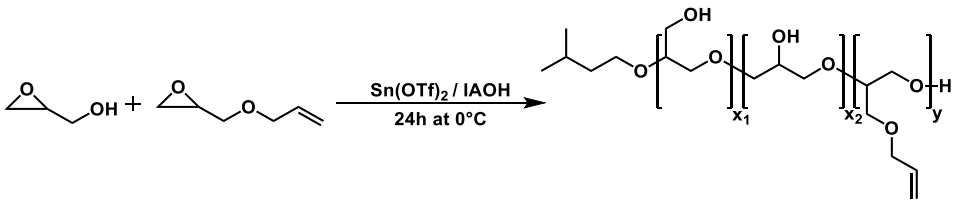

Figure II-4: Synthesis of poly(glycidol-co-allyl glycidyl ether) with $Sn(OTf)_2$

The discovery of this method was substantial, but to fully exploit the synthesis the formation of functionalized poly(glycidol) structures was desired. For this reason allyl glycidyl ether (AGE), a readily available glycidol derivative, was chosen to impart allyl functionality into the polymer backbone (See Figure II-4). Although not quite as reactive as the glycidol, by using $Sn(OTf)_2$ as a catalyst, AGE was easily incorporated into the backbone of the polymer at varying percentages. These reactions were run at room temperature following a similar procedure as the glycidol homopolymer. After the catalyst and initiator were complexed, the AGE was added dropwise followed by the dropwise addition of the glycidol monomer. Reactions were complete after 24 hours and after purification it was determined that the allyl monomer was successfully incorporated. The significance of this was twofold. The polymer formed was more readily capable of secondary modification, through the incorporation of another reactive unit, and the fact that AGE is an AB and not AB_2 type monomer led to species with still lower degrees of branching affording a second parameter that can be exploited for the formation of semibranched structures.

Advent of Green Synthesis Methods

Although the newly discovered polymerization proved to be very advantageous, there is a characteristic of glycidol that can still be exploited. It has been reported that in the presence of

water glycidol can undergo an autopolymerization, yielding short species of no real utility[9]. However, it was hypothesized that this inherent ability could be exploited, under the right conditions, to form both homopolymers, as well as functionalized copolymers, to be used in subsequent research goals. Previous work has shown that thermal cracking of the glycidol epoxide, in the presence of a weak nucleophile, can lead to ring opening of either the substituted or unsubstituted side, thus affording another parameter that can be investigated to determine the best manner conditions for this novel polymerization route[9].

Optimization of Reaction Conditions

Region	Shift (ppm)	60°C (13.5M)	80°C (13.5M)	100°C (13.5M)
$L_{1,3}$	81.0-82.0	1	1	1
D	79.5-80.5	1.5017	1.2115	1.2699
2 $L_{1,4}$	73.5-74.5	12.483	11.7599	10.6349
2D, 2T	72.0-73.5	9.5734	9.7469	10.154
$L_{1,3}$, $L_{1,4}$	70.5-72.0	6.6037	6.1915	5.6924
T	64.0-65.0	3.274	3.4851	3.6807
$L_{1,3}$	62.0-63.5	1.1331	1.2588	1.4066
Degree of Branching		0.29	0.25	0.27
Percent Yield		2.7	31.8	37.1

Figure II-5: Green polymer synthesis temperature studies

In order to fully investigate this intriguing idea, three reaction temperatures were chosen, 60°C, 80°C, and 100°C (See Figure II-5), with unique reaction times for each temperature (5 days, 3 days, and 1 day respectively). For the purpose of initiation of the homopolymerization reaction, it was decided that slightly acidic phosphate buffer (pH 6.0) would be added to the stirring

Region	Shift (ppm)	2x GLY (14.3M)	3x GLY (14.5M)	2x PB (12.3M)	3x PB (11.2M)	4x PB (10.4M)
$L_{1,3}$	81.0-82.0	1	1	1	1	1
D	79.5-80.5	1.2789	1.1456	1.2074	0.8681	0.8332
2 $L_{1,4}$	73.5-74.5	10.9784	11.577	11.7041	12.1723	12.7717
2D, 2T	72.0-73.5	8.8949	9.758	9.3083	9.6674	9.8932
$L_{1,3}$, $L_{1,4}$	70.5-72.0	5.7718	5.8661	5.9154	5.2936	5.3063
T	64.0-65.0	3.0503	3.7491	3.4265	5.081	5.4274
$L_{1,3}$	62.0-63.5	1.1353	1.0645	1.0847	1.2939	1.3443
Degree of Branching		0.28	0.25	0.26	0.19	0.18
Percent Yield		49.6	65.0	46.6	48.9	29.1

Figure II-6: Green polymer synthesis concentration studies

Region	Shift (ppm)	pH=3.75 (13.5M)	pH= 6.00 (13.5M)	pH=7.99 (13.5M)	DI Water (13.5M)
$L_{1,3}$	81.0-82.0	1	1	1	1
D	79.5-80.5	1.2285	1.2115	1.2447	1.0542
2 $L_{1,4}$	73.5-74.5	10.4149	11.7599	10.7286	11.2358
2D, 2T	72.0-73.5	8.8071	9.7469	8.9013	8.346
$L_{1,3}$, $L_{1,4}$	70.5-72.0	5.4975	6.1915	5.6529	5.4162
T	64.0-65.0	2.9902	3.4851	2.9783	3.5474
$L_{1,3}$	62.0-63.5	1.2266	1.2588	1.2039	1.4076
Degree of Branching		0.28	0.25	0.27	0.23
Percent Yield		31.9	31.8	24.5	1.2

Figure II-7: Green polymer synthesis pH studies

monomers prior to submersion in the oil baths, as it was believed that the slight acidity would elevate the potential for homopolymerization All three reaction temperatures yielded polymer products, but the lowest branching product was achieved at 80°C, and so this temperature was chosen for studies that investigated the effects of monomer concentration and pH on the polymer

Unit	2x GLY (14.3M)	3x GLY (14.5M)	2x PB (12.3M)	3x PB (11.2M)	4x PB (10.4M)
Terminal	**28**	**32**	**30**	**38**	**39**
Linear 1,3	**10**	**9**	**9**	**10**	**10**
Linear 1,4	**50**	**49**	**51**	**45**	**45**
Dendritic	**12**	**10**	**10**	**7**	**6**

Figure II-8: Green polymer synthesis: relative abundance of repeat units from concentration studies

products formed. It was seen that the manipulation of these three parameters yielded products that were similar in size but somewhat different in degree of branching and relative abundance of the numerous glycidol repeat units.

The first parameter that was studied was monomer concentration, which was varied by either increasing the amount of glycidol present or the amount of PB used (See Figure II-6 and Figure II-8). Interestingly, it was seen that as the concentration was increased through the addition of more monomer, as well as when the concentration was decreased by the use of more PB, there was a decrease in the DB observed for the polymer products, with very low branching of below 0.20 seen for the low concentration reactions. However, the low concentration reactions saw a marked decrease in yield proportional to the decrease in concentration while the yield for the higher concentration reactions was increased. The real difference was seen in the relative

abundance of repeat units, with the lower concentration polymers exhibiting increased amounts of terminal units and decreased amounts of branched units, pointing toward polymers of shorter size.

The final parameter that was studied was the pH of the PB used to catalyze the polymerizations (See Figure II-7). This was an interesting study as it was determined that an increase or decrease in pH led to polymers of higher DB. Furthermore, by running a reaction in DI water it was seen that little polymerization was possible, further alluding to the fact that some acidity or basicity is necessary to truly drive the autopolymerization process and yield polymers of viable length, capable of undergoing the precipitation process for purification.

Determination of Green Polymer Molecular Weight

The ability to form polymers in this novel green method was exciting, and the low degrees of branching meant that, once again, a new class of poly(glycidol) structures had been formed. As such, thorough investigation of the size of the synthesized polymers was desired. The first characterization method used was gel permeation chromatography and the results were intriguing. Historically, it has been difficult to characterize the size of branched structures due to their inherently high PDI values of 1.5 and higher, which arises from the low degree of control over the polymerization method due to multiple possible initiation points. However, the new systems showed good polymer control with PDIs of 1.2 and lower. This low PDI meant that the sizes of the polymers could be directly determined using MALDI-TOF-MS measurements, which was accomplished by spotting the polymers with a dithranol matrix. The data resulting from this investigation showed that the polymers formed from this new method were around 1500-1000 Da and that the concentration of the reactions is able to shift the polymer size obtained (See Figure II-9).

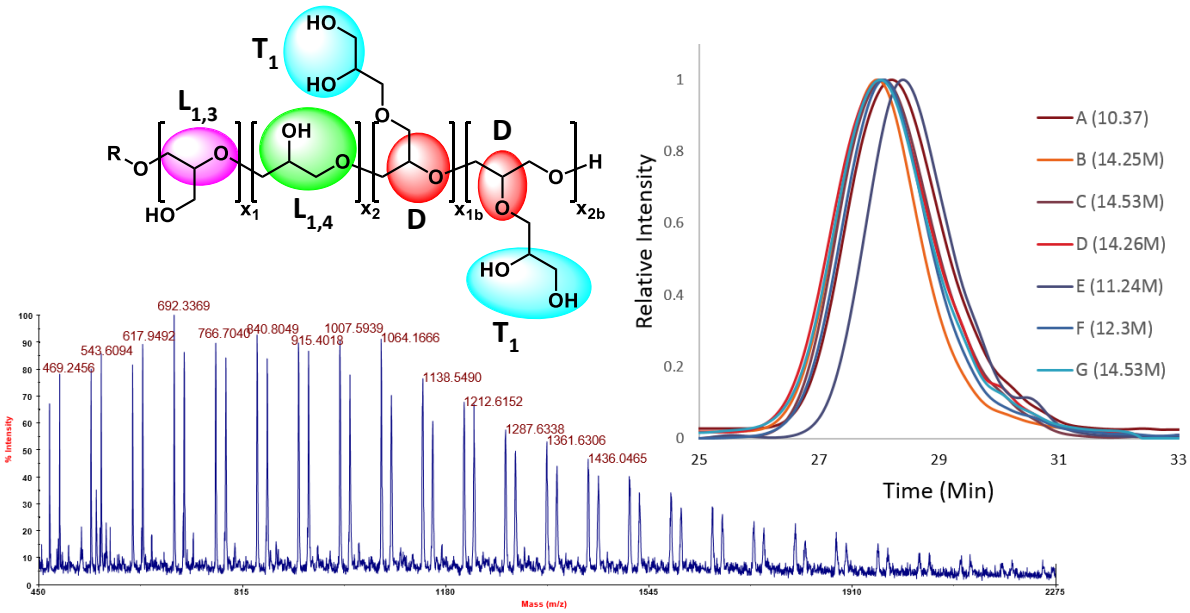

Sample	GLY (mL)	GLY (mmol)	PB (mL)	Concentration (mM)	Mn (MALDI)	Mw (MALDI)	PDI (MALDI)	PDI (GPC)
A	2.2	26.6	1.0	10.4	978.45	1074.57	1.098	1.206
B	4.4	53.2	0.25	14.3	1480.45	1645.11	1.111	1.193
C	6.6	79.8	0.25	14.5	1116.56	1247.76	1.117	1.086
D	2.2	26.6	0.125	14.3	1245.83	1302.57	1.046	1.125
E	2.2	26.6	0.75	11.2	863.00	959.96	1.112	1.144
F	2.2	26.6	0.5	12.3	1048.73	1189.00	1.134	1.073
G	3.3	26.6	0.125	14.5	1158.79	1320.15	1.139	1.099

Figure II-9: GPC and MALDI data for polymers formed with varying concentration

Introduction of Comonomers for Added Functionality

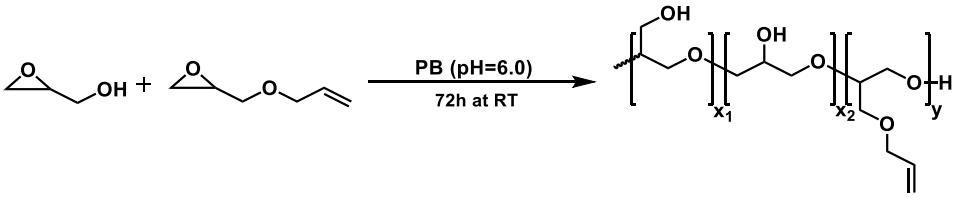

Figure II-10: Green synthesis of poly(glycidol-co-allyl glycidyl ether)

In the case of copolymers with AGE, we were successful in incorporating the allyl monomer but to a lower degree as was seen in the metal catalyzed system, a fact explained by the exaggerated difference in the reaction rate of glycidol and AGE (See Figure II-10). For these reactions, a similar strategy was developed whereby both monomer units were added to the dry reaction vessel followed by the addition of PB prior to submersion into the oil bath at 80°C. To

combat the lower than desired incorporation of AGE into the growing polymer chain, due to the reaction mechanism, a range of molar equivalences were chosen to study the capability of this technique to impart substantial allyl functionality into the system. The three reactions performed utilized GLY:AGE ratios of 1:1, 3:2, and 7:3, with the allyl incorporation seen to be 8.6%, 7.5%, and 5.6% respectively. Furthermore, in order to obtain even higher incorporation, and taking into consideration the slower reaction rate of AGE, another reaction with 1:1 molar equivalences was allowed to run for 5 days rather than the 3 days used in the original reactions. These reaction conditions afforded a polymer with 11.7% allyl incorporation. This set of experiments demonstrates the utility of this new method as a route for the formation of functionalized poly(glycidol) systems.

Comparison of Novel Polymerization Methods

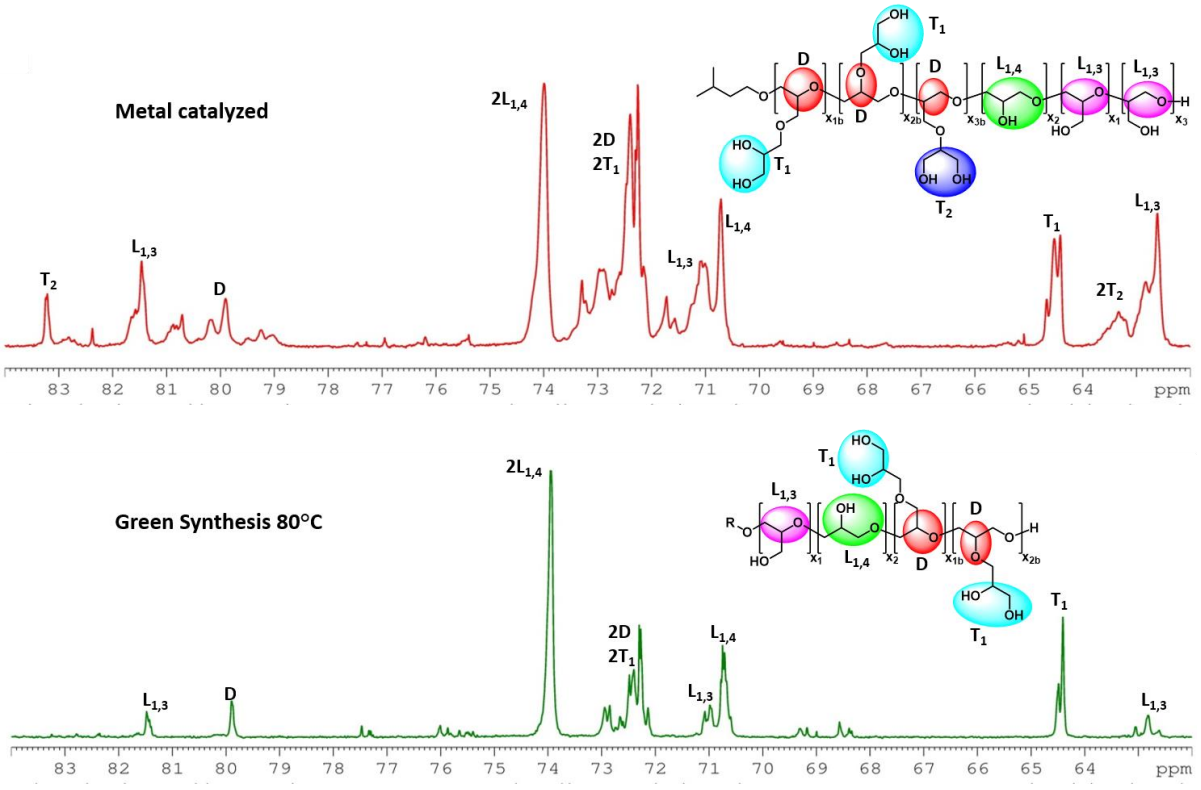

Figure II-11: Metal based polymer vs. the newly synthesized green polymer system

The ability to exploit the glycidol monomers inherent reaction in the presence of water was a very exciting discovery that led to the first reported synthesis of useful poly(glycidol) based polymers through a completely green synthesis method. However, we were very interested to determine the differences between the tin based synthesis and the green method. For this investigation we chose to use inverse gated quantitative NMR (See Figure II-11). It has been shown that this technique can be used to directly calculate both the degree of branching within the polymer species as well as the relative abundance of each type of repeat unit. The exhaustive characterization of these new systems showed a distinctly different backbone for each of the

Reaction Conditions	T	L 1,3	L 1,4	D
80°C	29	11	50	10
Metal	24	32	26	18

Figure II-12: Difference in relative abundance of repeat units between green synthesis and tin based system

polymer synthesis routes. The difference between the two systems was visually apparent upon performing the NMR measurements, with the green synthesis polymer exhibiting a much simpler NMR spectra, pointing to a polymer with fewer distinct ring opening possibilities. Without the presence of the tin, no T_2 termination units were observed, a fact that points to exclusive ring opening from the unsubstituted side of the glycidol ring in the green synthesis method. This intriguing fact is further accentuated when comparing the relative abundances of the different repeat units in the polymers where it was calculated that the green synthesis polymer contained 50% $L_{1,4}$ characteristic, almost twice that seen in the tin-based polymer (See Figure II-12). This

repeat unit is the dominating unit for the production of more linear species and explains why the green synthesis polymers have such a reduced degree of branching from the tin-based system.

The Elucidation of a Unique Polymerization Mechanism

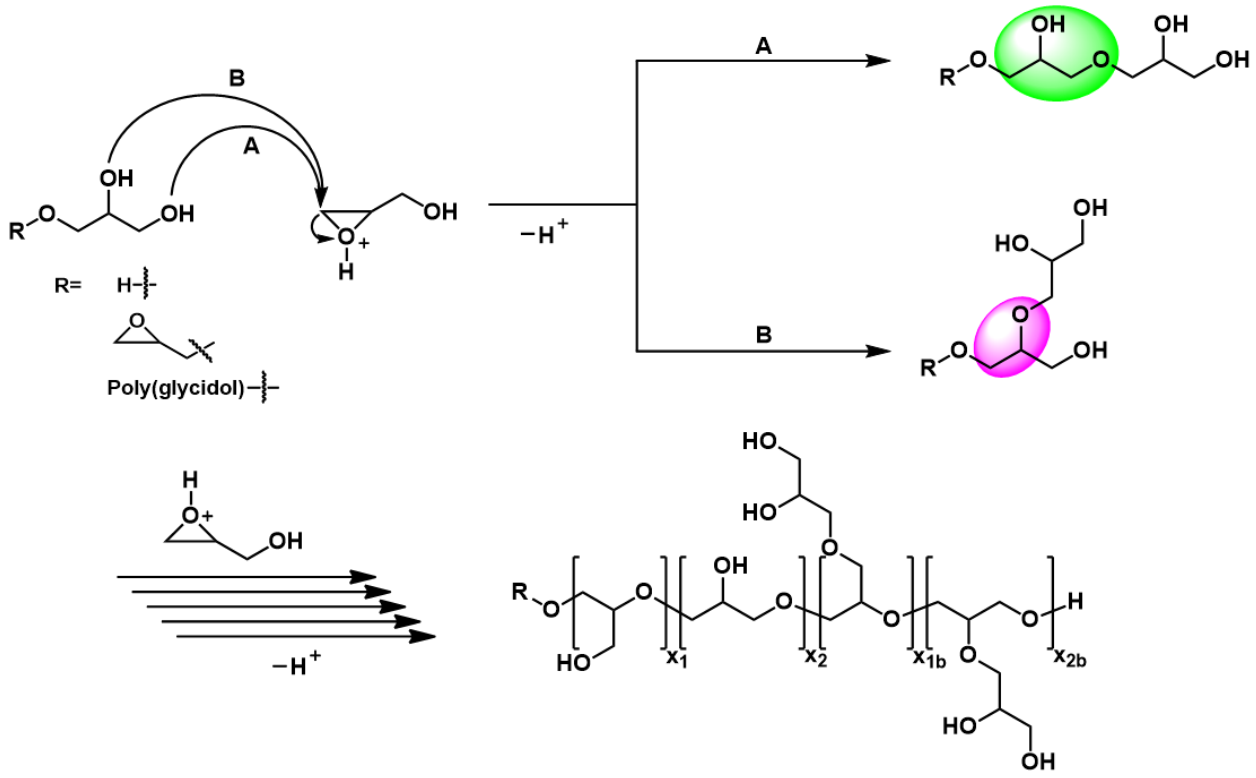

Figure II-13: New mechanism for the green synthesis method

Now that we knew the green synthesis products were unique and new to the field of poly(glycidol) structures, we were interested in determining how these structures were formed, and for this a new mechanism was necessary. The two known mechanisms for glycidol are the activated chain end (ACE), which we can rule out as this method gives large amounts of $L_{1,3}$ characteristic, and activated monomer mechanism (AM), which is most likely the prevailing mechanism in our case since the acidic pH buffer affords the ability to protonate the epoxide oxygen. However, the AM mechanism usually requires the presence of an activated oxoanion for sufficient nucleophilic attack. This issue is overcome in our reaction due to the elevated reaction

temperature, which allows not only the glycidol monomer to attack another monomer unit, but also the hydroxyls on the growing polymer chain, as well as water, which was determined from the obtained MALDI data. This unique convergence of thermal activation, with the activated monomer mechanism, leads to a mechanism with sole attack at the unsubstituted side of the monomer unit (See Figure II-13). This argument is made since attack at the substituted side of the glycidol ring could potentially yield a T_2 termination, which is not seen in the NMR data. Together, these arguments answer all of the structural anomalies seen in this novel polymer system and allow us to propose a new type of polymerization mechanism named Aqueous Epoxide Ring Opening Polymerization (AEROP). This mechanism combines the classic AM mechanism with elevated temperature and slight acidity to facilitate a facile yet controlled polymerization yielding well controlled poly(glycidol) structures.

Conclusion

The polymerization techniques described here represent two novel synthesis routes for the formation of poly(glycidol) based structures with reduced degrees of branching. The utilization of tin triflate as a benchtop catalyst gives control over the polymerization process while simplifying the reaction conditions and reducing reaction time relative to previously published polymerization techniques. The newly developed green synthesis method is the first reported example of a green synthesis route capable of forming poly(glycidol) structures of real utility. Furthermore, both methods are capable of yielding functionalized polymer products that can be employed for the formation of novel nano- and micronscale polymer architectures.

Experimental

Materials

All reaction solvents used were HPLC quality and purchased from Sigma Aldrich. All NMR solvents were purchased from Cambridge Isotope Laboratories, Inc. and used without further purification. Allyl glycidyl ether (AGE), ≥99%, sodium hydroxide, ≥97%, and dithranol, ≥98%, was purchased from Sigma Aldrich and used without further purification. Hydrochloric acid, 11.65M, was purchased from EMD and used without further purification. Glycidol (GLY), 96%, was purchased from Sigma Aldrich and vacuum distilled prior to use with a Kugelrohr short-path distillation device. Dulbecco's Phosphate Buffered Saline (PBS), no calcium, no magnesium, was purchased from life technologies and the pH was attenuated using either sodium hydroxide or hydrochloric acid prior to use.

Characterization

^{1}H and ^{13}C NMR spectroscopy was performed using a Bruker 600 spectrometer operating at 600 and 150 MHz, respectively. The instrument is equipped with a 14.1 Tesla Bruker magnet, which is controlled by a Bruker AV-II console, and a 5mm Z-gradient TCI Cryo-probe. A 20 second recycle delay was used to insure full relaxation for quantitative measurements, which allowed for the elucidation of specific monomer unit peaks and subsequent calculation of the degree of branching present in each glycidol homopolymer. MALDI measurements were accomplished using a Voyager DE-STR MS in linear TOF mode equipped with a nitrogen gas laser at λ= 337nm with external calibration. The individual instrument parameters varied based on the samples being characterized. Size exclusion measurements were obtained with a Waters chromatograph system equipped with a Waters 2414 refractive index detector, a Waters 1525 binary HPLC pump, and four 5 mm Waters columns (300 mm x 7.7 mm), connected in series with increasing pore size

(100, 1000, 100,000 and 1,000,000 Å respectively). All runs were performed with N-N-dimethylformamide (DMF) as the eluent at a flow rate of 1 mL/min.

General Procedure for GLY based polymers

In order to maintain a consistent temperature throughout the entirety of the polymerization, a specialized round bottom flask and cooling system were employed. The round bottom flask was formed with a 25mL reaction vessel enveloped by a glass "jacket" with an inlet at the bottom and an outlet at the top. This allowed for a temperature controlled liquid to constantly surround the reaction vessel, thus allowing for sustained reaction temperature. The pump system used was a 7 Liter Refrigerated Circulator obtained from PolyScience with a temperature range of -40°C to 200°C and a temperature stability of ±0.01°C.

Two 1-dram vials were fitted with septa and flame dried under N_2(g). The first 1-dram vial was used to make a 1.7M Iso-Amyl alcohol (IAOH) stock solution using dry THF, while the second was used to create a $3.7x10^{-2}$M tin triflate stock solution, also using dry THF. Stock IAOH (0.20mL, $3.33x10^{-4}$ mol, 0.066eq) and $Sn(OTf)_2$ (0.26mL, $9.45x10^{-6}$ mol, 0.00035 eq) were added to the jacketed reaction flask, equipped with a magnetic stir bar, at the chosen reaction temperature, and the reaction solution was allowed to stir for 30 minutes to allow for the alcohol/catalyst conjugation. The reaction flask was then brought to the proper reaction temperature before addition of the monomers and the polymerization was allowed to run to completion.

CAUTION: When the scale of the reaction is above 1g, the reaction can become very exothermic during monomer addition and dropwise monomer addition is required in order to deter decomposition.

Synthesis of GLY Homopolymer

To the jacketed reaction flask equilibrated to the desired temperature was added $Sn(OTf)_2$ (0.26mL; $9.45x10^{-6}$ mol; 0.00035 eq) and EtOH (0.20mL; $3.33x10^{-4}$ mol; 0.066 eq). After the complexation of the initiator to the catalyst, glycidol (2.00g; 27.0 mmol; 1.0 eq) was added dropwise. After stirring was completely impeded (reaction time varied with temperature), the crude viscous polymer product was dissolved in a minimal amount of methanol and precipitated into vigorously stirring acetone, which was then decanted to afford the pure glycidol homopolymer product as translucent viscous material. The product was collected in methanol, transferred to a weighed 6-dram vial, and the excess solvent was removed. Yield: 1.89g (94.8%) ^{1}H-NMR (600MHz, $CDCl_3$) δ: 3.31-3.94 (6H). ^{13}C-NMR (150MHz, $CDCl_3$) δ: 81.37, 79.81, 75.12, 73.88, 72.01-72.94, 70.42-71.17, 64.41, 62.53, 62.06.

Synthesis of GLY/AGE Polymer (80/20)

$Sn(OTf)_2$ (0.23mL; $8.52x10^{-6}$ mol; 0.00035 eq) and EtOH (0.196mL; $3.33x10^{-4}$ mol; 0.066 eq) were added to the reaction flask. After the complexation of the initiator to the catalyst, the glycidol (1.44g; 19.47 mmol; 4.0 eq) and allyl glycidyl ether (0.56g; 4.87 mmol; 1.0 eq) were added dropwise. After stirring was completely impeded (reaction time varied with temperature), the crude viscous polymer product was dissolved in a minimal amount of methanol and precipitated into vigorously stirring acetone, which was then decanted to afford the pure GLY/AGE polymer product as translucent viscous material. The product was collected in methanol, transferred to a weighed 6-dram vial, and the excess solvent was removed. Yield: 1.23g (68.3%). ^{1}H-NMR (600MHz, $CDCl_3$) δ: 5.92 (1H), 5.21 (2H), 4.04 (2H), 3.38-3.94 (27.30H). ^{13}C-NMR (150MHz, $CDCl_3$) δ: 136.31, 117.42, 81.56, 80.01, 74.09, 73.43, 72.51, 70.87, 64.60, 62.69.

Synthesis of GLY Homopolymer in Phosphate Buffer

To prepare the GLY homopolymers, glycidol monomer (33mmol, 1.0eq) was added to a flame dried 25mL round bottom flask (RBF). The reaction vessels were then lowered into oil baths of varying temperature (60°C, 80°C, or 100°C) to ensure consistent reaction temperatures, followed by the addition of DPBS (0.25mL; pH= 6.0). After a predetermined reaction time based on the reaction temperature (120h, 72h, and 24h respectively), the crude viscous polymer product was dissolved in a minimal amount of methanol and precipitated into vigorously stirring acetone. The resulting solution was decanted to afford the pure GLY product as a translucent viscous material. The product was collected in methanol, transferred to a weighed 6-dram vial, and the excess solvent was removed. Once it had been determined that the reaction at 80°C yielded the product with the most desirable DB, other reaction conditions were altered at this temperature, including reaction concentration and the pH of DPBS used. ^{1}H-NMR (600MHz, $CDCl_3$) δ: 3.42-3.87 (6H). ^{13}C-NMR (150MHz, $CDCl_3$) δ: 81.33, 79.75 73.84, 72.36, 70.90, 70.62, 64.32, 62.71

Synthesis of GLY/AGE Copolymer in Phosphate Buffer

To prepare GLY/AGE copolymers, glycidol monomer (17.5mmol, 2.3 eq,) was added to a flame dried 25mL RBF equipped with a stir bar. The allyl glycidyl ether monomer (7.5mmol, 1.0 eq) was then added via syringe and the reaction vessel was lowered into an oil bath at 80°C before the addition of DPBS (0.25mL; pH= 6.0). The reaction was then allowed to run for 72 hours before being removed from the oil bath, dissolved in a minimal amount of methanol and precipitated into vigorously stirring ethyl acetate. After allowing the solution to settle, the supernatant was decanted and the resulting polymer product was collected in methanol, transferred to a weighed 6-dram vial, and dried on the pump to remove all solvent. In order to determine the amount of allyl characteristic that could be incorporated into the final copolymer product, a molar equivalent ratio of GLY:AGE

of 1:1 was used in a subsequent reaction. ^{1}H-NMR (600MHz, CDCl3) δ:6.0-5.90 (m, –OCH2C*H*CH2), 5.37–5.17 (m, –OCH2CHCH_2) .3.97-3.42 (6H). ^{13}C-NMR (150MHz, CDCl3) δ: 136.31, 117.39, 81.37, 79.81, 75.12, 73.88, 72.01-72.94, 70.42-71.17, 64.41, 62.53, 62.06, 27.99, 27.60.

Quantitative NMR Measurements

^{1}H and ^{13}C NMR spectroscopy was obtained using a Bruker 600 spectrometer operating at 600 and 150 MHz, respectively. The instrument is equipped with a 14.1 Tesla Bruker magnet, which is controlled by a Bruker AV-II console, and a 5mm Z-gradient TCI Cryo-probe. A 10 second recycle delay was used to insure full relaxation between pulses, allowing for quantitative measurements. This data was then used to assign individual monomer peaks specific to the ring opening structure, thus allowing for the calculation of the polymer's degree of branching and relative abundance of repeat units.

Gel Permeation Chromatography (GPC)

Size exclusion chromatography of the glycidol based polymers was performed in DMF at 70°C with a flow rate of 1.0mL/min (Waters 1525 binary HPLC pump; columns: 7.8x300mm; Styragel HR 5, Styragel HR 4E, and Styragel HR 3: molecular weight range 50,000 to 4x10^{6}, 50 to 100,000, and 500 to 30,000 g/mol, respectively). A Waters 2414 refractive index detector was employed for detection of the polymer species. Polystyrene standards were used for molecular weight determination. Polymer samples were measured at a concentration of 10mg/mL and the dn/dc value for poly(glycidol) was determined using off-line refractive index measurements.

Size-Exclusion Chromatography Tandem Electrospray Ionization Ion Mobility Time-of-Flight Mass Spectrometry (SEC-Tandem-ESI-IM-TOF-MS)

In order to fully characterize the polymer structures being formed, a SEC-tandem-MS method was developed. SEC of the poly(glycidol) based samples was performed in water at 37°C, to simulate ambient body temperature, with a flow rate of 0.8mL/min (Waters 515 HPLC pump; columns:7.8x300mm; Ultrahydrogel 250, Ultrahydrogel 120, and Ultrahydrogel DP 120; molecular weight range 1,000-80,000, 100-5,000, and 100-5,000 respectively). After SEC was complete, the sample was run through a T joint with one end going to a waste collector and the other attached to a Synapt G2-S equipped with a ZSpray ESI source. The instrument settings were set to: Polarity: positive; Capillary: 2kV; Source T: 80°C. Polymer samples were measured at a concentration of 100µg/mL. Although an interesting trend was seen with the drift time of species with different charge states, the hardness of the ESI source made the determination of molecular weight with this method overly difficult. Thus, MALDI-TOF was chosen as the preferred method for molecular weight calculation.

Matrix Assisted Laser Desorption-Ionization Time-of-Flight Mass Spectrometry (MALDI-TOF-MS).

MALDI-TOF-MS measurements were performed using a Voyager DE-STR MS in reflector mode equipped with a nitrogen gas laser of wavelength 337nm utilizing external calibration. The instrument parameters were set to: 25,000 V; 90% grid; 600ns delay; 1000 shots per spectrum. The poly(glycidol) based samples were formed using solutions of 10mg/mL polymer in water and saturated CHCA matrix solution in 2:1 water:acetonitrile. In order to determine the molecular

weight of the polymer species, direct integration of the obtained peaks was performed. This allowed for the calculation of Mn and Mw values, which also allows for the determination of PDI.

References

1. Gong, C., Xie, Y., Wu, Q., Wang, Y., Deng, S., Xiong, D., Liu, L., Xiang, M., Qian, Z., and Wei, Y. (2012) Improving anti-tumor activity with polymeric micelles entrapping paclitaxel in pulmonary carcinoma, *Nanoscale 4*, 6004-6017.
2. Tyrrell, Z., Shen, Y., and Radosz, M. (2012) Multilayered Nanoparticles for Controlled Release of Paclitaxel Formed by Near-Critical Micellization of Triblock Copolymers, *Macromolecules 45*, 4809-4817.
3. Parveen, S., and Sahoo, S. (2014) Long circulating chitosan/PEG blended PLGA nanoparticle for tumor drug delivery (vol 670, pg 372, 2011), *European Journal of Pharmacology 727*, 186-186.
4. Alconcel, S. N. S., Baas, A. S., and Maynard, H. D. (2011) FDA-approved poly(ethylene glycol)-protein conjugate drugs, *Polymer Chemistry 2*, 1442-1448.
5. Fam, C., Eisenberg, S., Carlson, S., Chlipala, E., Cox, G., and Rosendahl, M. (2014) PEGylation Improves the Pharmacokinetic Properties and Ability of Interferon Gamma to Inhibit Growth of a Human Tumor Xenograft in Athymic Mice, *Journal of Interferon and Cytokine Research 34*, 759-768.
6. Vine, K., Lobov, S., Chandran, V., Harris, N., and Ranson, M. (2015) Improved Pharmacokinetic and Biodistribution Properties of the Selective Urokinase Inhibitor PAI-2 (SerpinB2) by Site-Specific PEGylation: Implications for Drug Delivery, *Pharmaceutical Research 32*, 1045-1054.

7. Niidome, T., Yamagata, M., Okamoto, Y., Akiyama, Y., Takahashi, H., Kawano, T., Katayama, Y., and Niidome, Y. (2006) PEG-modified gold nanorods with a stealth character for in vivo applications, *Journal of Controlled Release 114*, 343-347.

8. Vasilache, V., Popa, C., Filote, C., Cretu, M.-A., and Benta, M. (2011) NANOPARTICLES APPLICATIONS FOR IMPROVING THE FOOD SAFETY AND FOOD PROCESSING, 7th International Conference on Materials Science and Engineering, Conference Paper.

9. Levene, P. A., and Walti, A. (1927) On Condensation Products of Propylene Oxide and of Glycidol, *The Journal of Biological Chemistry 75*.

10. Tokar, R., Kubisa, P., Penczek, S., and Dworak, A. (1994) Cationic Polymerization of Glycidol - Coexistence of the Activated Monomer and Active Chain-End Mechanism, *Macromolecules 27*, 320-322.

11. Dworak, A., Walach, W., and Trzebicka, B. (1995) Cationic Polymerization of Glycidol - Polymer Structure and Polymerization Mechanism, *Macromolecular Chemistry and Physics 196*, 1963-1970.

12. Sunder, A., Hanselmann, R., Frey, H., and Mulhaupt, R. (1999) Controlled synthesis of hyperbranched polyglycerols by ring-opening multibranching polymerization, *Macromolecules 32*, 4240-4246.

13. Sunder, A., Turk, H., Haag, R., and Frey, H. (2000) Copolymers of glycidol and glycidyl ethers: Design of branched polyether polyols by combination of latent cyclic AB(2) and ABR monomers, *Macromolecules 33*, 7682-7692.

14. Sunder, A., Frey, H., and Mulhaupt, R. (2000) Hyperbranched polyglycerols by ring-opening multibranching polymerization, *Macromolecular Symposia 153*, 187-196.

15. Khan, M., and Huck, W. T. S. (2003) Hyperbranched polyglycidol on Si/SiO2 surfaces via surface-initiated polymerization, *Macromolecules 36*, 5088-5093.

16. Slagt, M., Stiriba, S., Kautz, H., Gebbink, R., Frey, H., and van Koten, G. (2004) Optically active hyperbranched polyglycerol as scaffold for covalent and noncovalent immobilization of platinum(II) NCN-pincer complexes. Catalytic application and recovery, *Organometallics 23*, 1525-1532.

17. Sun, X., Yang, X., Liu, Y., and Wang, X. (2004) Synthesis and characterization of a multiarm star polymer, *Journal of Polymer Science Part a-Polymer Chemistry 42*, 2356-2364.

18. Wang, S. X., Zhou, Y., Yang, S. C., and Ding, B. J. (2008) Growing hyperbranched polyglycerols on magnetic nanoparticles to resist nonspecific adsorption of proteins, *Colloids and Surfaces B-Biointerfaces 67*, 122-126.

19. Feng, X., Taton, D., Chaikof, E., and Gnanou, Y. (2009) Fast Access to Dendrimer-like Poly(ethylene oxide)s through Anionic Ring-Opening Polymerization of Ethylene Oxide and Use of Nonprotected Glycidol as Branching Agent, *Macromolecules 42*, 7292-7298.

20. Mendrek, A., and al., e. (2010) Amphiphilic behaviour of poly(glycidol)-based macromonomers and its influence on homo-polymerisation in water and in water/benzene mixture, *Polymer 51*, 342-354.

21. Wilms, D., Schomer, M., Wurm, F., Hermanns, M. I., Kirkpatrick, C. J., and Frey, H. (2010) Hyperbranched PEG by Random Copolymerization of Ethylene Oxide and Glycidol, *Macromolecular Rapid Communications 31*, 1811-1815.

22. Wilms, D., Stiriba, S. E., and Frey, H. (2010) Hyperbranched Polyglycerols: From the Controlled Synthesis of Biocompatible Polyether Polyols to Multipurpose Applications, *Accounts of Chemical Research 43*, 129-141.

23. Schull, C., Nuhn, L., Mangold, C., Christ, E., Zentel, R., and Frey, H. (2012) Linear-Hyperbranched Graft-Copolymers via Grafting-to Strategy Based on Hyperbranched Dendron Analogues and Reactive Ester Polymers, *Macromolecules 45*, 5901-5910.

24. Spears, B. R., Waksal, J., McQuade, C., Lanier, L., and Harth, E. (2013) Controlled branching of polyglycidol and formation of protein-glycidol bioconjugates *via* a graft-from approach with "PEG-like" arms, *Chemical Communications 49*, 2394-2396.

25. Weber, T., Bechthold, M., Winkler, T., Dauselt, J., and Terfort, A. (2013) Direct grafting of anti-fouling polyglycerol layers to steel and other technically relevant materials, *Colloids and Surfaces B-Biointerfaces 111*, 360-366.

26. Thomas, A., Muller, S., and Frey, H. (2014) Beyond Poly(ethylene glycol): Linear Polyglycerol as a Multifunctional Polyether for Biomedical and Pharmaceutical Applications, *Biomacromolecules 15*, 1935-1954.

27. Wurm, F., Dingels, C., Frey, H., and Klok, H.-A. (2012) Squaric Acid Mediated Synthesis and Biological Activity of a Library of Linear and Hyperbranched Poly(Glycerol)-Protein Conjugates, *Biomacromolecules 13*, 1161-1171.

28. Haag, R., Sunder, A., and Stumbe, J. F. (2000) An approach to glycerol dendrimers and pseudo-dendritic polyglycerols, *Journal of the American Chemical Society 122*, 2954-2955.

29. Zhang, J. G., Krajden, O. B., Kainthan, R. K., Kizhakkedathu, J. N., Constantinescu, I., Brooks, D. E., and Gyongyossy-Issa, M. I. C. (2008) Conjugation to hyperbranched polyglycerols improves RGD-mediated inhibition of platelet function in vitro, *Bioconjugate Chemistry 19*, 1241-1247.

30. Calderon, M., Quadir, M. A., Sharma, S. K., and Haag, R. (2010) Dendritic Polyglycerols for Biomedical Applications, *Advanced Materials 22*, 190-218.

31. Debaig, C., Benvegnu, T., and Plusquellec, D. (2002) Synthesis of linear and cyclic polyglycerols. Polyglyceryled surfactants: synthesis and characterization, *Ocl-Oleagineux Corps Gras Lipides 9*, 155-162.

32. Kainthan, R. K., Janzen, J., Levin, E., Devine, D. V., and Brooks, D. E. (2006) Biocompatibility Testing of Branched and Linear Polyglycidol, *Biomacromolecules 7*, 703-709.

33. Kawagishi, T., Yoshikawa, K., Ubukata, M., Hamada, M., and Nakajima, N. (2006) Synthesis of cyclic polyglycerols, *Heterocycles 69*, 107-111.

34. Holder, K., Spears, B., Huff, M., Priolo, M., Harth, E., and Grunlan, J. (2014) Stretchable Gas Barrier Achieved with Partially Hydrogen- Bonded Multilayer Nanocoating, *Macromolecular Rapid Communications 35*, 960-964.

CHAPTER III

FORMATION OF BIOCONJUGATES UTILIZING POLY(GLYCIDOL)

Introduction

The ability to increase the plasma half-life and decrease immunogenicity of readily available biological structures has led to some of the most efficacious treatments for many debilitating diseases. Since its conception, the field of protein therapeutics has been dominated by poly(ethylene glycol) (PEG)[1, 2]. PEGylation has contributed greatly to the success of treatment methods aimed at the delivery of biological therapeutics that would otherwise be of little consequence due to the body's natural desire to rapidly remove anything deemed to be a foreign entity. The 'stealth' ability of PEG is well documented and as such this method continues to be utilized for the formation of protein-polymer conjugates where it is capable of providing a protective barrier around the therapeutic, facilitating increased circulation time, greatly increasing the utility of the proteins[3-5]. However, as many of the diseases treated with PEGylated structures require lifetime administration of the therapeutic, new studies have seen an increase in immune response to the historically used linear PEG species. For this reason, the utilization of branched PEG structures, as well as the search for alternatives to PEG with different, and potentially better characteristics, is a field that has seen marked growth in the past decade[6-9].

Polymers that are biologically compatible can be conjugated to proteins with therapeutic properties to afford systems that have enhanced pharmacokinetic properties. This functionalization results in enhanced therapeutic potential, and increased stability of the structures, allowing less stringent storage and transfer restrictions[7, 10]. In order to form the most effective structures, a high degree of control is desirable, as well as location specific attachment of the polymer chains to the

proteins being functionalized, as both of these factors contribute to the overall efficiency of the polymer-protein products[6, 11, 12]. In hopes of addressing these issues, researchers will often utilize genetically engineered proteins which exhibit well defined and readily accessible conjugation sites that can be effectively targeted. The formation of protein therapeutics coated in a protective layer of PEG is a multi-billion dollar field that has afforded some of the most potent biological therapeutics on the market, including treatments for diseases such as diabetes, hepatitis C, and even cancer[7, 13].

The new push for better PEG alternatives has explored many avenues, including acrylamide derivatives, poly(vinylpyrrolidone), and poly(glycidol) based systems. However, much of the work requires the synthesis and purification of polymers with reactive groups that can be utilized as anchors for the secondary attachment of these polymers to the surface of the desired protein therapeutic. While this method affords some advantages over the possible sizes and functionalities of the polymers used, it is a process that requires numerous synthesis and purification steps to achieve the protein-polymer conjugate product[14, 15]. Therefore, it would be advantageous to develop a method capable of arriving at a functionalized species through a graft-from approach. In such an approach, the protein to be conjugated, modified to act as a macroinitiator, would be incubated with the monomers necessary for the desired polymerization to occur. This method would allow for the directed formation of protein-polymer conjugates in a one-step polymerization affording the conjugated species ready for administration[9].

Poly(glycidol) (PG) contains a polyether backbone similar to that seen in PEG and has been studied previously as a potential PEG alternative. The synthesis methods used to form these PG polymers leads to either purely linear systems, through the utilization of protected monomer species, or to hyperbranched polymers similar in architecture to dendrimers[14-19]. Work with these

PG products has shown successful graft-on approaches affording protein-polymer conjugates with similar activity as their PEG counterparts. Furthermore, the research has shown that PG polymers of semibranched architecture perform better than the linear and hyperbranched structures[14, 15]. This data, together with the ability to control the branching of PG polymers, led to the desire for the formation of PG based protein-polymer conjugates using a graft-from method.

Results and Discussion

The facile polymerization of poly(glycidol) is utilized for the formation of protein-polymer conjugates with potentially enhanced therapeutic potential. The one pot formation of these graft-from conjugates allows for direct functionalization of the protein macroinitiators with the poly(glycidol) polymer, thus decreasing the steps necessary to arrive at a protein-polymer conjugate. This method will be employed for the formation of protein-polymer conjugates of both bovine serum albumin (BSA) and lysozyme (LYZ).

Bovine Serum Albumin Bioconjugates

The first protein to be PEGylated in 1977 was BSA, and for this reason it was chosen as the first protein to be functionalized with the newly proposed GLYcidation method. It is well established that BSA has an easily accessible free thiol on the exterior of the protein which has shown the ability for functionalization. As the method of polymerization to be used is ring opening polymerization (ROP), the synthesized BSA macroinitiator needs to have an easily accessible alcohol group. Therefore, it was decided that a maleimide alcohol would be employed to impart the desired hydroxyl characteristic. To facilitate this reaction, the native BSA protein was incubated in nitrogen purged phosphate buffer (PB) followed by the addition of the maleimide alcohol. After completion, the newly formed macroinitiator was dialyzed and ready to be used for the polymerization procedure.

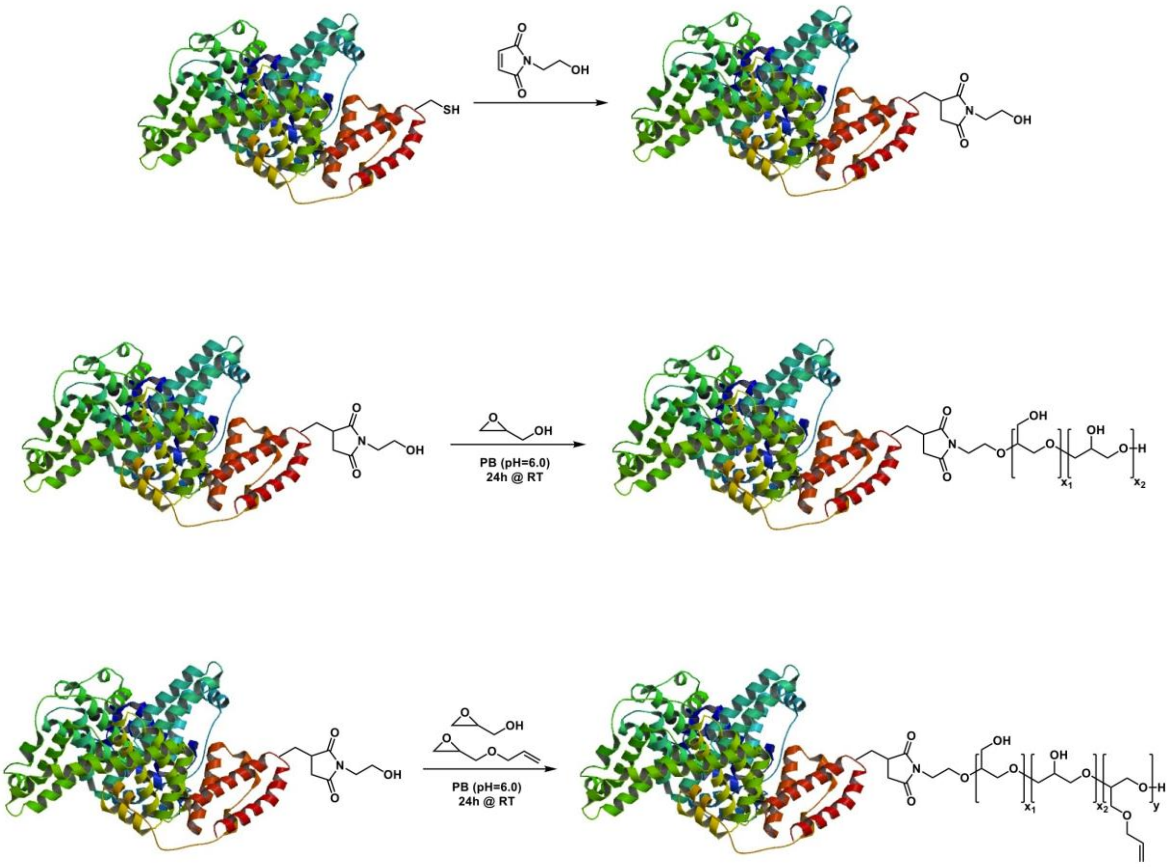

Figure III-1: (Top) Maleimide attachment to BSA protein. (Center) Polymerization of GLY Homopolymer from BSA-OH. (Bottom) Polymerization of GLY/AGE Polymer from BSA-OH

In order to determine the ability to form polymers of different sizes on the surface of the proteins, two separate concentrations of glycidol were investigated. Initial polymerization reactions were performed in DMSO and DMF with $Sn(OTf)_2$ catalyst present. However, the products from these reactions exhibited poor water solubility and led to the need for a different approach. It is known that glycidol can undergo autopolymerization in the presence of water, and that anionic polymerization mechanisms are capable of forming poly(glycidol) structures (See Figure III-1). Therefore, it was decided that a green synthesis route would be followed in which the newly formed macroinitiator was solubilized in slightly acidic phosphate buffer (pH= 6.0)

followed by the addition of glycidol to facilitate the formation of protein-polymer conjugates. The products resulting from this reaction were well soluble in water and easily purified through dialysis.

Introduction of a Functional Monomer Unit

The newly discovered method for the facile formation of protein-polymer conjugates was very exciting, but the ability to incorporate functional monomers, capable of undergoing secondary reactions once attached to the protein, is an intriguing notion. In order to investigate this possibility, subsequent reactions were run in which allyl glycidyl ether (AGE), a readily available glycidol derivative, was added to the reaction mixture. The resulting products were investigated using ^{1}H NMR and showed successful incorporation of the allyl moiety. Containing a range of thiolated structures, which can be used for secondary modifications such as targeting units, through the use of thiolene-click reactions, these newly formed species can be utilized as protein-polymer conjugates with elevated potential

Characterization of Bioconjugate Sizes

MALDI-TOF mass spectrometry was found to be an ideal tool to determine the success of the graft-from approach and to quantify the molecular weight increase (Figure III-2). The first set of experiments afforded a 1kDa increase in the molecular weight of BSA. To demonstrate a more apparent change in molecular weight, the amount of glycidol was increased to 4 fold and an increase in the molecular weight of the BSA of up to 10K was observed.

Most surprisingly, the reactions conducted in buffer yielded species with the highest molecular weight increase. This finding may indicate a catalytic promotion of the slightly acidic buffer (pH 6.0) accelerating the polymerization of the glycidol and is the subject of further studies.

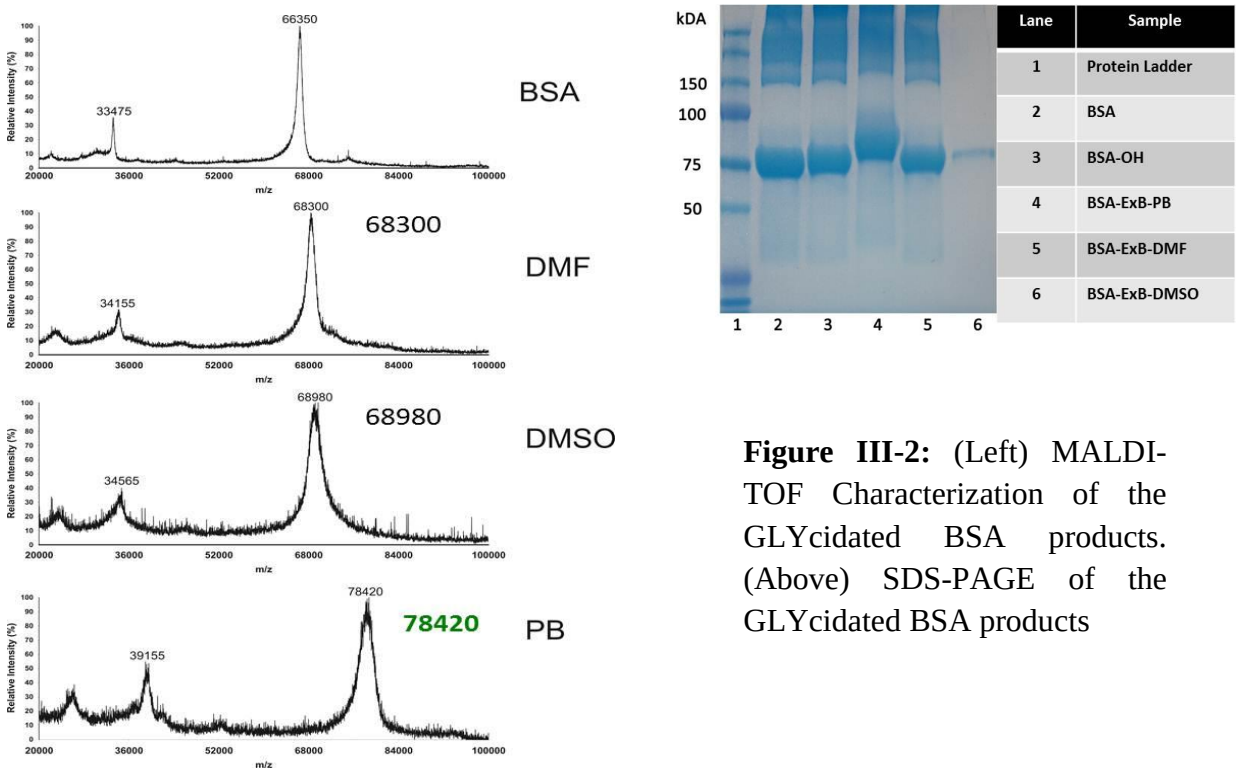

Figure III-2: (Left) MALDI-TOF Characterization of the GLYcidated BSA products. (Above) SDS-PAGE of the GLYcidated BSA products

With this, a practical method to grow polyglycerols from proteins in physiological environments was created.

Polyacrylamide electrophoresis (PAGE) was employed to further support the evidence of a successful polymer-protein conjugation. Figure III-3 shows lanes with BSA (lane 2), BSA-OH macroinitiator (lane 3) and conjugated protein-polymer products (lanes 4-6) in the three selected solvents and at the highest glycidol monomer concentration. The PAGE confirmed the molecular weight increases of the samples via the graft-from method and the products appear as high molecular weight bands slightly above the BSA standard. The polymer-protein conjugate reaction conducted in buffer showed a substantial molecular weight increase in PAGE in comparison with the other samples and confirmed the MALDI-TOF measurements.

Measurement of Retained Bioactivity

To determine the bioactivity of the polymer-protein conjugates, the species were allowed to react with 4-nitrophenyl acetate and the absorbance of the resulting hydrolysis product was

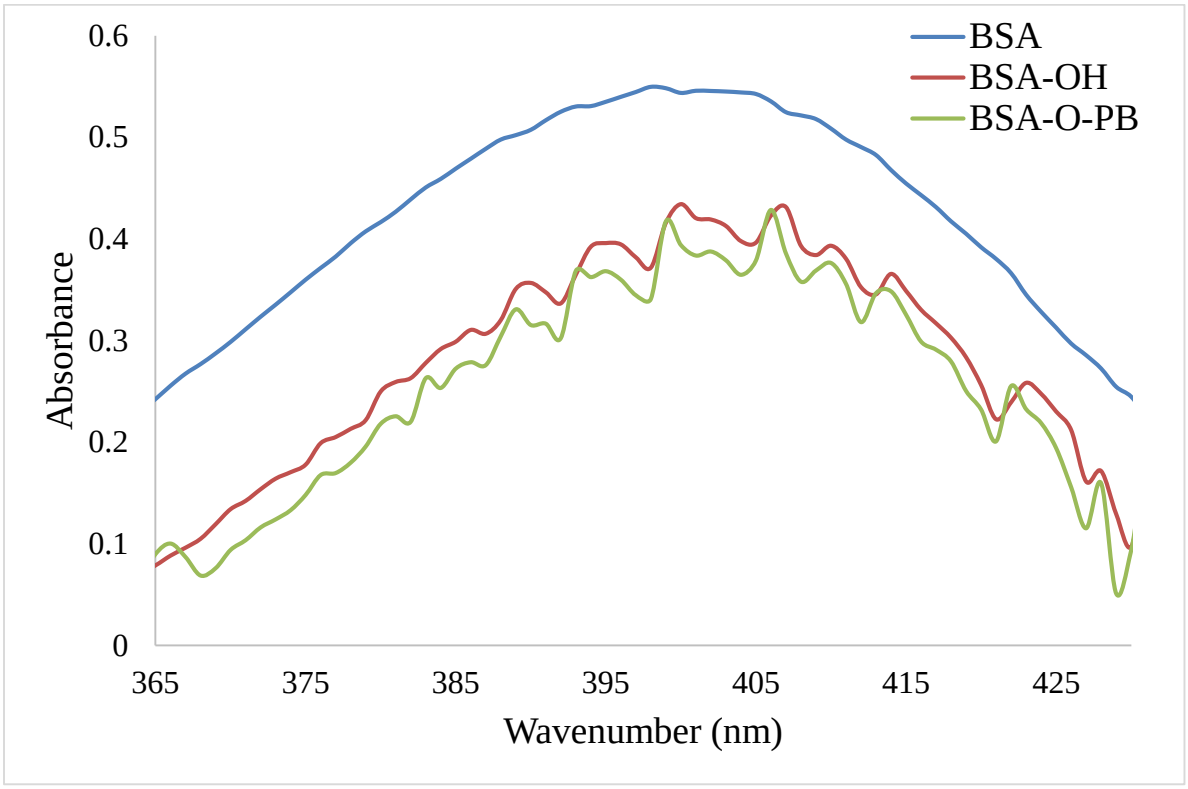

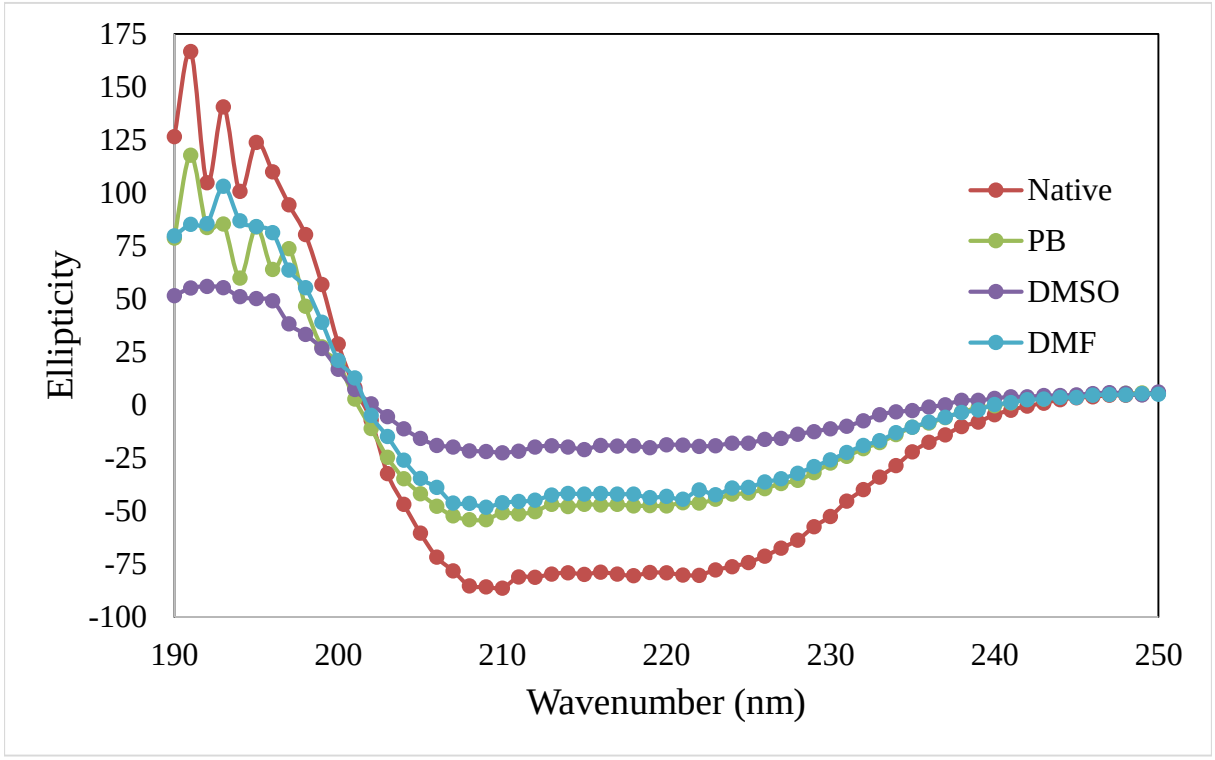

Figure III-3: (Top) Bioactivity investigation of BSA polymer-protein conjugates. (Bottom) Circular Dichroism investigation of BSA polymer-protein conjugates

measured using UV/Vis spectroscopy (See Figure III-3). The results of the bioactivity assay indicated only a slight decrease in activity in comparison with the unmodified BSA protein. Protein-polymer conjugates formed with the lower concentration of 0.33M are shown in Figure III-4. All samples show a high activity that is close to or higher than the BSA-OH macroinitiator. The lowest bioactivity is observed for the sample conducted in DMSO. The polymer-protein conjugate obtained from reactions with 1.33M in PB, which yielded the highest increase in molecular weight (10K), showed a lower bioactivity of 0.02. Since the reactions run at 1.33M were performed to validate the developed method, future studies will attempt to achieve sufficient solubilization and stability with the shortest polyglycerol chains possible to limit the adverse effect on bioactivity.

Investigation of Structural Changes

The final characterization method employed was circular dichroism (Figure III-3). This particular measurement is able to determine the influence that the polymer conjugation reaction has on the 3-dimensional structure of the BSA protein. These structural characteristics must be maintained in order to ensure the protein will behave as it should. The measurements taken show a similar trend to the bioactivity measurements, with the DMSO reaction exhibiting a significant change in structure while the reactions conducted in PB and DMF have a minimal effect on the BSA protein. This information affords another argument in favor of the GLYcidation of the protein and allows for the assumption that the formulated process does not overtly influence the structure of the protein being functionalized.

Lysozyme Bioconjugates

The intriguing data garnered from the work done with BSA, coinciding with the minor reduction in protein activity, led the researcher to experiment with a more biologically relevant

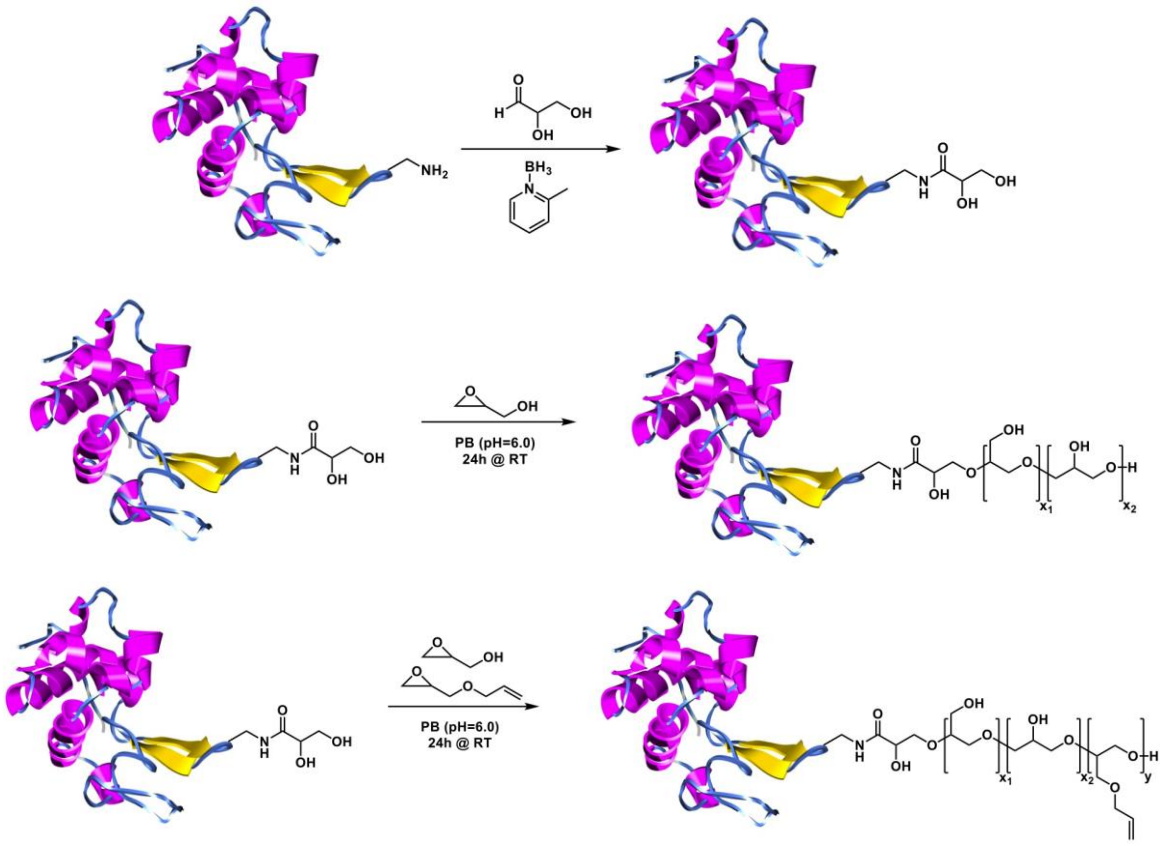

Figure III-4: (Top) Maleimide attachment to LYZ protein. (Center) Polymerization of GLY Homopolymer from LYZ-OH. (Bottom) Polymerization of GLY/AGE Polymer from LYZ-OH

protein, the antimicrobial lysozyme (LYZ). Unlike BSA, LYZ possess seven pendant amine groups, though only one functionalized group is desired. In order to afford a LYZ macroinitiator, the LYZ was incubated with an aldehyde thiol to allow for the formation of a Schiff base which was subsequently reduced with 2-picoline borane complex to yield the desired diol functionalized product (Figure III-4). Due to their green nature, and based on the fact that they yielded the least disrupted BSA products, only the PB reaction conditions were used, though a more thorough time and concentration study was performed. The reaction time was not limited to 24h, but reaction times included 4h, 8h, 16h, 24h, and 48h, and each reaction time was used to form LYZ products at both 1.33M and 2.66M with respect to GLY concentration. This range of reactions provided protein conjugates with a seemingly more linear time dependent polymer growth, while the more

concentrated reactions did not yield species with drastically increased molecular weights as was observed in the BSA study. The synthesis of a LYZ-GLY/AGE species was also performed to afford a product species with readily available allyl units.

Effect of Reaction Time and Concentration on Functionalization

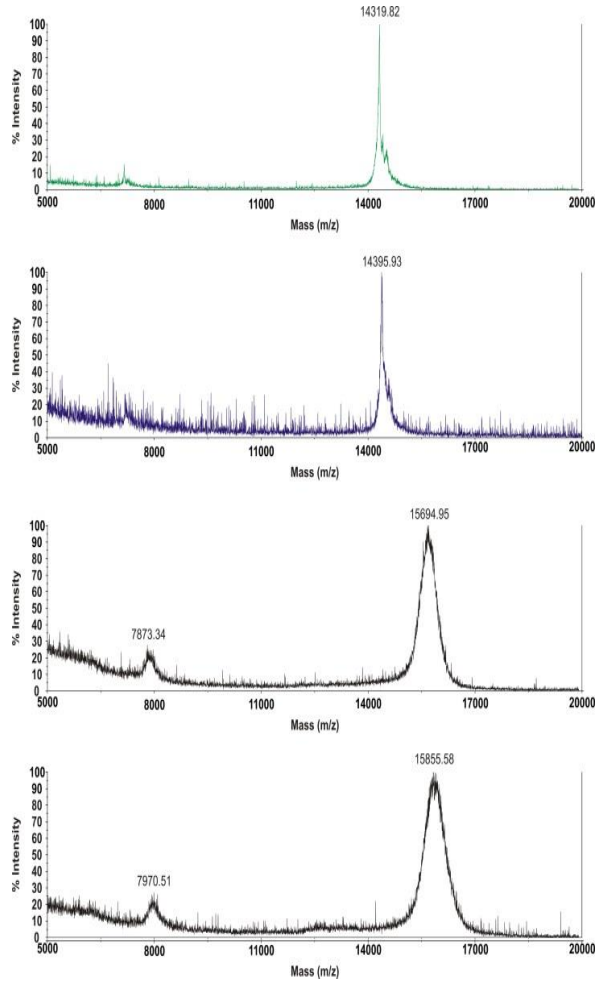

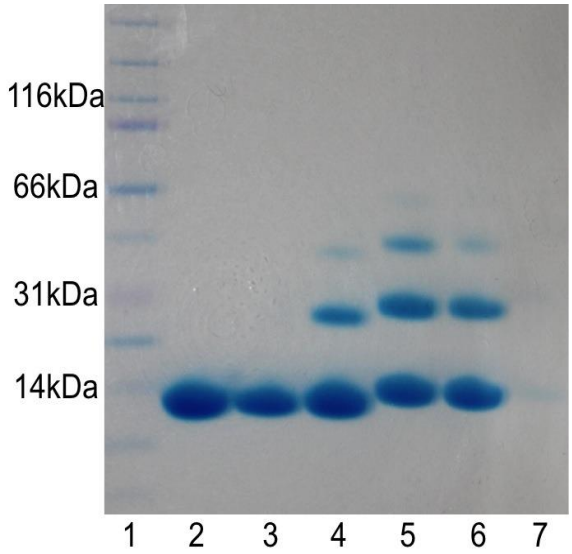

Figure III-5: (Left) MALDI-TOF Characterization of the GLYcidated Lysozyme products. (Above) SDS-PAGE of the GLYcidated LYZ products. LYZ (lane 2), LYZ-OH (lane 3), 4h at 1.33M (lane 4), 24h at 1.33M (lane 5), 24 h at 2.66M (lane 6), LYZ-O-GLY/AGE (lane 7)

The use of PAGE was quantitatively useful to demonstrate the increase in conjugate size with respect to reaction time as well as concentration. Figure III-5 shows lanes with LYZ (lane 2), LYZ-OH (lane 3), a 4h reaction at 1.33M (lane 4), a 24h reaction at 1.33M (lane 5), a 24h reaction at 2.66M (lane 6), and the polymerization of GLY/AGE using the LYZ-OH macroinitiator (lane 7). While the PAGE confirms an increase in size of the conjugates based upon reaction time as

well as concentration, the concentration of the reaction is a more subtle variation that becomes more prevalent upon the acquisition of subsequent measurements.

In order to further investigate the change in mass achieved, MALDI-TOF was employed to obtain quantitative measurements of the polymer that was grown from the surface of the LYZ protein. Figure III-5 illustrates the functionalization that was achieved by attachment of the aldehyde diol and subsequent growth of the glycidol polymer from the surface of the functionalized LYZ protein. The LYZ protein is shown in green while the synthesized macroinitiator appears in blue. The two product species shown are 24h reactions at 1.33M and 2.66M respectively. This data alludes to the fact that the reaction time more directly influences the length of the polyglycerol grown from the surface than does the reaction concentration.

Measurement of Retained Bioactivity

Since LYZ is an antimicrobial protein, the activity of the GLYcidated LYZ products can be measured against *Micrococcus lysodeikticus* (Ml) cells and compared to the activity of the native LYZ protein. As the LYZ conjugates lyse the micrococcus cells, a reduction in absorption at λ=450nm was measured over the course of 3 minutes using UV/Vis Spectroscopy. The results were similar to those seen with PEG systems wherein an increase in molecular mass of the attached polymer structure leads to a reduction in overall protein activity and are illustrated in Figure III-6. The activity values obtained ranged from ~40% down to 3% which, compared to hyperbranched structures of similar molecular mass, are slightly lower than the values seen for hyperbranched polyglycerol.[14] This observation may be due to the formation of multiple polymer chains on the surface of the protein, and is an issue that will be investigated further in hopes of providing systems with higher degrees of activity retention. However, it is hypothesized that, as is the case with PEG

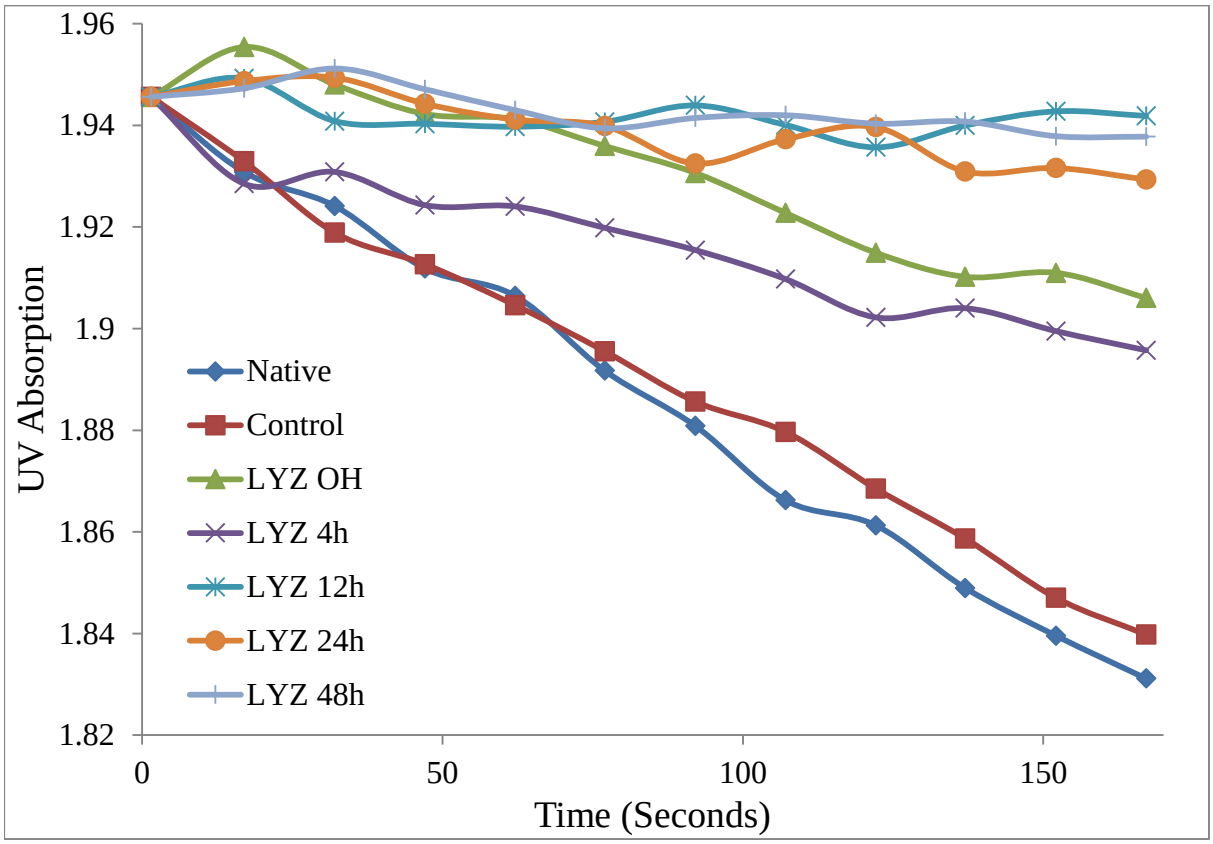

Figure III-6: Bioactivity of the lysozyme-polymer conjugates is measured using Ml cells. As the conjugates lyse the Ml cells, a change in absorbance can be measured using UV-Vis Spectroscopy

structures, this decrease in activity will be greatly overshadowed by an increase in circulation time within the body, thus allowing for an overall increase in the therapeutic ability of the protein.

Conclusion

The research describes the first method developed for the direct functionalization of protein species via a graft-from reaction to form poly(glycidol) based protein-polymer products. This is an exciting new technique providing a facile method for the formation of these species, which opens the door for new and more versatile protein therapeutics. Furthermore, the incorporation of secondary reactive groups affords readily functionalized protein architectures that can be tagged with fluorophores, targeting agents, or incorporated into nanonetworks.

Experimental

Materials

Glycidol (Sigma Aldrich, 96%) was vacuum distilled prior to use. The m-CPBA (77%) was purified as previously reported in the literature. Allyl glycidyl ether (Sigma Aldrich, ≥99%), Phosphate Buffer (Sigma Aldrich), DL-glyceraldehyde (Strem Chemicals Inc., 98%), 2-picoline borane (Sigma Aldrich Inc., 95%), sodium nitrate (Sigma Aldrich Inc., 99%), Lysozyme from chicken egg white lyophilized powder (Sigma Aldrich Inc., 90%), sinapic acid (Sigma Aldrich Inc., 98%), Micrococcus lysodeikticus ATCC No. 4698 lyophilized cells (Sigma Aldrich Inc.), 3-Buten-1-ol (Sigma Aldrich Inc.), tin(II) trifluoromethanesulfonate (Strem Chemicals Inc., 99%), N,N-dimethylformamide (DMF, Sigma Aldrich 99.8%), N,N,N′,N′-ethylenediaminetetraacetic acid (EDTA, Sigma Aldrich, 99.4-100.6%), triethylamine (Sigma Aldrich, ≥99%), bovine serum albumin (BSA, Aldrich, Approx. 99%), 5,5′- dithio-bis-(2-nitrobenzenzoic acid) (Ellman's reagent, Aldrich, 99%), tris(2-carboxyethyl)phosphine hydrochloride (Sigma Aldrich, TCEP, ≥98 %),and 4-nitrophenyl acetate (Fluka, ≥99%) were used as received. Dialysis membranes (SnakeSkin, molecular weight cut-off (MWCO): 10,000 Da) were obtained from Thermo Scientific. Dialysis membranes (Spectra/Por® 7, molecular weight cut-off (MWCO): 25,000 and 50,000 Da) were obtained from Spectrum Laboratories, Inc. Precise Tris-glycine 12% pre-cast PAGE gels were obtained from Fisher Scientific Company.

Characterization

^{1}H and ^{13}C NMR spectroscopy was performed using a Bruker 600 spectrometer operating at 600 and 150 MHz, respectively. The instrument is equipped with a 14.1 Tesla Bruker magnet, which is controlled by a Bruker AV-II console, and a 5mm Z-gradient TCI Cryo-probe. A 20 second recycle delay was used to insure full relaxation for quantitative measurements, which allowed for

the elucidation of specific monomer unit peaks and subsequent calculation of the degree of branching present in each glycidol homopolymer. MALDI measurements were accomplished using a Voyager DE-STR MS in linear TOF mode equipped with a nitrogen gas laser at λ= 337nm with external calibration. The individual instrument parameters varied based on the samples being characterized. PAGE measurements were accomplished using an Invitrogen x-cell electrophoresis system from Life Technologies. 12% Precise Tris-glycine gels from Thermo Scientific were used for BSA conjugates. Novex NuPage 4-12% Bis-Tris gels were used for LYZ Conjugates. The gels were then removed from their cartridges and washed three times with DI water, with one 30 minute water soak, before being stained with Coomassie Blue gel stain. Gels were then stored in DI water. Size exclusion measurements were obtained with a Waters chromatograph system equipped with a Waters 2414 refractive index detector, a Waters 1525 binary HPLC pump, and four 5 mm Waters columns (300 mm x 7.7 mm), connected in series with increasing pore size (100, 1000, 100,000 and 1,000,000 Å respectively). All runs were performed with N-N-dimethylformamide (DMF) as the eluent at a flow rate of 1 mL/min. Ultraviolent/Visible spectroscopy data was obtained using an Agilent 8453 UV/Vis spectrometer with a photodiode array detector. Kinetic measurements were obtained by collecting the absorbance at 450nm every 15s for 3 minutes.

Conjugation of BSA with Maleimide Alcohol to obtain BSA Alcohol Conjugate

BSA (0.5g, 7.5 μmol, 1 eq) was dissolved in phosphate buffer (PB) solution (37.5mL, pH 7.2) in a 100mL round bottom flask equipped with a magnetic stir bar and was then purged under N_2(g) for 1h. 1-(2-hydroxyethyl)-1H-pyrrole-2,5-dione (21.23mg; $6x10^{-5}$ mol; 20 eq) was solubilized in nitrogen-purged DMF (2.5mL). The maleimide solution was then added dropwise to the stirring BSA solution and the reaction was allowed to run for 20h @ 25°C. The resulting reaction mixture

was dialyzed against deionized (DI) water for 36h using a MWCO of 25,000 Da, and then lyophilized to isolate the BSA Alcohol Conjugate (BSA-OH). Yield: 32.7mg (79.2%)

General Procedure for the Polymerization of GLY using BSA-OH in different Solvent Systems

$Sn(OTf)_2$ (0.87mg, 2.1μmol), BSA-OH (80mg, 1.2μmol), and DMF (3.6mL) were added to a 25mL round bottom flask equipped with a magnetic stir bar and purged with N_2(g) for 30 minutes in an ice bath. The glycidol monomer (79.4μL, 1.19mmol) was then added by syringe and the reaction was allowed to run for 24h at 25°C. The resulting reaction mixture was dialyzed against DI water for 36h using a MWCO of 25,000 Da, and then lyophilized to isolate the BSA Glycidol Conjugate (BSA-GLY).

This reaction was repeated with the DMF replaced with either PB (pH=6.0; no Sn catalyst) or DMSO in order to ascertain the optimal reaction conditions. The products obtained from these three solvent systems were visibly different with a seeming decrease in solubility in the trend: PB>DMF>DMSO. However, apart from this caveat, the reaction procedure remained unchanged.

Polymerization of GLY/AGE using BSA-OH

This procedure was modified from an earlier reported procedure. BSA (1g, 15.1μmol), and PB pH 6.0 (46.8mL) were added to a 100mL round bottom flask equipped with a magnetic stir bar and purged with N_2(g) for 30 minutes in an ice bath. The GLY (15.1mmol, 1.03mL) and AGE (15.1mmol, 1.79mL) was then added by syringe and the reaction was allowed to run for 24h at 25°C. The resulting reaction mixture was dialyzed against DI water for 36h using a MWCO of 10,000 Da, and then lyophilized to isolate the BSA GLY/AGE Conjugate (BSA-GLY/AGE). Yield: 27.4mg (84.1%). Relevant ^{1}H-NMR peaks at 5.86 , 5.23 , 3.57, show inclusion of AGE into the polymer backbone attached to the BSA protein.

PAGE Characterization of BSA-Polymer Conjugates

PAGE was accomplished using an Invitrogen Novex Mini-Cell system. Precast 12% Precise™ Protein Gels (Thermo Scientific) were run at 100V and 120mA for 1.75 hours. Solutions were prepared with a BSA concentration of 6g/L in DI water. PAGE samples were formed by mixing 7.5μL of BSA solution with 2.5μL 4x LDS sample buffer (Invitrogen) before loading the 10μL solutions onto the gel plate. Staining of the gels was accomplished using Coomassie Blue.

MALDI Characterization of BSA Based Bioconjugates

MALDI-TOF MS was employed to confirm the addition of the maleimide alcohol initiator to the BSA protein and the subsequent glycidol polymer growth from the BSA-OH conjugate. The MALDI samples were formed using 6mg/mL product samples in DI water and a 5mg/mL matrix solution of sinapic acid dissolved in 2 parts 0.1% formic acid, 1 part acetonitrile. The sample and matrix were mixed in a 1:1 ratio and 1.4μL was spotted onto the MALDI plate for characterization. The instrument parameters were set to: 25,000V; 90% grid; 600ns delay; 1000 shots per spectrum.

Determination of BSA-Polymer Conjugates Bioactivity

The bioactivity of the synthesized BSA-OH conjugates and subsequent polymer coated species was determined and compared to the native BSA protein by measuring the absorbance related to the hydrolysis product with 4-nitrophenyl acetate. Sample preparation was performed by combining a BSA or BSA conjugate solution (50μL, [BSA]=0.27mM) in PB (pH=8.0) with a 10mM solution of 4-nitrophenyl acetate dissolved in acetonitrile (10μL) and PB (0.94mL, pH=8.0) and centrifuging the samples for 5 minutes at 6,000 rpm. The samples were allowed to incubate for 30 minutes at room temperature before measuring the absorbance at λ= 405nm to determine the bioactivity of each sample.

Circular Dichroism

The use of CD spectrophotometry was employed to verify the retention of the secondary structure of the BSA protein. Spectra were obtained with a Jasco J-720 at 25 ± 1 °C in DI water ($1.5x10^{-5}$ M) in a cell with a path length of 1cm (bandwidth=1 nm; step resolution = 0.5 nm; scan speed = 50nm/min; response time = 0.5s). Spectral data was collected from 190-275 nm to ascertain information about the a-helix structure of the BSA protein as well as the structure of the BSA conjugates formed.

Conjugation of LYZ with Aldehyde Diol to Obtain LYZ Alcohol Initiator

In a 500mL RBF, equipped with stir bar, was added DL-glyceraldehyde (6.3mg; 70µmol) along with 50mM $NaNO_3$ (250mL). Lysozyme (1.0g; 70µmol) was solubilized in a minimal amount of 50mM $NaNO_3$ solution and added dropwise to the stirring reaction. After 1h, the 2-picoline borane complex (150mg; 1.4mmol) was added proportionally and the reaction was allowed to stir overnight. The product solution was then placed in dialysis tubing (SnakeSkin; 10,000 MWCO) and dialyzed against 50mM $NaNO_3$ solution for 72 hours. The product was then lyophilized to afford the pure LYZ-OH product. Yield: 767.4 mg (76.7%)

Polymerization of GLY using LYZ-OH

LYZ-OH (200mg; 14µmol), and PB (pH 6.0; 42.1mL) were added to a 100mL RBF equipped with a stir bar. The glycidol monomer (4.14g; 56mmol) was then added by syringe and the reaction was allowed to run for 24h at 25°C. The resulting reaction mixture was dialyzed against DI water for 36h using a MWCO of 10,000 Da, and then lyophilized to isolate the LYZ-Glycidol Conjugate (LYZ-GLY). Yield: 26.2mg (83.4%)

Polymerization of GLY/AGE using LYZ-OH

LYZ-OH (112mg; 7.8μmol), and PB (pH 6.0; 42.1mL) were added to a 100mL RBF equipped with a stir bar. The glycidol monomer (2.31g; 31.3mmol) and allyl glycidyl ether monomer (3.57g; 31.3mmol) were then added by syringe and the reaction was allowed to run for 24h at 25°C. The resulting reaction mixture was dialyzed against DI water for 36h using a MWCO of 10,000 Da, and then lyophilized to isolate the LYZ-Glycidol Conjugate (LYZ-GLY). Yield: 17.4mg (55.8%)

PAGE Characterization of LYZ-Polymer Conjugates

PAGE was accomplished using an Invitrogen Novex Mini-Cell system. Precast 12% Precise™ Protein Gels (Thermo Scientific) were run at 100V and 120mA for 1.75 hours. Solutions were prepared with a LYZ concentration of 6g/L in DI water. PAGE samples were formed by mixing 7.5μL of BSA solution with 2.5μL 4x LDS sample buffer (Invitrogen) before loading the 10μL solutions onto the gel plate. Staining of the gels was accomplished using Coomassie Blue.

MALDI Characterization of LYZ Based Bioconjugates

MALDI-TOF MS was employed to confirm the addition of the DL-glyceraldehyde diol initiator to the LYZ protein and the subsequent glycidol polymer growth from the LYZ-OH conjugate. The MALDI samples were formed using 6mg/mL product samples in DI water and a 5mg/mL matrix solution of sinapic acid dissolved in 2 parts 0.1% formic acid, 1 part acetonitrile. The sample and matrix were mixed in a 1:1 ratio, and 1.4μL was spotted onto the MALDI plate for characterization. The instrument parameters were set to: 25,000V; 90% grid; 500ns delay; 500 shots per spectrum.

Determination of the LYZ-Polymer Conjugates Bioactivity

A suspension of M1 cells (19.4mg) was formed in PBS buffer solution (90mL, pH 7.0), while lysozyme solutions were formed (1.0 mg/mL in PBS buffer, pH 6.5). In order to measure the

bioactivity, a small aliquot of the lysozyme solution (5.0µL) was transferred to a blanked cuvette. The M1 cell suspension (3.0mL) was then added to the cuvette, and a kinetic UV-Vis measurement was performed by measuring the absorbance at wavelength 450nm every 15s for 3 min.

References

1. Parveen, S., and Sahoo, S. (2014) Long circulating chitosan/PEG blended PLGA nanoparticle for tumor drug delivery (vol 670, pg 372, 2011), *European Journal of Pharmacology 727*, 186-186.
2. Alconcel, S. N. S., Baas, A. S., and Maynard, H. D. (2011) FDA-approved poly(ethylene glycol)-protein conjugate drugs, *Polymer Chemistry 2*, 1442-1448.
3. Niidome, T., Yamagata, M., Okamoto, Y., Akiyama, Y., Takahashi, H., Kawano, T., Katayama, Y., and Niidome, Y. (2006) PEG-modified gold nanorods with a stealth character for in vivo applications, *Journal of Controlled Release 114*, 343-347.
4. Vine, K., Lobov, S., Chandran, V., Harris, N., and Ranson, M. (2015) Improved Pharmacokinetic and Biodistribution Properties of the Selective Urokinase Inhibitor PAI-2 (SerpinB2) by Site-Specific PEGylation: Implications for Drug Delivery, *Pharmaceutical Research 32*, 1045-1054.
5. Fam, C., Eisenberg, S., Carlson, S., Chlipala, E., Cox, G., and Rosendahl, M. (2014) PEGylation Improves the Pharmacokinetic Properties and Ability of Interferon Gamma to Inhibit Growth of a Human Tumor Xenograft in Athymic Mice, *Journal of Interferon and Cytokine Research 34*, 759-768.

6. Styslinger, T., Zhang, N., Bhatt, V., Pettit, N., Palmer, A., and Wang, P. (2012) Site-Selective Glycosylation of Hemoglobin with Variable Molecular Weight Oligosaccharides: Potential Alternative to PEGylation, *Journal of the American Chemical Society 134*, 7507-7515.

7. Pelegri-O'Day, E., Lin, E., and Maynard, H. (2014) Therapeutic Protein-Polymer Conjugates: Advancing Beyond PEGylation, *Journal of the American Chemical Society 136*, 14323-14332.

8. Mero, A., Pasut, G., Via, L., Fijten, M., Schubert, U., Hoogenboom, R., and Veronese, F. (2008) Synthesis and characterization of poly(2-ethyl 2-oxazoline)-conjugates with proteins and drugs: Suitable alternatives to PEG-conjugates?, *Journal of Controlled Release 125*, 87-95.

9. Spears, B. R., Waksal, J., McQuade, C., Lanier, L., and Harth, E. (2013) Controlled branching of polyglycidol and formation of protein-glycidol bioconjugates *via* a graft-from approach with "PEG-like" arms, *Chemical Communications 49*, 2394-2396.

10. Shakya, A., Sami, H., Srivastava, A., and Kumar, A. (2010) Stability of responsive polymer-protein bioconjugates, *Progress in Polymer Science 35*, 459-486.

11. Wan, X., Zhang, G., Ge, Z., Narain, R., and Liu, S. (2011) Construction of Polymer-Protein Bioconjugates with Varying Chain Topologies: Polymer Molecular Weight and Steric Hindrance Effects, *Chemistry-an Asian Journal 6*, 2835-2845.

12. Li, M., De, P., Gondi, S., and Sumerlin, B. (2008) Responsive polymer-protein bioconjugates prepared by RAFT polymerization and copper-catalyzed azide-alkyne click chemistry, *Macromolecular Rapid Communications 29*, 1172-1176.

13. Dimitrov, D. S. (2012) *Therapeutic Proteins*, *Methods of Molecular Biology 899*, 1-26

14. Wurm, F., Dingels, C., Frey, H., and Klok, H.-A. (2012) Squaric Acid Mediated Synthesis and Biological Activity of a Library of Linear and Hyperbranched Poly(Glycerol)-Protein Conjugates, *Biomacromolecules 13*, 1161-1171.

15. Wilms, D., Stiriba, S. E., and Frey, H. (2010) Hyperbranched Polyglycerols: From the Controlled Synthesis of Biocompatible Polyether Polyols to Multipurpose Applications, *Accounts of Chemical Research 43*, 129-141.

16. Sunder, A., Hanselmann, R., Frey, H., and Mulhaupt, R. (1999) Controlled synthesis of hyperbranched polyglycerols by ring-opening multibranching polymerization, *Macromolecules 32*, 4240-4246.

17. Sunder, A., Turk, H., Haag, R., and Frey, H. (2000) Copolymers of glycidol and glycidyl ethers: Design of branched polyether polyols by combination of latent cyclic AB(2) and ABR monomers, *Macromolecules 33*, 7682-7692.

18. Sunder, A., Frey, H., and Mulhaupt, R. (2000) Hyperbranched polyglycerols by ring-opening multibranching polymerization, *Macromolecular Symposia 153*, 187-196.

19. Wilms, D., Schomer, M., Wurm, F., Hermanns, M. I., Kirkpatrick, C. J., and Frey, H. (2010) Hyperbranched PEG by Random Copolymerization of Ethylene Oxide and Glycidol, *Macromolecular Rapid Communications 31*, 1811-1815.

CHAPTER IV

NANOSCALE NETWORK FORMATION

Introduction

The realm of medicinal chemistry is full of highly efficacious small molecule drugs. Unfortunately, this high degree of effectiveness is often accompanied by a low degree of solubility and/or permeability[1-4]. This unfavorable combination means that the majority of these drug molecules can never be employed directly to combat the diseases they were synthesized to cure. Due to these facts, a good amount of polymer research has been focused on the development of drug delivery platforms capable of imparting the necessary solubility to hitherto unused drug molecules[5-8]. Furthermore, research in the polymer nanoparticle field has endeavored to create delivery vehicles capable of sustaining the release of their cargo over an extended period of time in order to decrease the time patients spend with their doctors, and increase the patients' quality of life. The goal tying all this research together is the development of a facile fabrication method yielding a platform capable of providing a single therapeutic dose of a highly efficacious drug by imparting solubility and extended release of the desired therapeutic[5, 7, 9-12].

Current research in the field of nanoparticle drug delivery focuses mainly on the development of a single delivery vehicle with minimal adjustability in drug delivery rate or cargo specificity. Drug release from such platforms is often very fast at first, a burst effect, followed by the complete clearance of the payload within the first 48 hours. Nanoparticles formed through emulsion reactions, often from the utilization of block copolymer building blocks, afford products with definable size and release rate, but these characteristics rely heavily on the type of copolymer and surfactant used, and allow little ability for tuning without large changes to the reaction

parameters[1, 2, 13-15]. Similar structures can be easily developed using micelle based delivery systems, but again these platforms suffer from rapid delivery of their therapeutic cargo[3, 11, 16, 17]. In order to combat these shortcomings, a number of platforms have focused on the formation of prodrug based delivery wherein the desired therapeutic is covalently attached to the polymer structure and can be released in the presence of a predetermined stimuli.[18-20]. Unfortunately, this method is not well adapted for broad application, and thus the door is open for a delivery vehicle capable of sustained release of therapeutics with minimal limitations based upon cargo and highly tunable parameters based on polymer characteristics.

While the majority of nanoparticle fabrication relies heavily on self-assembly, the ability to direct the formation of nanoparticle structures through covalent bonding allows for the introduction of an easily tunable characteristic. Furthermore, by altering the degree of crosslinking one can easily change the density of the formed structure and impart varying release kinetics to the delivery vehicle. For these reasons it was decided that polymeric nanoparticles would be synthesized from two separate polymer species. First, a linear poly(ester) based polymer will be used to form semi-hydrophobic structures for the delivery of highly hydrophobic cargo. Second, a branched poly(glycidol) based polymer will be employed to form hydrophilic delivery vehicles for the purpose of biological cargo delivery. These two systems will utilize the thiolene-click reaction for nanoparticle formation and will be directly compared to investigate the level of control possible over the size of the formed nanoparticles.

Results and Discussion

Synthesis of Monomer Building Blocks

The utilization of thiolene-click chemistry for nanoparticle formation necessitates the presences of allyl functionality within the backbone of the synthesized polymer products.

However, such monomers are not always easily purchased. Therefore, a number of monomer units for the proposed research were synthesized in order to impart variable hydrophilicity as well as the necessary allyl functionality. For the hydrolytically degradable poly(ester) system, monomers previously described in the literature were chosen, while for the poly(glycidol) system a novel monomer was synthesized.

Synthesis of an Allyl Functionalized Lactone

The ability of lactones to undergo ring opening polymerization for the formation of linear poly(ester) structures has been described previously in the literature[4, 6, 21-23]. Furthermore, it has been shown that the introduction of an allyl functionality to the ring structure can be easily facilitated to afford an allyl functionalized random copolymer capable of undergoing secondary modification or direct utilization, via thiolene-click chemistry, as a nanoparticle building block. For this reason it is necessary to synthesize the desired α-allyl-δ-valerolactone monomer species. The method chosen, described previously in the literature, involved the activation of the lactone ring with diisopropylamine and n-butyl lithium followed by the addition of the desired allyl functionality through reaction of the activated ring with allyl bromide[21].

Synthesis of an Ester Monomer with Increased Hydrophilic Potential

Though the poly(ester) polymer structure is hydrolytically degradable, the polymer suffers from low solubility. In an effort to combat this undesirable characteristic it was decided that 2-oxepane-1,5-dione would be added as a comonomer in the poly(ester) synthesis. This monomer introduces a keto group into the backbone of the polymer with each incorporated monomer unit, facilitating an increase in hydrophilicity while maintaining the desired ester moiety. This monomer was formed as previously described in the literature, and is synthesized by the reaction between

1,4-cyclohexanedione and purified meta-chloroperoxybenzoic acid, leading to the insertion of an oxygen adjacent to one of the ketones on the ring[23].

Synthesis of Novel Allyl Glycidyl Ester Monomers

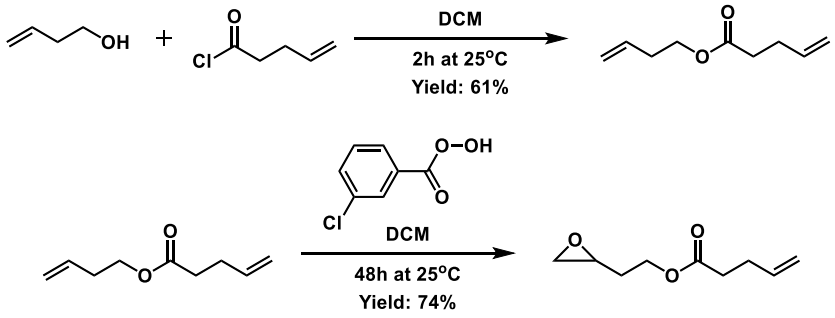

Figure IV-1: Synthesis of a novel glycidol based monomer unit

In the case of glycidol based monomers, there is a readily available allyl functionalized monomer, allyl glycidyl ether, which can afford poly(glycidol) based copolymers with the desired allyl functionality. However, as the goal of this project is to create a biologically degradable drug delivery vehicle, a monomer was needed that would not only impart the desired allyl functionality but also introduce an easily cleavable moiety, such as an ester. For this reason a novel monomer species was synthesized to combine their desired regions: an epoxide for rapid ring opening, an ester for inherent degradability, and an allyl for secondary utilization for crosslinking and nanoparticle formation. This monomer was successfully formed using a two-step process (See Figure IV-1). First, allyl alcohol was reacted with 4-pentenoyl chloride under dry conditions to afford a diallyl species with an ester in the middle. Subsequently, this product was treated with 1 molar equivalent of m-CPBA to facilitate the epoxidation of a single allyl species. The resultant glycidyl ester allyl monomer unit successfully incorporated the three desired regions and was utilized as a comonomer for the synthesis of functionalized poly(glycidol) polymers.

Synthesis of Polymer Building Blocks

Allyl Functionalized Poly(ester) Polymers

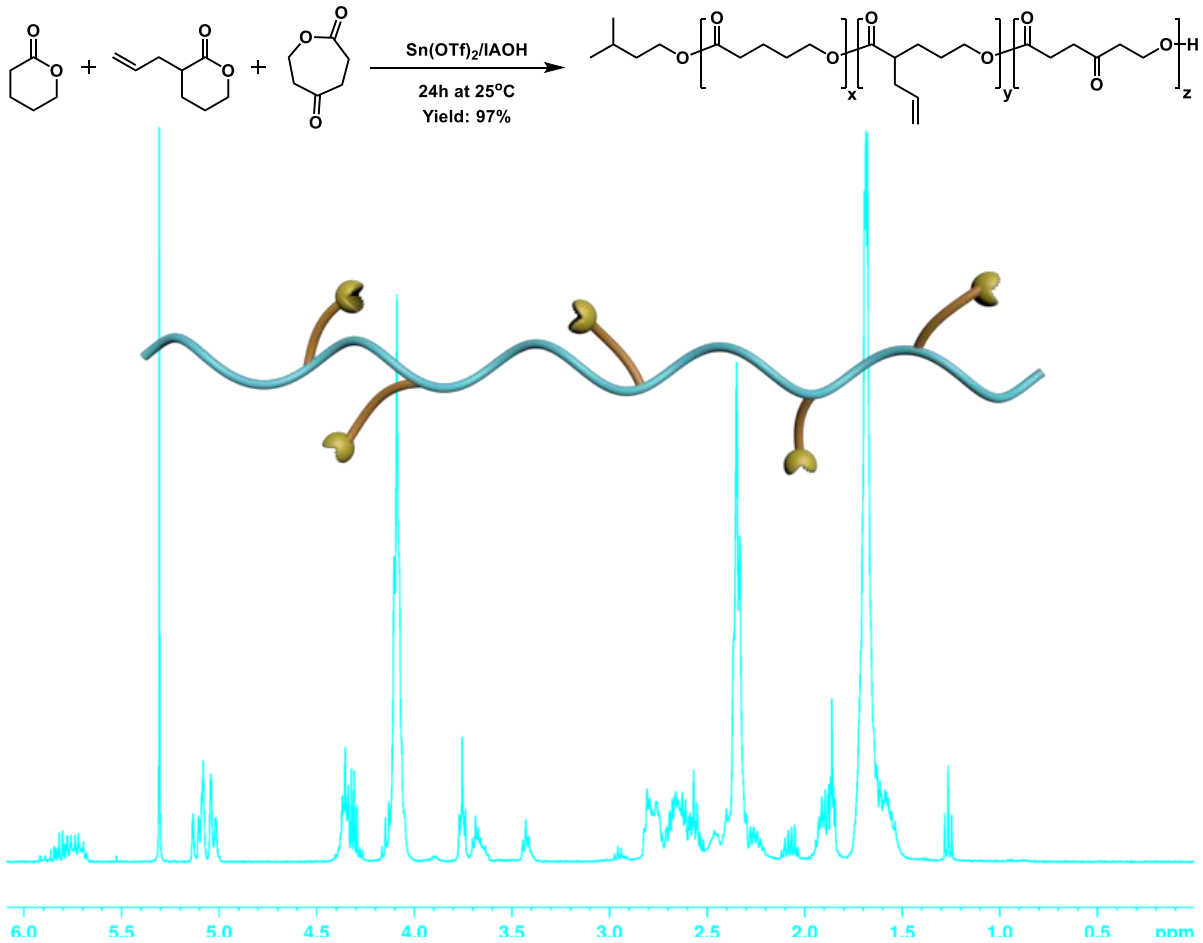

Figure IV-2: Synthesis of the poly(ester) building block with allyl functionality and increased hydrophilicity

The allyl functionalized polymer products were synthesized similarly to those described previously, with the caveat that the oxepane-2-dione monomer was added at varying percentages to produce products of variable hydrophilic character (See Figure IV-2). The polymerization was performed in bulk conditions utilizing $Sn(OTf)_2$ as a catalyst and isoamyl alcohol as the ring opening initiator. Random copolymers were obtained after 24 hours and characterized using ^1H NMR and GPC measurements. The ability to incorporate variable amounts of both AVL and OPD

means that the synthesized polymers contain a range of crosslinking and hydrophilic character, allowing for numerous particle formulations. The ability to tune the crosslinking density of the formed nanoparticles is very important as this characteristic has been shown to dictate the release rate of the loaded therapeutic cargo.

Allyl Functionalized Poly(glycidol) Polymers

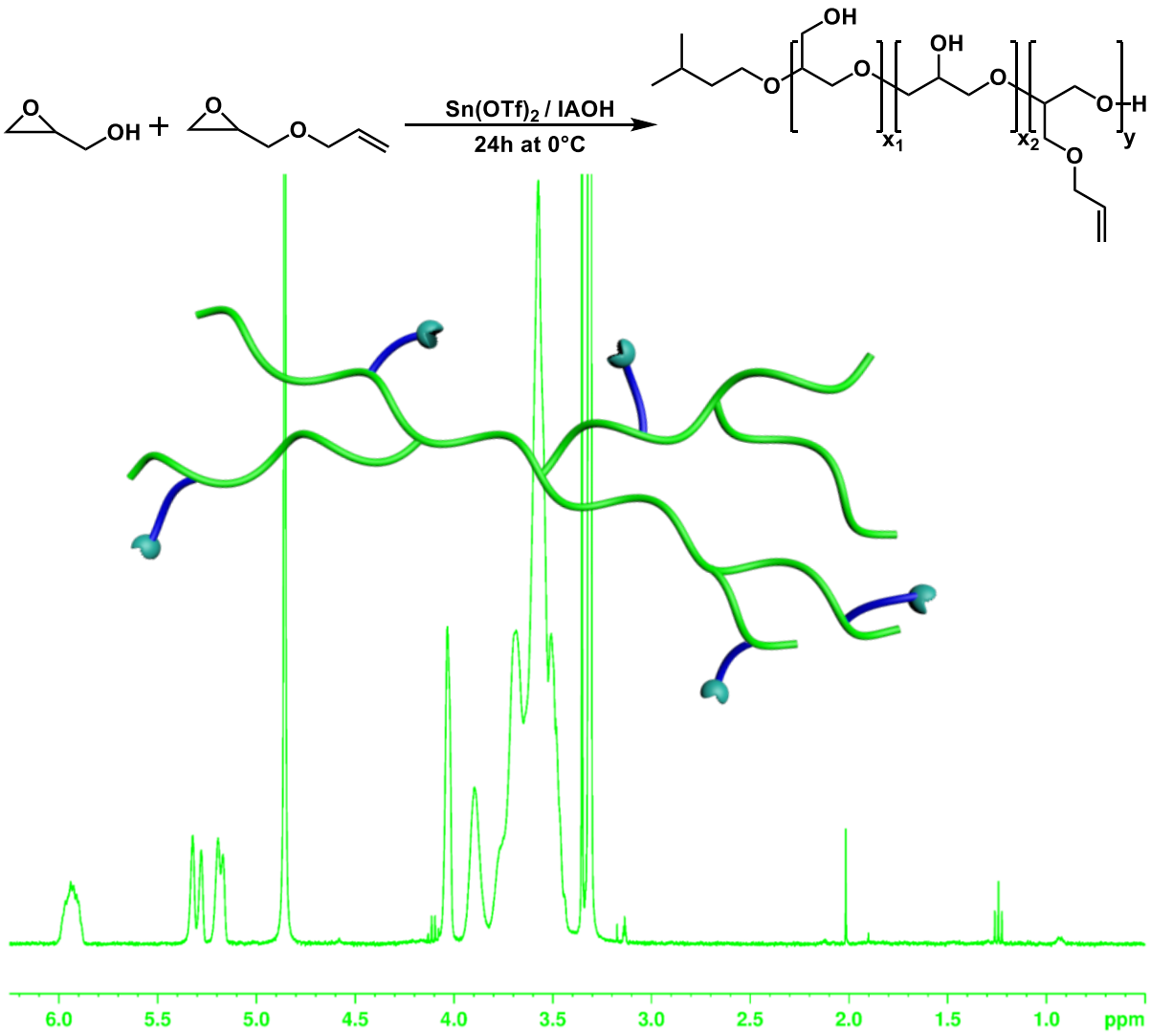

Figure IV-3: Synthesis of the poly(glycidol) building block with allyl functionality

Though the synthesis of glycidol polymers has been a topic of research for many years, the post-modification of the polymer systems in order to afford structures with enhanced reaction

capability is a fledgling field of study[24-28]. The majority of previously synthesized structures have been used directly for applications such as biomineralization, solid phase catalysis, etc.,[18, 27, 29, 30] and few researchers have sought to fundamentally change the composition of these glycidol structures. However, the advantages of the formation of functionalized glycidol polymers are vast and attracted our interest in the hopes of expanding the usefulness of the glycidol based polymers. A range of post-modification reactions, as well as the implementation of glycidol derivatives, were considered with numerous end goals for the proposed products. These included the introduction of ester functionalities to impart hydrolytic degradability, as well as the addition of either allyl or primary thiol moieties for intra and intermolecular interactions. The ester functionalities allow for a polymer system capable of hydrolytic release of bound molecules, be these other polymer chains in the case of nanoparticle formation, or therapeutic cargo. As this ester functionality yields a desired characteristic, allyl and thiol containing molecules were chosen that afforded functionalized polymers with both the ester and desired allyl or thiol moiety.

Utilization of Functional Monomer Units

Allyl functionalized poly(glycidol) precursors were formed using both the available allyl glycidyl ether monomer (See Figure IV-3) and the newly synthesized glycidyl ester allyl. Furthermore, a range of allyl percentages were formed in order to facilitate the synthesis of nanoparticles with variable crosslinking densities. The polymerization reaction was similar to that utilized for the poly(ester) systems, though the allyl monomer was added prior to the addition of the glycidol monomer due to the relative difference in reaction rate, with glycidol being a highly reactive species. Random copolymers were obtained after 16 hours and using ^{1}H NMR and GPC measurements. The resulting polymers showed good incorporation, though the GEA monomer was

not incorporated at the same level as the AGE monomer, with 7% and 13% allyl incorporation achieved, respectively, when attempting 20% allyl incorporation.

Secondary Functionalization of Poly(glycidol) Homopolymers

In the formation of the GEA monomer, 4-pentenoyl chloride is used to form the DAE intermediate molecule. It stands to reason that the acid chloride would rapidly react with the pendant hydroxyl groups on the glycidol polymer structure. This theory was tested through a neat reaction with the glycidol polymer, acid chloride, and pyridine as a base to scavenge the HCl byproduct. The synthesis route afforded polymer systems with predictable allyl functionalization and ester incorporation.

In order to incorporate the desired thiol functionalization, the previously synthesized DSL molecule was utilized.[31] As this molecule contains a carboxylic acid rather than an acid chloride, the DSL was treated first with thionyl chloride to afford the acid chloride derivative DSL-Cl. This product was then used to functionalize the glycidol polymer backbone in a method similar to that used for 4-pentenoyl chloride. The purification of the synthesized product proved to be more difficult than expected but was accomplished through the implementation of HPLC separation. This afforded the functionalized glycidol product with both ester incorporation and a readily cleavable dithiol species.

Structural Comparison Between Poly(ester) and Poly(glycidol) Nanosponges

In order to investigate the inherent differences conferred on the nanoparticle structures based upon the polymers chosen for their creation, a number of nanosponges were formed. All reactions use thiolene-click reactions to facilitate the rapid reaction between the free thiols of the PEG crosslinker and the pendant allyl functionalities on the synthesized polymer species. The nanosponge formation is accomplished by solubilizing the synthesized polymers with a PEG

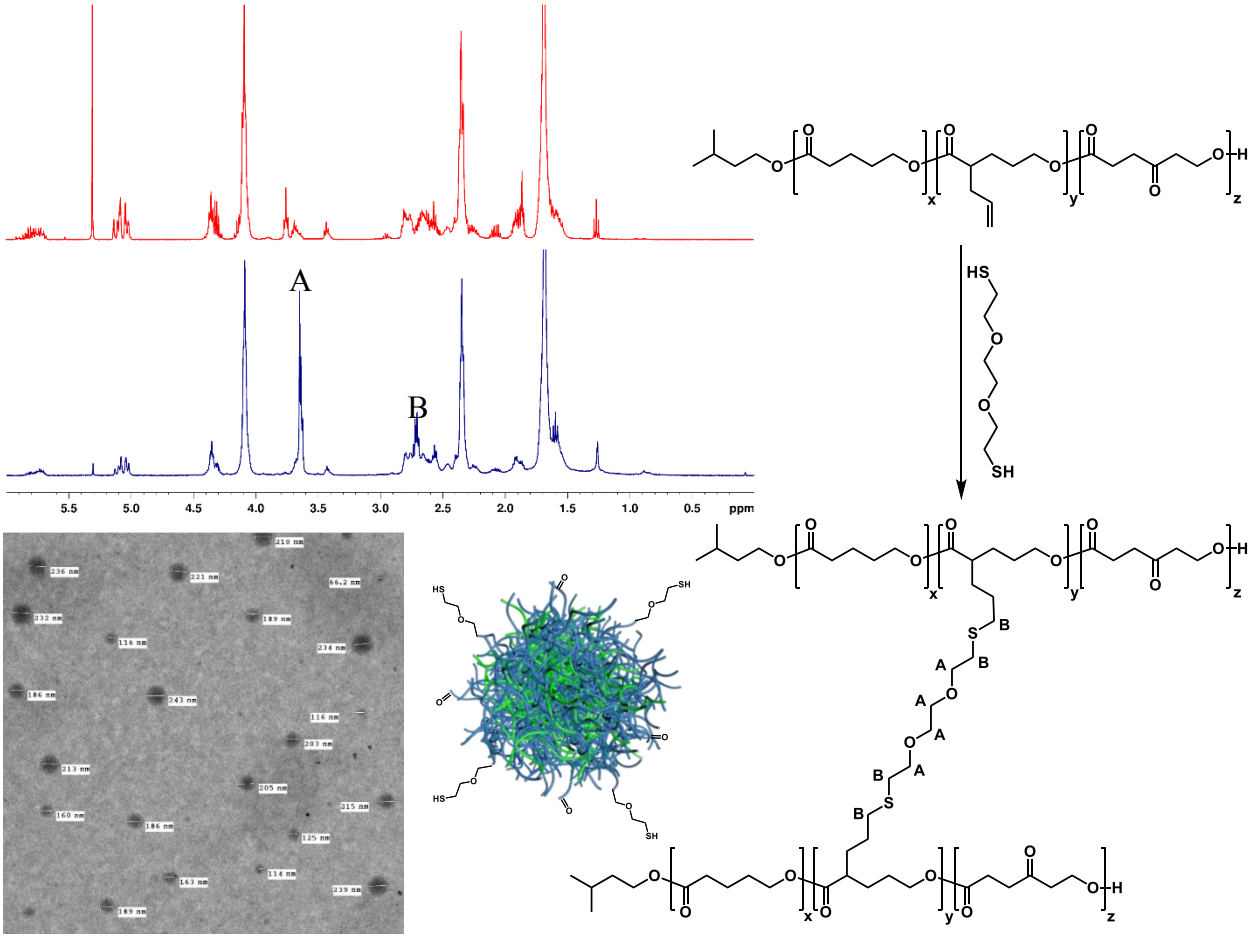

Figure IV-4: Synthesis and characterization of the poly(ester) based nanoparticle structure

spaced dithiol crosslinker and subsequently refluxing the solution for 12 hours to allow the thiolene-click reaction to covalently bond the polymers together. For the poly(ester) systems this was accomplished in dichloromethane, while the poly(glycidol) systems were formed in methanol. To fully investigate the relative influence that crosslinking density has on the synthesized particles, a range of cross linking equivalents and allyl percentages was studied. This investigation showed that the use of different molar equivalents of cross linker causes a shift in the size of the particles formed, with the smallest particle species coming when there is a 1:1 relationship between allyl and thiol. When comparing the two separate polymer based particles however, it was interesting to see that polymers with similar allyl incorporation and the same molar equivalents of crosslinker yielded particles of disparate sizes, with smaller particles formed from the poly(glycidol) based

systems. However, the poly(ether) systems tended to form particle structures with lower size disparity, which is a logical occurrence since the poly(glycidol) structures are branched and less

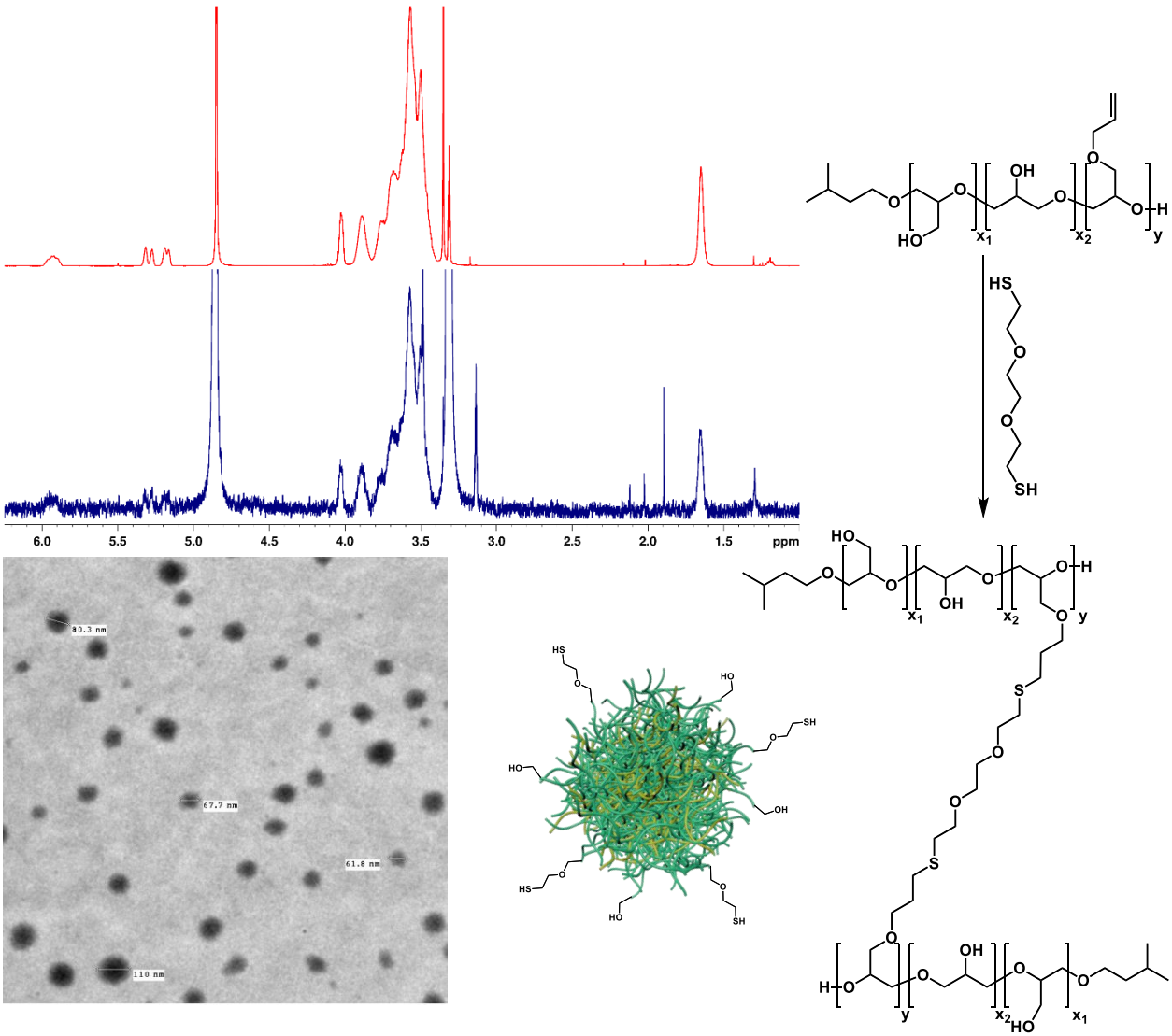

Figure IV-5: Synthesis and characterization of the poly(glycidol) based nanoparticle structure able to form consistent interactions between the polymer chains.

Loading of Poly(ester) Nanosponges with Therapeutic Cargo

The ability to load a small molecule therapeutic into the formed nanosponge networks is paramount to their ability to be utilized as drug delivery vehicles. Furthermore, it is desirable to load therapeutics with specific thoughts in mind as to the desired delivery method. Building on

previous work in the lab that sought to shuttle brimonidine across the optic nerve, bypassing the blood brain barrier, the synthesized poly(ester) nanosponges were loaded with temozolomide, a brain cancer therapeutic with notoriously low bioavailability. As the desired delivery method involved deposition of the drug loaded particles to the region adjacent to the optic nerve, larger particles were chosen for their ability to carry more of the temozolomide molecule. The drug was loaded into the nanosponge structure as previously described, and successful incorporation of the drug was determined using UV/Vis.

Conclusion

In summary, we have successfully shown that nanoparticles can be formed from both poly(ester) and poly(glycidol) based starting materials. Work with the poly(ester) nanoparticle platform has been accomplished previously in the lab. However, the research in this section represents the first successful formation of poly(glycidol) based nanoparticles using similar reaction conditions as those utilized for the poly(ester) system. The pendant allyl groups on the back of both polymer systems were utilized for the successful crosslinking of the particles using a dithiol molecule in order to form nanoparticle products. Furthermore, these nanoparticles were formed at different sizes by using varying crosslinking densities and amount of allyl functionality available. This exciting discovery opens the door for the utilization of these novel nanosponge architectures as delivery platforms for therapeutic cargo.

Experimental

Materials

All reagent chemicals were purchased from Sigma-Aldrich, Strem Chemicals, or Acros and used as received unless otherwise noted. The m-CPBA (77%) was purified as previously reported in the literature while δ-valerolactone and glycidol was further purified through vacuum distillation.

SnakeSkin® Pleated Dialysis Tubing, regenerated cellulose, was purchased from Pierce Biotechnology. Spectra/Por® Dialysis membrane was purchased from Spectrum Laboratories Inc. α-allyl-δ-valerolactone, α-propargyl-δ-valerolactone, and 2-oxepane- 1,5-dione were synthesized as previously reported in the literature.

Characterization

^{1}H and ^{13}C NMR were obtained from a Bruker AV-I 400 MHz, a Bruker DRX 500 MHz, or a Bruker AV-II 600 MHz spectrometer. The reported chemical shifts are in ppm and are in reference to the corresponding residual nuclei in deuterated solvents. Gel-permeation chromatography (GPC) was carried out with a Waters chromatograph system equipped with a Waters 2414 refractive index detector, a Waters 2481 dual λ absorbance detector, a Waters 1525 binary HPLC pump, and four 5 mm Waters columns (300 mm x 7.7 mm), connected in series with increasing pore size (100, 1000, 100,000 and 1,000,000 Å respectively). All runs were performed with N-N-dimethylformamide (DMF) as the eluent at a flow rate of 1 mL/min. Samples for transmission electron microscopy (TEM) imaging were prepared by dissolving 0.5 mg nanoparticles in 1 mL isopropanol, 0.3 mL acetonitrile and 0.2 mL toluene. The samples were sonicated for 5 min and were stained with 3 drops of 3% phosphotungstic acid. The carbon grids were prepared by slowly dipping an Ultrathin Carbon Type-A 400 Mesh Copper Grid (Ted Pella, Inc., Redding, CA) into the particle solutions three times and drying the grid at ambient temperature. A Philips CM20T transmission electron microscope operating at 200 kV in bright-field mode was used to obtain TEM micrographs of the polymeric nanoparticles.

Synthesis of α-allyl-δ-valerolactone (AVL)

This reaction was performed as previously described in the literature with the use of vacuum distilled δ-valerolactone (VL) rather than using the purchased purity. ^{1}H-NMR (400MHz, $CDCl_3$)

δ: 5.80 (1H, m, CH) 5.04 (2H, m, CH_2), 4.27 (2H, m, CH_2), 2.42 (2H, m, CH_2, CH), 2.18 (1H, m, CH_2), 2.00-1.72 (4H, m, CH_2). ^{13}C-NMR (100MHz, $CDCl_3$) δ: 173.98, 135.03, 117.54, 68.84, 39.13, 35.42, 22.13, 21.05.

Synthesis of 2-oxepane-1,5-dione (OPD)

This reaction was performed as previously described in literature with the use of purified m-CPBA rather than using the purchased purity. ^{1}H-NMR (400MHz, $CDCl_3$) δ: 4.36 (2H, t, CH_2), 2.76 (2H, m, CH_2), 2.65 (2H, m, CH_2), 2.59 (2H, m, CH_2). ^{13}C-NMR (125MHz, $CDCl_3$) δ: 205.14, 173.57, 63.74, 44.86, 38.94, 28.31.

Synthesis of Diallyl Ester

To a round bottom flask equipped with a stir bar, was added 3-buten-1-ol (3.27g; 45.3 mmol; 1.0 eq) and DCM (25mL; excess). A diluted solution of 4-pentenoyl chloride (5.37g; 45.3 mmol; 1.0 eq) and DCM (25mL; excess) was created in an addition funnel. The 4-pentenoyl chloride solution was then added drop wise to the stirring reaction mixture over 30 minutes and the reaction was allowed to run for 3h until TLC indicated the reaction was complete. The excess solvent was then removed on the rotary evaporator to afford the crude product. The resulting crude liquid product was purified using flash chromatography to yield the pure clear liquid product. ^{1}H-NMR (500MHz, $CDCl_3$/TMS) δ 5.78 (2H, m, CH), 5.07 (4H, m, CH_2), 4.12 (2H, t, CH_2O), 2.38 (6H, m, $3CH_2$). ^{13}C-NMR (125MHz, $CDCl_3$) δ 173.22, 136.89, 134.22, 117.38, 115.65, 63.61, 33.73, 33.28, 29.07.

Synthesis of Glycidyl Ester Allyl

To a round bottom flask equipped with a stir bar, was added the previously synthesized diallyl ester (2.90g; 18.8 mmol; 1.0 eq), m-CPBA (3.24g; 18.8 mmol; 1.0 eq), and DCM (53.66mL; $5.4x10^{-2}$ g/mL). The oxidation reaction was then allowed to run for 48h. The crude product was

then vacuum filtered to remove the white precipitate before extracting the filtrate with saturated sodium bicarbonate to remove any unreacted m-CPBA. The excess DCM was then removed on the rotary evaporator to afford the clear crude liquid product. The resulting crude liquid product was purified on the Biotage column system to yield the pure clear liquid product. ^{1}H-NMR (500MHz, $CDCl_3$) δ 5.82 (1H, m, CH), 5.09 (2H, m, CH_2), 4.41 (1H, dd, CH_2), 3.93 (1H, q, CH_2), 3.21 (1H, sext, CH), 2.85 (1H, t, CH_2), 2.65 (1H, q, CH_2), 2.47 (2H, m, CH_2), 2.40 (2H, m, CH_2). ^{13}C-NMR (125MHz, $CDCl_3$) δ 174.27, 138, 116.06, 66.23, 50.42, 45.13, 34.27, 29.96.

General Procedure for the synthesis of VL/AVL/OPD copolymers.

A 25mL and a 10mL round bottom flask were flame-dried under N_2(g), along with a 50mL 3-neck round bottom flask equipped with a stir bar. In the 25mL round bottom flask, an 1.7M IAOH stock solution was formed using dry THF, while the 10mL round bottom flask was used to create a 3.7 x 10^{-2}M tin triflate stock solution, also using dry THF. $Sn(OTf)_2$ (0.30mL; $8.83x10^{-6}$ mmol; 0.00035 eq) and IAOH (0.29mL; $3.33x10^{-4}$ mmol; 0.066 eq) were added to the reaction flask. The stock solutions were allowed to stir for 10 minutes before adding the δ-valerolactone (1.92g; 19.2mmol; 3.0 eq), 2-oxepane-1,5-dione (0.82g; 6.0mmol; 1.0 eq), and the previously synthesized α-allyl-δ-valerolactone (0.90g; 6.40mmol; 1.0 eq). The reaction was then allowed to run for 24h at room temperature. After 24h the resulting viscous polymer product was precipitated into cold diethyl ether to afford the off-white particulate polymer product. The diethyl ether was decanted from the product, which was then transferred to a 6-dram vial, using ethyl acetate. Yield: 97% ^{1}H-NMR (400MHz, $CDCl_3$) δ: 5.71 (1H, m, CH), 5.03 (2H, m, CH_2), 4.34 (2H), 4.08 (10.79H), 3.67 (1.04H), 2.52-2.86 (6.68H), 2.15-2.51 (13.22H), 1.67 (22.63H). ^{13}C-NMR (100MHz, $CDCl_3$) δ: 135.33, 117.73, 69.64, 68.76, 64.11, 39.57, 35.71, 33.89, 30.05, 28.26, 24.36, 22.53, 21.61, 19.33.

General Procedure for the synthesis of GLY/AGE copolymers.

A 25 mL round bottom flask, equipped with stir bar, was capped with a rubber septum and flame dried under nitrogen. $Sn(OTf)_2$ (5.2mg; 12.48μmol; 0.4 eq) was then added to round bottom flask and the reaction vessel was then immediately purged with nitrogen again prior to the addition of IAOH (43.7mg 496μmol; 17.4 eq) via microsyringe. The initiator-catalyst mixture was then allowed to stir at room temperature for 30 minutes before lowering the reaction vessel into an ice water bath. After the reaction vessel had been cooled for 5 minutes, the AGE monomer (834mg; 7.31mmol; 250 eq) was added drop wise to the stirring reaction. The GLY monomer (2.17g; 29.2mmol; 1000eq) was added dropwise in 4 separate aliquots, allowing 5 minute breaks between each aliquot, to ensure the exothermic reaction did not overheat and decompose. After stirring was completely impeded (~14 hours) the crude reaction mixture was solubilized in a minimal amount of methanol and precipitated into vigorously stirring ethyl acetate. The precipitation solvent was allowed to settle before carefully decanting the ethyl acetate. The resulting GLY/AGE copolymer was solubilized in methanol, removed to a weighed 6-dram vial, and dried on the rotary evaporator then high vacuum pump to afford the translucent, viscous product. Yield 73.2% ^{1}H-NMR (600MHz, MeOD) δ: 6.0-5.90 (m, –OCH2C*H*CH2), 5.37–5.17 (m, –OCH2CHC*H*2) .3.97-3.42 (6H). ^{13}C-NMR (150MHz, MeOD) δ: 136.31, 117.39, 81.37, 79.81, 75.12, 73.88, 72.01-72.94, 70.42-71.17, 64.41, 62.53, 62.06, 27.99, 27.60.

Synthesis of GLY/MLGEA Polymer (80/20)

A 25 mL round bottom flask, equipped with a stir bar, was capped with a rubber septum and flame dried under nitrogen. $Sn(OTf)_2$ (0.10g; $3.75x10^{-6}$ mol; 0.00035 eq) and EtOH (0.10mL; $1.67x10^{-4}$ mol; 0.066 eq) were added to the reaction flask. The initiator-catalyst mixture was then allowed to stir at room temperature for 30 minutes before lowering the reaction vessel into an ice water bath.

After the reaction vessel had been cooled for 5 minutes the previously synthesized mixed length glycidyl ester allyl (0.36g; 2.1 mmol; 1.0 eq) was added dropwise to the stirring mixture followed by the glycidol (0.64g; 8.6 mmol; 4.0 eq) monomer. After stirring was completely impeded (~14 hours) the crude reaction mixture was solubilized in a minimal amount of methanol and precipitated into vigorously stirring ethyl acetate. The precipitation solvent was allowed to settle before carefully decanting the ethyl acetate. The resulting GLY/MLGEA copolymer was solubilized in methanol, removed to a weighed 6-dram vial, and dried on the rotary evaporator, then under high vacuum, to afford the translucent, viscous product. Yield: 633.7mg (63.37%). ^{1}H-NMR (600MHz, $CDCl_3$) δ: 5.93 (1H), 5.27 (2.37H), 4.06-4.28 (2.91H) 3.26-3.98 (303.6H), 2.24-2.63 (8.25H), 1.84 (2.57H), 1.65 (18.67H). ^{13}C-NMR (150MHz, $CDCl_3$) δ: 138.53, 72.90, 71.32, 63.42, 61.52, 26.55.

Nanoparticle formation through thiolene-click reactions using VL/OPD/AVL copolymers (450nm)

To a round bottom flask equipped with a stir bar, was added the VL/OPD/AVL polymer (100.1mg; 0.18mmol; 1 eq), 3,6-dioxa-1,8-octanedithiol (197.3mg; 1.08mmol; 6 eq), and dichloromethane (55.66mL; $3.24x10^{-3}$M). The flask was then fitted with a reflux condenser and lowered into an oil bath at 45°C to reflux for 12h. The resulting solution was then transferred to 10K dialysis tubing and dialyzed for 72h against dichloromethane to remove any unreacted starting material. The remaining product solution was then concentrated into a preweighed vial and stored in the refrigerator at 4°C. ^{1}H-NMR (600MHz, $CDCl_3$) δ: 5.71 (1H, m, CH), 5.03 (2H, m, CH_2), 4.34 (2H), 4.08 (10.79H), 3.67 (1.04H), 2.52-2.86 (6.68H), 2.15-2.51 (13.22H), 1.67 (22.63H). ^{13}C-NMR (150MHz, $CDCl_3$) δ: 135.33, 117.73, 69.64, 68.76, 64.11, 39.57, 35.71, 33.89, 30.05, 28.26, 24.36, 22.53, 21.61, 19.33.

Nanoparticle formation through thiolene-click reactions using GLY/AGE copolymers (50nm)

To a round bottom flask equipped with a stir bar, was added the GLY/AGE polymer (111mg; $1.79x10^{-1}$mmol; 2 eq), 3,6-dioxa-1,8-octanedithiol (16.35mg; $8.97x10^{-2}$mmol; 1 eq), and methanol (55.36mL; $3.24x10^{-3}$M). The flask was then fitted with a reflux condenser and lowered into an oil bath at 45°C to reflux for 12h. The resulting solution was then transferred to 10K dialysis tubing and dialyzed for 72h against methanol to remove any unreacted starting material. The remaining product solution was then concentrated into a preweighed vial and stored in the refrigerator at 4°C. ^{1}H-NMR (600MHz, $CDCl_3$) δ: 6.0-5.90 (m, –OCH2C*H*CH2), 5.37–5.17 (m, –OCH2CHC*H*2) .3.97-3.42 (6H). 13C-NMR (150MHz, MeOD) δ: 136.31, 117.39, 81.37, 79.81, 75.12, 73.88, 72.01-72.94, 70.42-71.17, 64.41, 62.53, 62.06, 27.99, 27.60.

Temozolomide encapsulation into poly(ester) nanoparticles (NP-TMZ)

A solution of poly(ester) nanoparticle (50.0 mg) and temozolomide (10.9 mg) in DMSO (0.150 mL) was added dropwise to a vortexing solution of aqueous 1% d-α-tocopherol polyethyleneglycol (1000) succinate (Vit E-TPGS, 35.0 mL). As the nanoparticle solution was added, precipitation occured, and the resulting solution was centrifuged to remove the free drug from the encapsulated drug. In order to ensure all nonbound drug was removed, centrifugation was repeated three times with fresh water added after each run. The resulting product was freeze-dried to yield a white powder, and UV/Vis was employed to confirm temozolomide incorporation.

References

1. Killops, K., Rodriguez, C., Lundberg, P., Hawker, C., and Lynd, N. (2015) A synthetic strategy for the preparation of sub-100 nm functional polymer particles of uniform diameter, *Polymer Chemistry 6*, 1431-1435.

2. Ramos, J., Forcada, J., and Hidalgo-Alvarez, R. (2014) Cationic Polymer Nanoparticles and Nanogels: From Synthesis to Biotechnological Applications, *Chemical Reviews 114*, 367-428.

3. Tyrrell, Z., Shen, Y., and Radosz, M. (2012) Multilayered Nanoparticles for Controlled Release of Paclitaxel Formed by Near-Critical Micellization of Triblock Copolymers, *Macromolecules 45*, 4809-4817.

4. van der Ende, A. E., Sathiyakumar, V., Diaz, R., Hallahan, D. E., and Harth, E. (2010) Linear release nanoparticle devices for advanced targeted cancer therapies with increased efficacy, *Polymer Chemistry 1*, 93-96.

5. Stevens, D., Rahalkar, A., Spears, B., Gilmore, K., Douglas, E., Muthukumar, M., and Harth, E. (2015) Semibranched polyglycidols as "fillers" in polycarbonate hydrogels to tune hydrophobic drug release, *Polymer Chemistry 6*, 1096-1102.

6. Hariri, G., Edwards, A., Merrill, T., Greenbaum, J., van der Ende, A., and Harth, E. (2014) Sequential Targeted Delivery of Paclitaxel and Camptothecin Using a Cross-Linked "Nanosponge" Network for Lung Cancer Chemotherapy, *Molecular Pharmaceutics 11*, 265-275.

7. Dhanda, D., Tyagi, P., Mirvish, S., and Kompella, U. (2013) Supercritical fluid technology based large porous celecoxib-PLGA microparticles do not induce pulmonary fibrosis and

sustain drug delivery and efficacy for several weeks following a single dose, *Journal of Controlled Release 168*, 239-250.

8. Lee, B., Yun, Y., Choi, J., Choi, Y., Kim, J., and Cho, Y. (2012) Fabrication of drug-loaded polymer microparticles with arbitrary geometries using a piezoelectric inkjet printing system, *International Journal of Pharmaceutics 427*, 305-310.
9. Anselmo, A., and Mitragotri, S. (2014) An overview of clinical and commercial impact of drug delivery systems, *Journal of Controlled Release 190*, 15-28.
10. Li, B., Harich, K., Wegiel, L., Taylor, L., and Edgar, K. (2013) Stability and solubility enhancement of ellagic acid in cellulose ester solid dispersions, *Carbohydrate Polymers 92*, 1443-1450.
11. McCarley, R., Forsythe, J., Loew, M., Mendoza, M., Hollabaugh, N., and Winter, J. (2013) Release Rates of Liposomal Contents Are Controlled by Kosmotropes and Chaotropes, *Langmuir 29*, 13991-13995.
12. Ye, L., Letchford, K., Heller, M., Liggins, R., Guan, D., Kizhakkedathu, J. N., Brooks, D. E., Jackson, J. K., and Burt, H. M. (2011) Synthesis and Characterization of Carboxylic Acid Conjugated, Hydrophobically Derivatized, Hyperbranched Polyglycerols as Nanoparticulate Drug Carriers for Cisplatin, *Biomacromolecules 12*, 145-155.
13. Charleux, B., Delaittre, G., Rieger, J., and D'Agosto, F. (2012) Polymerization-Induced Self-Assembly: From Soluble Macromolecules to Block Copolymer Nano-Objects in One Step, *Macromolecules 45*, 6753-6765.
14. Ungaro, F., Bianca, R., Giovino, C., Miro, A., Sorrentino, R., Quaglia, F., and La Rotonda, M. (2009) Insulin-loaded PLGA/cyclodextrin large porous particles with improved

aerosolization properties: In vivo deposition and hypoglycaemic activity after delivery to rat lungs, *Journal of Controlled Release 135*, 25-34.

15. Riess, G., and Labbe, C. (2004) Block copolymers in emulsion and dispersion polymerization, *Macromolecular Rapid Communications 25*, 401-435.
16. Kim, M., and Lee, D. (2010) In Vitro Degradability and Stability of Hydrophobically Modified pH-Sensitive Micelles Using MPEG-Grafted Poly(beta-amino ester) for Efficient Encapsulation of Paclitaxel, *Journal of Applied Polymer Science*, 3431-3438.
17. Kotsuchibashi, Y., Ebara, M., Yamamoto, K., and Aoyagi, T. (2010) "On-Off" Switching of Dynamically Controllable Self-Assembly Formation of Double-Responsive Block Copolymers with Tunable LCSTs, *Journal of Polymer Science Part a-Polymer Chemistry*, 4393-4399.
18. Calderon, M., Quadir, M. A., Sharma, S. K., and Haag, R. (2010) Dendritic Polyglycerols for Biomedical Applications, *Advanced Materials 22*, 190-218.
19. Nichols, D., and Lewis, M. (2004) Mechanisms and issues relating to the use of D1-like dopamine receptor agonists for age-related illnesses: Parkinson's disease and memory and cognition, *Medicinal Chemistry Research*, 105-114.
20. Nichols, D., and Frescas, S. (1999) Improvements to the synthesis of psilocybin and a facile method for preparing the O-acetyl prodrug of psilocin, *Synthesis-Stuttgart*, 935-938.
21. van der Ende, A. E., Harrell, J., Sathiyakumar, V., Meschievitz, M., Katz, J., Adcock, K., and Harth, E. (2010) "Click" Reactions: Novel Chemistries for Forming Well-defined Polyester Nanoparticles, *Macromolecules 43*, 5665-5671.

22. van der Ende, A., Croce, T., Hamilton, S., Sathiyakumar, V., and Harth, E. (2009) Tailored polyester nanoparticles: post-modification with dendritic transporter and targeting units via reductive amination and thiol-ene chemistry, *Soft Matter 5*, 1417-1425.

23. van der Ende, A. E., Kravitz, E. J., and Harth, E. (2008) Approach to formation of multifunctional polyester particles in controlled nanoscopic dimensions, *Journal of the American Chemical Society 130*, 8706-8713.

24. Sunder, A., Turk, H., Haag, R., and Frey, H. (2000) Copolymers of glycidol and glycidyl ethers: Design of branched polyether polyols by combination of latent cyclic AB(2) and ABR monomers, *Macromolecules 33*, 7682-7692.

25. Wilms, D., Schomer, M., Wurm, F., Hermanns, M. I., Kirkpatrick, C. J., and Frey, H. (2010) Hyperbranched PEG by Random Copolymerization of Ethylene Oxide and Glycidol, *Macromolecular Rapid Communications 31*, 1811-1815.

26. Sunder, A., Frey, H., and Mulhaupt, R. (2000) Hyperbranched polyglycerols by ring-opening multibranching polymerization, *Macromolecular Symposia 153*, 187-196.

27. Sunder, A., Hanselmann, R., Frey, H., and Mulhaupt, R. (1999) Controlled synthesis of hyperbranched polyglycerols by ring-opening multibranching polymerization, *Macromolecules 32*, 4240-4246.

28. Wilms, D., Stiriba, S. E., and Frey, H. (2010) Hyperbranched Polyglycerols: From the Controlled Synthesis of Biocompatible Polyether Polyols to Multipurpose Applications, *Accounts of Chemical Research 43*, 129-141.

29. Haag, R., Sunder, A., and Stumbe, J. F. (2000) An approach to glycerol dendrimers and pseudo-dendritic polyglycerols, *Journal of the American Chemical Society 122*, 2954-2955.

30. Zhang, J. G., Krajden, O. B., Kainthan, R. K., Kizhakkedathu, J. N., Constantinescu, I., Brooks, D. E., and Gyongyossy-Issa, M. I. C. (2008) Conjugation to hyperbranched polyglycerols improves RGD-mediated inhibition of platelet function in vitro, *Bioconjugate Chemistry 19*, 1241-1247.

31. Hamilton, S. K., Ikizler, M. R., Wallen, C., Wright, P. F., and Harth, E. (2008) Effective delivery of IgG-antibodies into infected cells via dendritic molecular transporter conjugate IgGMT, *Molecular Biosystems*, 1209-1211.

CHAPTER V

MICRONSCALE NETWORKS THROUGH INKJET PRINTING

Introduction

The potential for a drug delivery platform capable of combining the release of not only therapeutics but secondary delivery vehicles is highly advantageous[1]. Furthermore, to be able to tune the release of individual cargo, to accommodate different release rates for each therapeutic based on need, is a goal with exciting possibilities[2]. Research in this realm has had success in utilizing non-covalently bound polymer mixtures to co-deliver BMP2 along with a MEK inhibitor to promote enhanced bone growth in mice with neurofibromatosis type I, a gene mutation based disease which contributes to non-bone union after fractures in children[3]. However, much of the work currently being done requires incision and implantation of macro sized structures to facilitate the desired delivery of therapeutics.

In contrast, microparticle drug delivery platforms are well researched and of particular interest due to their ability to provide sustained release of loaded therapeutic cargo. Research in this area is well established and has shown that microparticles are well suited for treating a range of issues, including cancer[4-6], diabetes[7], and tuberculosis[8]. The synthesis routes known for the formation of such structures include techniques such as emulsion synthesis[9-13], microfluidic devices[14, 15], and spray drying[16]. While these methods are rather well known, they suffer from shape inconsistency and high polydispersity of particles. Furthermore, the large scale utilization of such particles is hindered by the price, reproducibility, and scalability of the formed particle species. In an effort to overcome the shortcomings of other microparticle synthesis techniques, two synthesis methods, lithography and ink jet printing, have been utilized to form well-defined

and reproducible microparticle structures. However, of these two, the print speed is slower, and the costs larger with lithography[17]. For these reasons, a fabrication method employing ink jet printing for the directed formation of well-defined and easily reproducible microparticles, which can be easily scaled to accommodate distribution, would quickly find a place as a viable drug delivery platform.

Figure V-1: Desired hydrogel structures and tunable characteristics

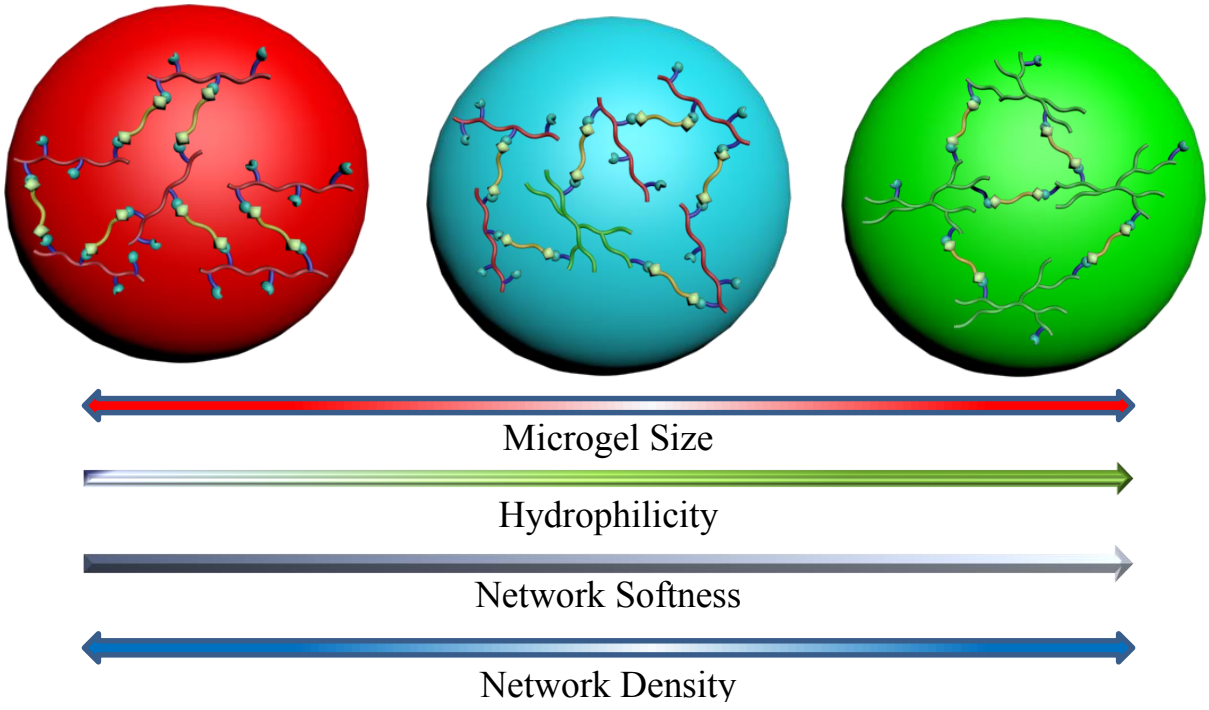

The integration of technology into the field of polymer research is leading to new and exciting possibilities, from automated polymerization machines to 3-D printing of tissue scaffolds[18-21]. One such instrument that has been employed is the piezoelectric ink jet printer, which has shown great potential for the formation of thin films as well as microparticle structures. This technique benefits greatly from its inherent ability to easily change the composition of the ink being used, affording an extremely tunable system with seemingly nonexistent limitations on the systems that can be formed[17, 22-24]. A fabrication method utilizing a commercially available instrument also means the scalability is not limited by reaction conditions but by the number of

printers that are operating at any given time. Finally, by tuning the instrument settings, such as nozzle size, accelerating voltage, and/or the voltage waveform used, one can easily direct the size of the formed particles (See Figure V-1).

Despite these numerous advantages, research utilizing ink jet printing is far from expansive. Much of the work has focused on the optimization of waveforms for the purpose of particle size manipulation, with little intention for the particles to be removed from the surface onto which they were printed[17]. The only structures printed for the purpose of drug delivery employed the solvent evaporation method for particle formation and released their entire payload within the first six hours, far from to the type of sustained release that is often desirable in microparticle based systems. This fast release rate arose from a number of factors, including degradations and excessive swelling. [17, 22-24]

Within the realm of microparticle research, size becomes exceedingly important[4, 14]. The size of the microparticles formed often dictates the available options for utilization of the formed structures. With this in mind, it becomes desirable to be able to dictate the size of the particles formed through the manipulation a simple reaction condition, such as wt% of the polymer within the hydrogel printing solution. This method of change allows for the desired change in particle size without the necessity for major changes to the fabrication method. For this reason, a number of wt% solutions were employed to afford particles that ranged in size from 12.5µm down to 2µm. The ability to directly form particles of a desired size with such a minor perturbation to the printing solution is further validation of the robustness of this new fabrication method.

One method that has been utilized to decrease the swelling seen in other microparticle formulations is to covalently cross link the polymers of the system to form hydrogel architectures. There are a number of methods by which hydrogels can be formed, but the method

chosen must be compatible with the ink jet printing system. For this reason, the crosslinking chemistry should be able to occur at room temperature without the need for excessive perturbation of the printed structures. One such crosslinking mechanism is the thiolene click reaction, which employs a dithiol crosslinker and allyl functionalized polymers that, in the presence of a photoinitiator, can be irradiated with UV to facilitate the radical click reaction. When this reaction is performed, in a solution of proper concentration, it will lead to the formation of a hydrogel structure. Furthermore, the combination of the prepared hydrogel solution and the ink jet printing platform will lead to the formation of micron sized gel structures with very well defined sizes and low dispersity in size and/or shape.

The research described here is focused on the formation of a delivery platform capable of co- and sequential-drug delivery with tunable characteristics, including hydrophilicity, size, network crosslinking density, and softness, on a size scale from 1-15μm, affording an injectable system with properties similar to their macroscale counterparts.

Results and Discussion

Synthesis of Polymer Building Blocks

The desire to deliver a range of cargo with varied solubility and size necessitates the use of inherently different materials as the basis for the hydrogel structures. For this reason, two dialectic polymer species were chosen. First was a poly(carbonate) based polymer with allyl functionality which was synthesized as previously described (See Figure V-2). This species is highly hydrophobic and has shown the ability to form hydrogel structures with sustained linear release of small molecule drugs[2]. Furthermore, the enzymatic degradability of the carbonate moiety allows the body a mechanism for elimination of the poly(carbonate) backbone while the ester containing side arm can be targeted for hydrolytic cleavage. The second polymer chosen was a poly(glycidol)

based system with allyl functionality (See Figure V-3). This polymer was synthesized using the comonomers glycidol and allyl glycidyl ether, with $Sn(OTf)_2$ catalyst, in a manner similar to

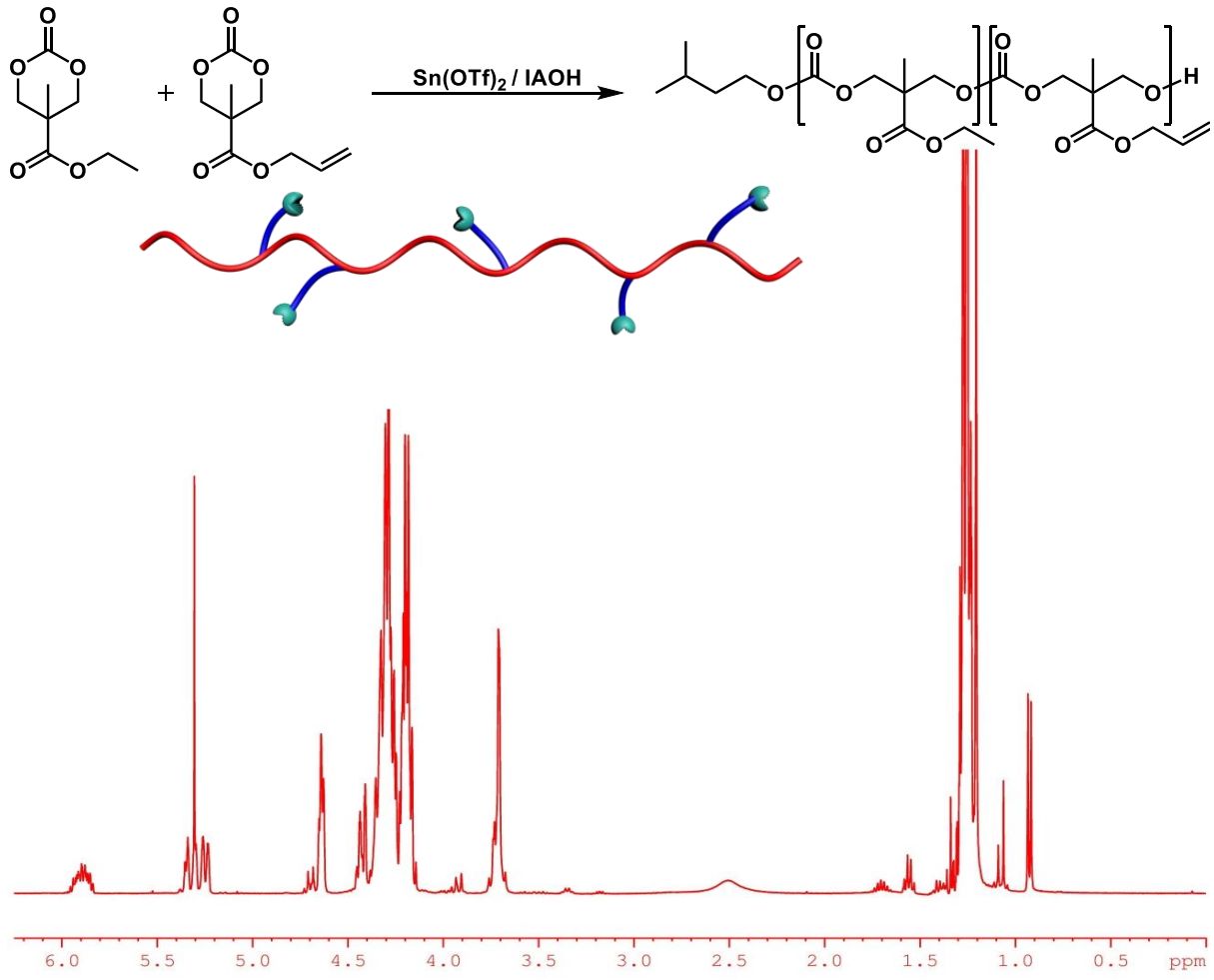

Figure V-2: Synthesis and ^{1}H-NMR spectra for allyl poly(carbonate)

information published previously. In contrast to the poly(carbonate), the poly(glycidol) system is completely water soluble, which allows for the investigation of water based gel formation, an advantageous characteristic when the delivery of biological cargo is desired. Also, the polyether backbone, and lack of hydrolytically cleavable esters in the side arms, presents a substantially different methodology for removal than is seen in the poly(carbonate) system. Both of these polymers present interesting characteristics that arise from their many differences, and for these reasons, three systems were chosen for investigation. The first system, consisting entirely of

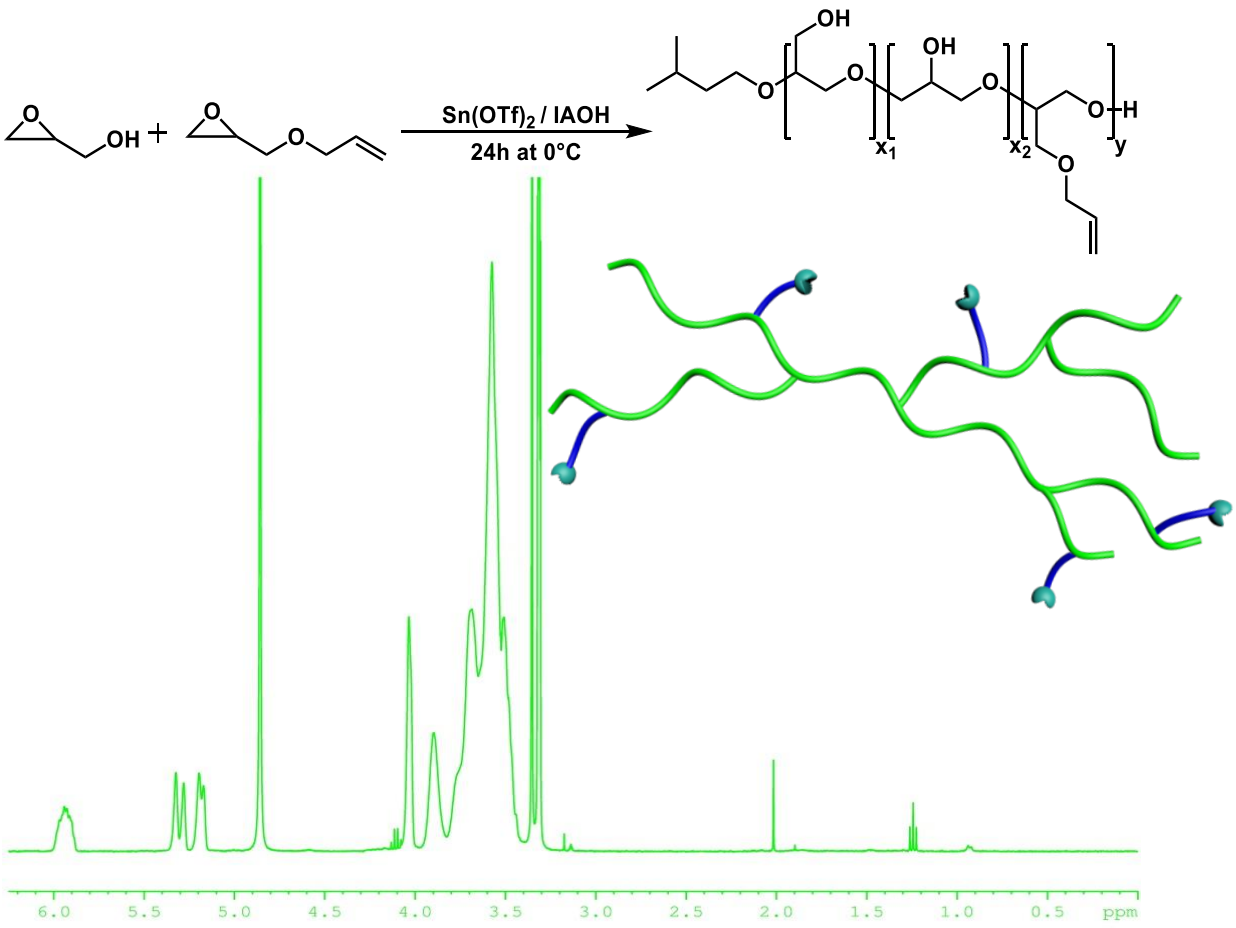

Figure V-3: Synthesis and ^{1}H-NMR spectra for allyl poly(glycidol)

poly(carbonate), represents a purely hydrophobic system. The second system is composed of a 70/30 w% mixture of poly(carbonate)/poly(glycidol), which affords a system that is still mostly

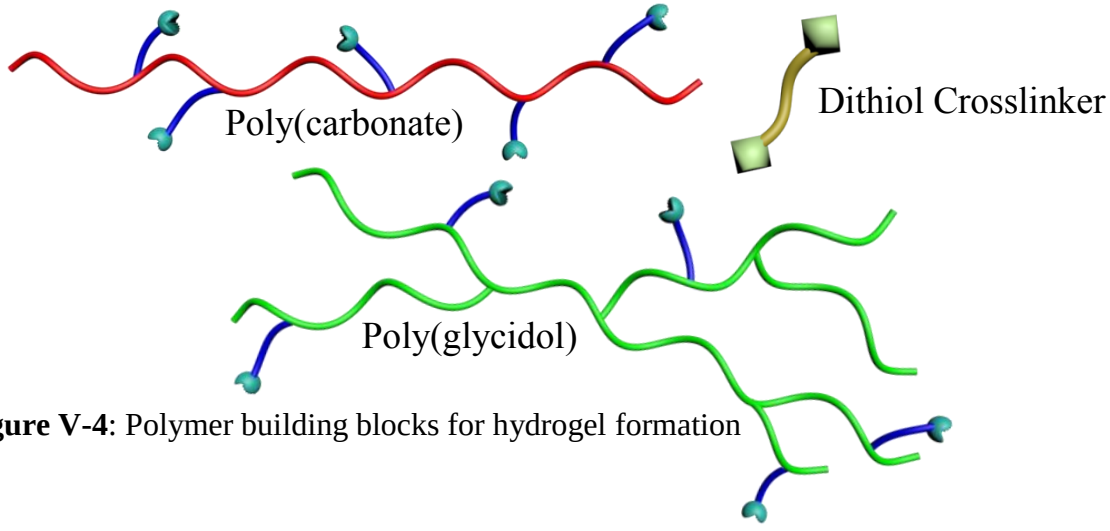

Figure V-4: Polymer building blocks for hydrogel formation

hydrophobic by mass but will have some increased hydrophilicity and softness due to the poly(glycidol). The third system is comprised purely of poly(glycdidol) and represents a completely hydrophilic species.

Formation of Macroscale Hydrogel Structures

The use of thiolene click crosslinking was employed in order to form hydrogel samples utilizing the synthesized allyl functionalized polymers and dithiol species of varying molecular weight (See Figure V-4). For samples 1 and 2, the polymers were solubilized in DMSO before the addition of DMPA (0.2eq per alkene). After thorough mixing with the tip of a needle, the dithiol crosslinker (0.5eq per alkene) was added via micro syringe and the hydrogel solution was again mixed with a needle to ensure complete solubilization and the formation of a homogenous solution (See Figure V-5). A similar procedure was followed for the formation

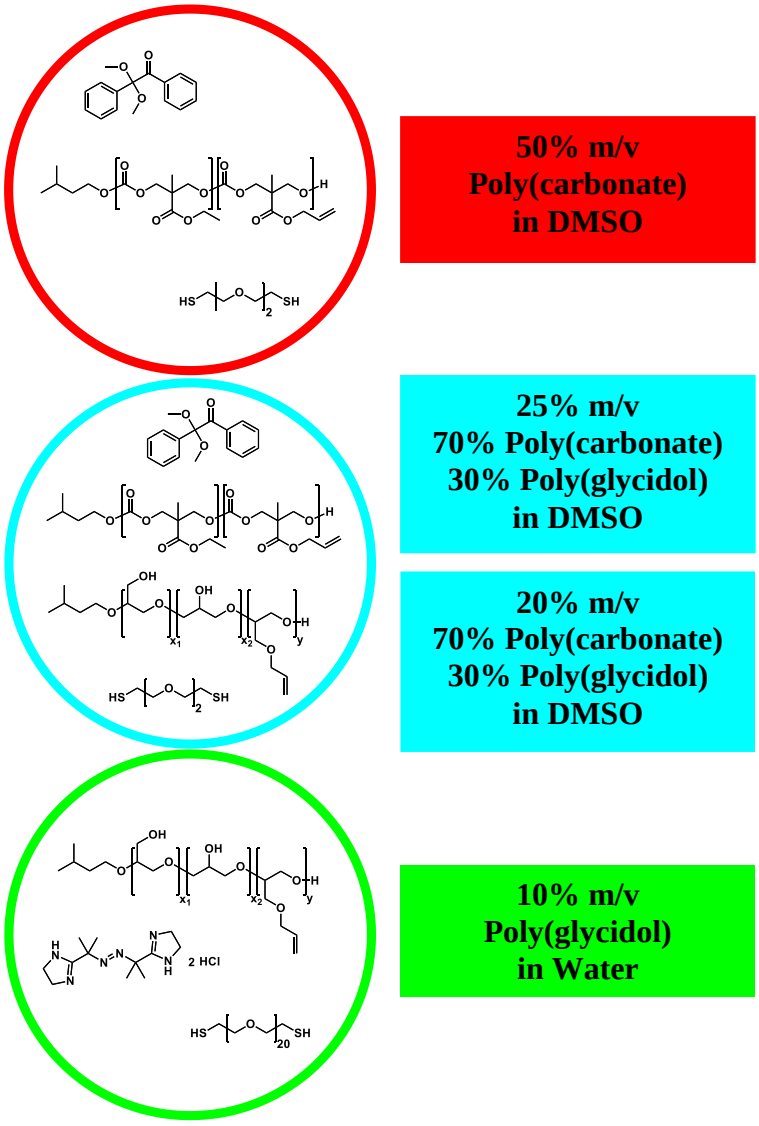

Figure V-5: Three separate polymer mixtures were used for printing, and the influence of % m/v was investigated using the poly(carbonate)/poly(glycidol) system

of a mixed poly(carbonate)-poly(glycidol) hydrogel sample with both polymers being weighed together prior to solubilizaiotn in DMSO. As the use of a larger molecular weight dithiol was preferred for the poly(glycidol) based sample, and it was necessary to employ a water soluble photoinitiator (VA-044), the order for the addition of reagents was varied, with the solid dithiol (0.5eq per alkene) being added to a mixture of polymer in half the total desired amount of water. This solution was stirred, again with the tip of a needle, until the crosslinker was completely in solution before the addition of the second half of water containing the VA-044 (0.2eq per alkene) initiator (See Figure V-5).

Once the hydrogel solutions had been completely solubilized, the samples were irradiated with long wave UV light (365nm) for five minutes to induce gelation. Upon completion of the gel formation, the samples were rinsed thoroughly with water, methanol, and methylene chloride to remove any unreacted starting materials and replace the reaction solvent with water so as to dry the samples via lyophilization. In order to determine the yields from the gelation, dry masses were compared to the total mass of the unreacted starting materials, with typical yields exceeding 90%.

Determination of Limiting Hydrogel Concentration

As the method being utilized in this research involves the ejection of a solution from a small printer head, the viscosity of the hydrogel solution plays a very important role. However, the mechanism of gel formation used has a threshold concentration below which hydrogel formation is not observed. For this reason it was imperative that a concentration be found that was as dilute as possible while still affording a hydrogel product. In order to determine this concentration, a dilution assay was performed on all three hydrogel samples wherein the dilution was increased linearly from 1:1 w/v to 1:15 w/v (polymer/solvent). As would be expected, the threshold concentration varied for each of the gel solutions with the addition of the branched poly(glycidol)

structure affording gelation at ever lower concentrations. The optimal dilution for samples 1, 2, and 3 was found to be 1:2, 1:4, and 1:10 respectively, and with this information it was hypothesized that there would be a decrease in size of the printed gels with the decrease in concentration as less polymer was present for gelation in each dot.

Determination of Mechanical Properties of Model Hydrogel Structures

Initial macroscale structures were formed using poly(carbonate) that was either doped with unfunctionalized poly(glycidol), which acted as a filler, or pure poly(carbonate). Furthermore, two separate dithiol crosslinkers were used to investigate the change this would have on the hydrogel's properties. These systems were studied using unconfined compression to determine the mechanical properties of the structures, and yielded interesting results. The implantation of poly(glycidol) as a filler led to drastic increases in the deformability of the formed hydrogels, while the use of a longer crosslinker had a similar but less exaggerated effect. Subsequently, the compression modulus for the structures decreased with the increase in deformability. Despite this intriguing shift in hydrogel behavior, it was determined that the utilization of functionalized poly(glycidol) would be more advantageous as it affords a system that has hydrophilic and hydrophobic polymer chains covalently bound together, which should yield a system with enhanced delivery potential due to the ability to take advantage of favorable interactions between cargo and the hydrogel structure.

Swelling Studies of Model Hydrogel Structures

The ability of a gel to swell while in water is a characteristic that can directly influence the behavior of the gel system. Rapid swelling often leads to the rapid release of cargo as well as increased rates of degradation due to the increase in surface area. For these reasons it was important to find the swelling capability of each of the hydrogel solutions (See Figure V-6). As the amount

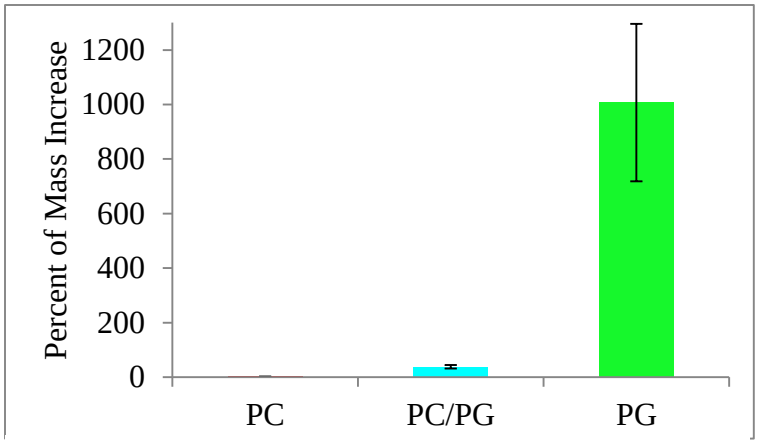

Figure V-6: Swelling of Model Hydrogel Structures

of poly(glycidol) was increased there was a distinct increase in swelling of the gels, which is to be expected due to the hydrophilic nature of the poly(glycidol) polymer. Furthermore, in the pure poly(carbonate) systems it was observed that the use of a longer crosslinker further enhanced the increase in swelling, a fact that can be explained by the high affinity PEG has for water.

Fabrication and Characterization of Micronsized Hydrogel Structures

The utilization of a Dimatix Materials printer was chosen in order to produce individual microgel spheres in a facile method with reproducible sizes. The hydrogel solutions were formed using the same methodology as was utilized for the bulk samples with the addition of a separate fluorescent dye for each hydrogel solution. Once the mixtures were in solution, they were carefully loaded into a Dimatix printer cartridge and the cartridge was placed within the Dimatix instrument. Initially, the substrates chosen for the printing process were glass slides. However, the relative surface area interaction for each dot afforded a situation in which the gels could not be easily removed from the glass surface. This issue was combated in two separate phases. For samples 1 and 2, which are decisively more hydrophobic, the glass slides were coated with a sacrificial layer of poly(glycidol) by spin-coating a solution of poly(glycidol) in methanol (50/50 mass%). This method yielded surfaces that, once printed onto, could be easily removed with water to liberate the hydrogel structures. Unfortunately, this method could not work for the poly(glycidol) based system as the favorable hydrophilicities cause mixing of the gel solution and poly(glycidol) coating. For

this reason, a new and uniform surface was sought which could be used for all of the hydrogel systems. Chosen to fit this role was Teflon, which provides an excellent surface that proved useful for the overtly hydrophilic poly(glycidol) system. Once the printing substrates had been placed on the printing area, the Dimatix program was used to create a pattern which printed individual dots, with spacing of 100μm, in a continuous grid over the entire surface of the printing substrates. The ejection of the hydrogel solution from the printing cartridge was controlled by varying the voltages applied to the piezoelectric plate within the cartridge. A number of waveforms were tried before one was chosen which afforded the most consistent and uniform formation of drops[17]. Once the desired waveform had been determined, the hydrogel solution was printed onto the appropriate substrates. Upon completion, the substrate was carefully removed from the printing surface and irradiated with long wave UV (365nm) for 5 minutes in order to form the microgel spheres. The product gels could then be visualized using fluorescent microscopy. To investigate the printed gels on the substrate surface, a Nikon AZ100M microscope with a halogen lamp was utilized. This instrument allows for the determination of spatial resolution between the dots as well as confirmation of encapsulation of the fluorescent dye. Once it had been confirmed that the microdots were successfully printed onto the surface, water was used to rinse the gels from the surface into MakTek glass bottom culture dishes for investigation with confocal microscopy. The gels, now suspended in water, were thoroughly investigated using a Zeiss LSM Inverted Confocal Microscope to study their sizes, shapes, and, as the gels are relatively transparent, Z-stack images were obtained at progression rates of 0.05μm-0.25 μm. The data obtained from these cross sectional readings shows good integration of the fluorescent molecules throughout the hydrogel structure, meaning that any drug loaded into the system should be evenly distributed throughout the formed microgels.

Poly(carbonate) Particles

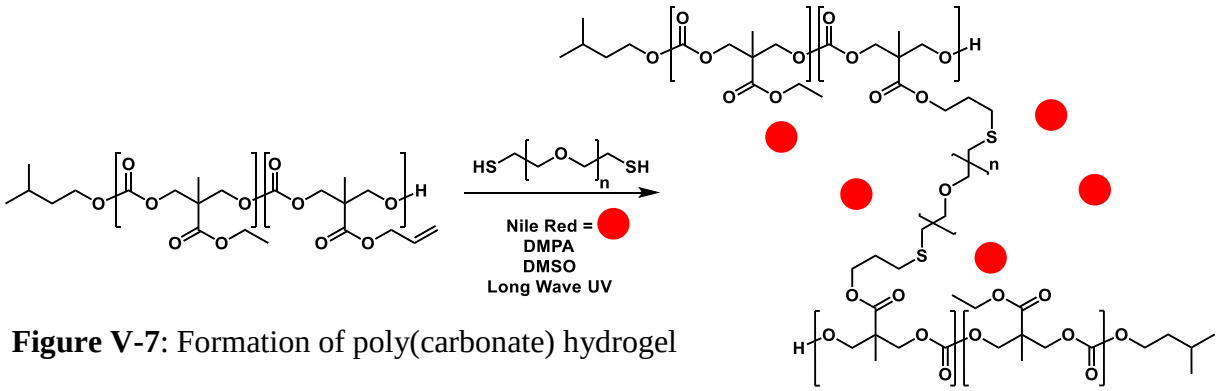

Figure V-7: Formation of poly(carbonate) hydrogel

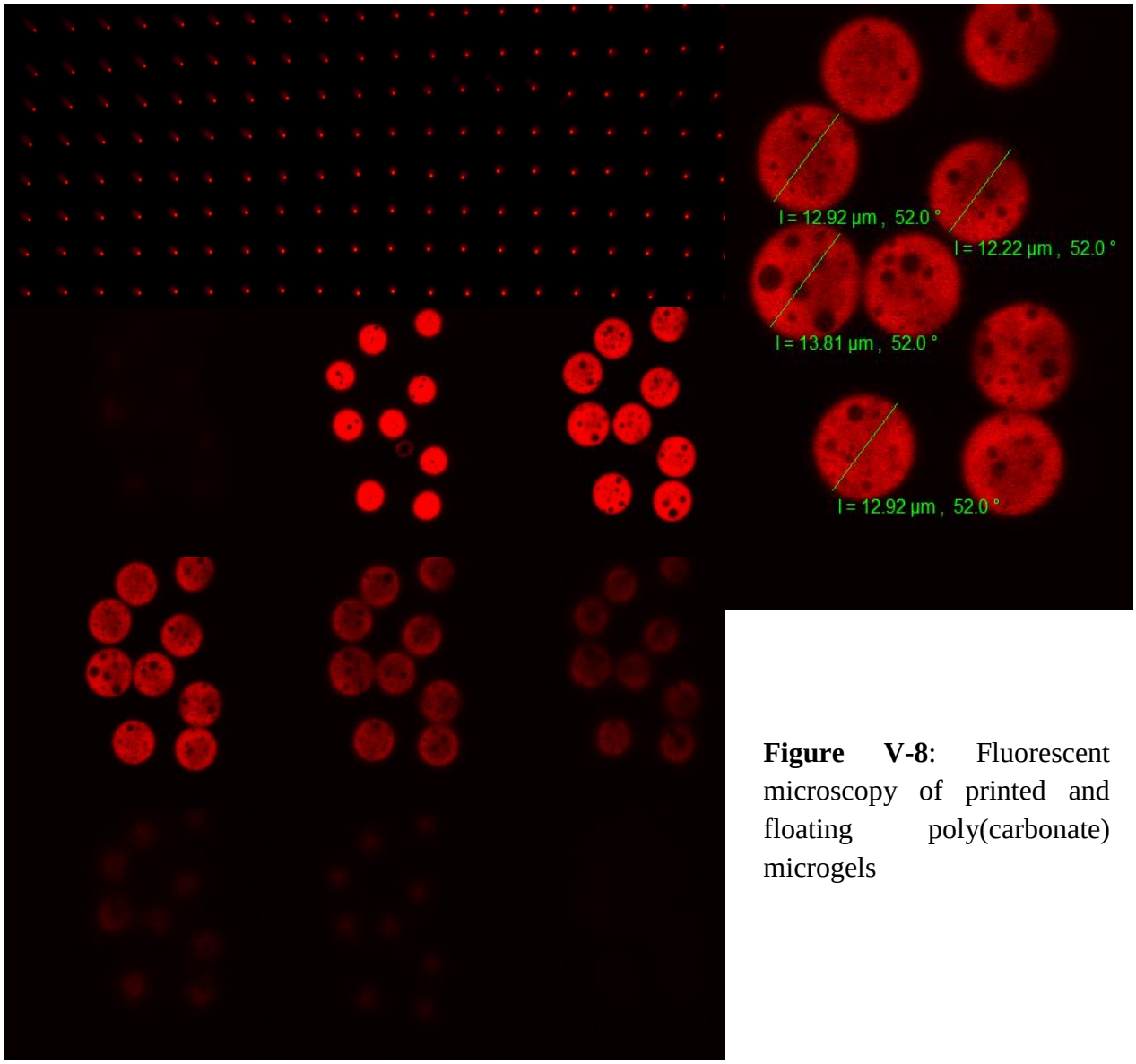

Figure V-8: Fluorescent microscopy of printed and floating poly(carbonate) microgels

The first printing system investigated was a pure poly(carbonate) based ink primed with dithiol crosslinker, DMPA initiator, and Nile Red as a model hydrophobic drug (See Figure V-7). For this composition, poly(glycidol) coated slides were employed to give a hydrophilic surface for the hydrophobic hydrogel solution to be printed onto. The resulting printed particles were easily visualized using fluorescent microscopy, due to the incorporation of Nile Red, and showed good uniformity and spacing on the poly(glycidol) coated surface (See Figure V-8). Once washed from the surface and resuspended, the particles could be visualized using confocal microscopy, and the results were fascinating. Utilizing the facile new particle fabrication method, particles with an average size of 12.5μm were obtained. The size disparity among the printed particles was seen to be minimal and the Nile Red dye was observed to be distributed evenly throughout the particle structure, which suppirts the argument that any therapeutic loaded into the system should also exhibit this homogenous distribution. Furthermore, the particles exhibited good porosity, a characteristic that increases surface area and decreases overall particle mass. This characteristic is highly advantageous for delivery methods such as inhalation, where the low particle mass affords better aerosolization[4]. Also, the particle size of 12.5μm falls nicely in the size range of particles capable of accomplishing both good nasal cavity and throat distribution, as well as entry into the lower portions of the lungs for directed delivery of therapeutic cargo.

Poly(carbonate)/Poly(glycidol) Particles

The ability to form hydrogel networks with both hydrophobic and hydrophilic character expands the potential for cargo delivery and tunable release. In order to investigate this possibility, a hybrid system was formed using 70/30 m/m combination of poly(carbonate)/poly(glycidol) polymer chains. The hydrogel ink for this investigation was primed with dithiol crosslinker,

Figure V-9: Formation of polycarbonate/poly(glycidol) hydrogel

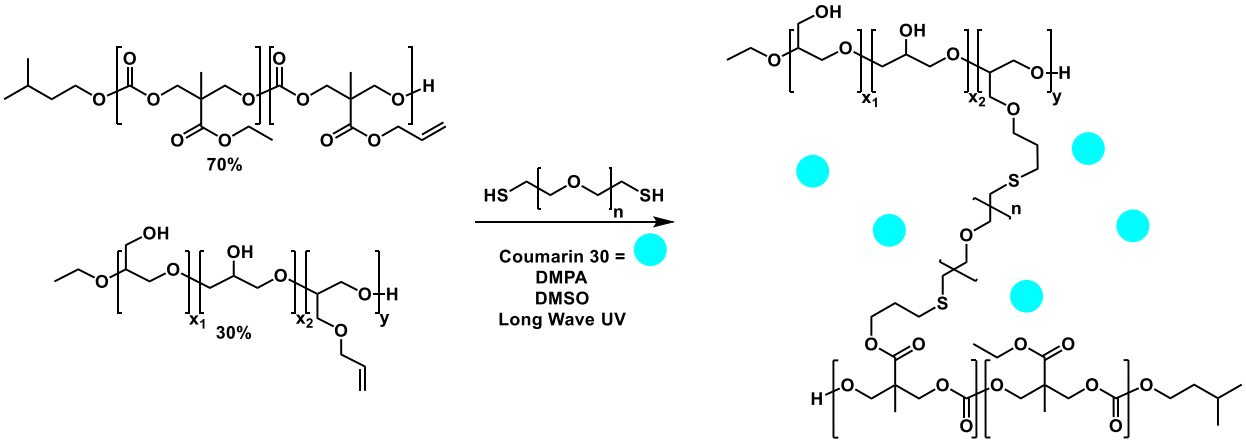

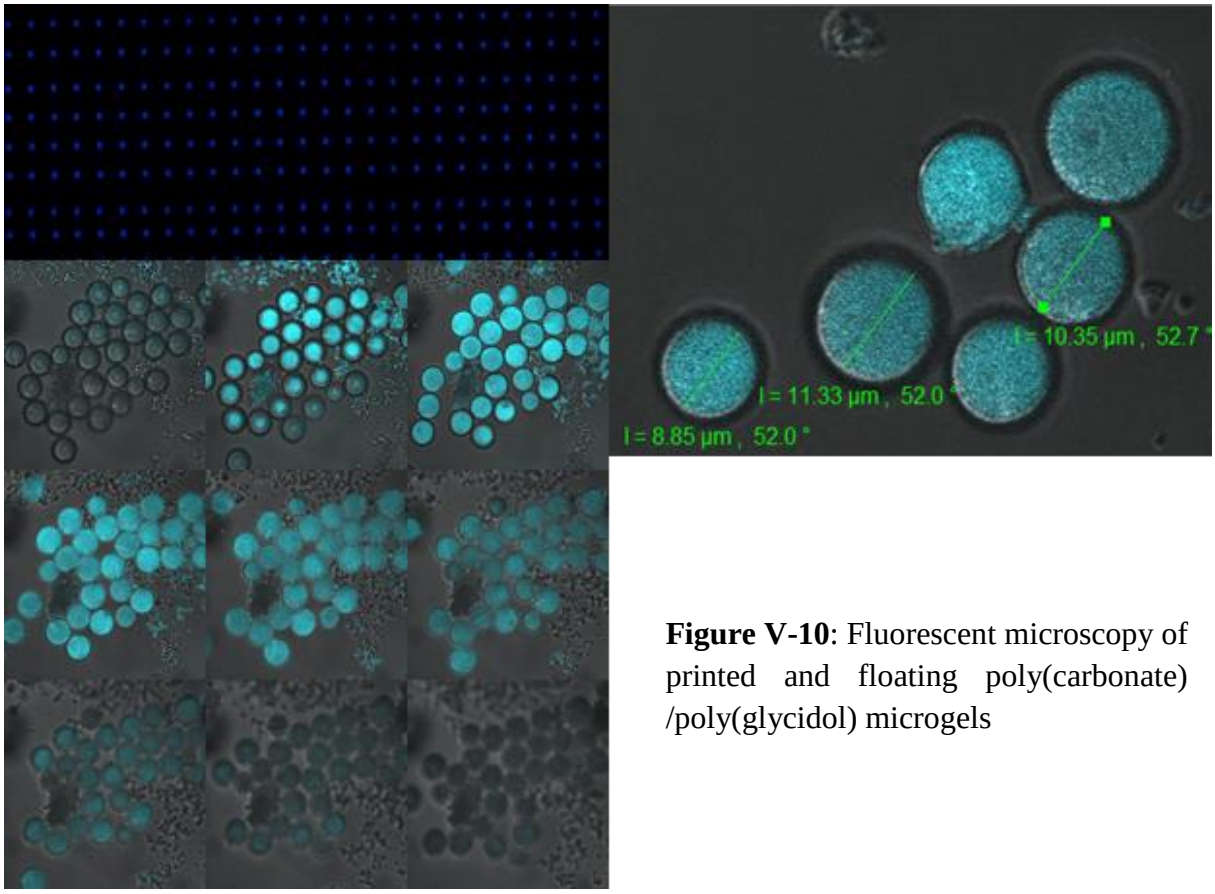

Figure V-10: Fluorescent microscopy of printed and floating poly(carbonate) /poly(glycidol) microgels

DMPA initiator, and coumarin 30 as a model hydrophobic drug (See Figure V-9). Since these gels are still mostly hydrophobic, the poly(glycidol) coated slides were used as a printing surface, and the printed particles were again visualized using fluorescent microscopy. Interestingly, when the

hydrogel products were rinsed from the slide for confocal investigation, it was observed the particles were smaller in size than those formed purely from poly(carbonate), with the average size of the products around 10μm, though the uniformity of the system was decreased (See Figure V-10). However, these hybrid particles were seen to be much more mobile and able to bump into each other and continue moving without any perceived aggregation. This fact is very important when considering the utilization of these systems for intravenous delivery, where aggregation leads to potentially deadly side effects. The size of the particles formed is again well suited for inhalation and direct injection therapies, and the formation of these hybrid systems is a great representation of the potential of this method to form covalently bound hydrogel structures with tunable hydrophilicity.

Poly(glycidol) Particles

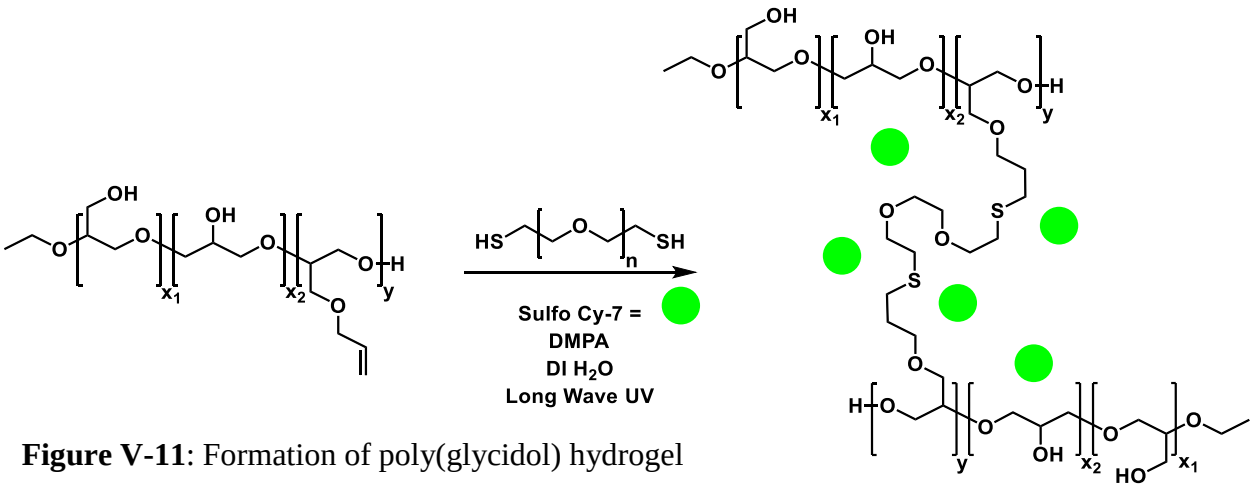

Figure V-11: Formation of poly(glycidol) hydrogel

The final printing composition investigated was pure poly(glycidol). In this case the solvent used was water, an exciting point that further expands the possible cargo. For this ink a larger crosslinker was used to allow for water solubility, and a water soluble photoinitiator, in this case VA-044, was employed. Finally, the use of a thiolated Cy2 dye served as a model hydrophilic drug and readily visible fluorophore. For this formulation the use of poly(glycidol) coated slides is not

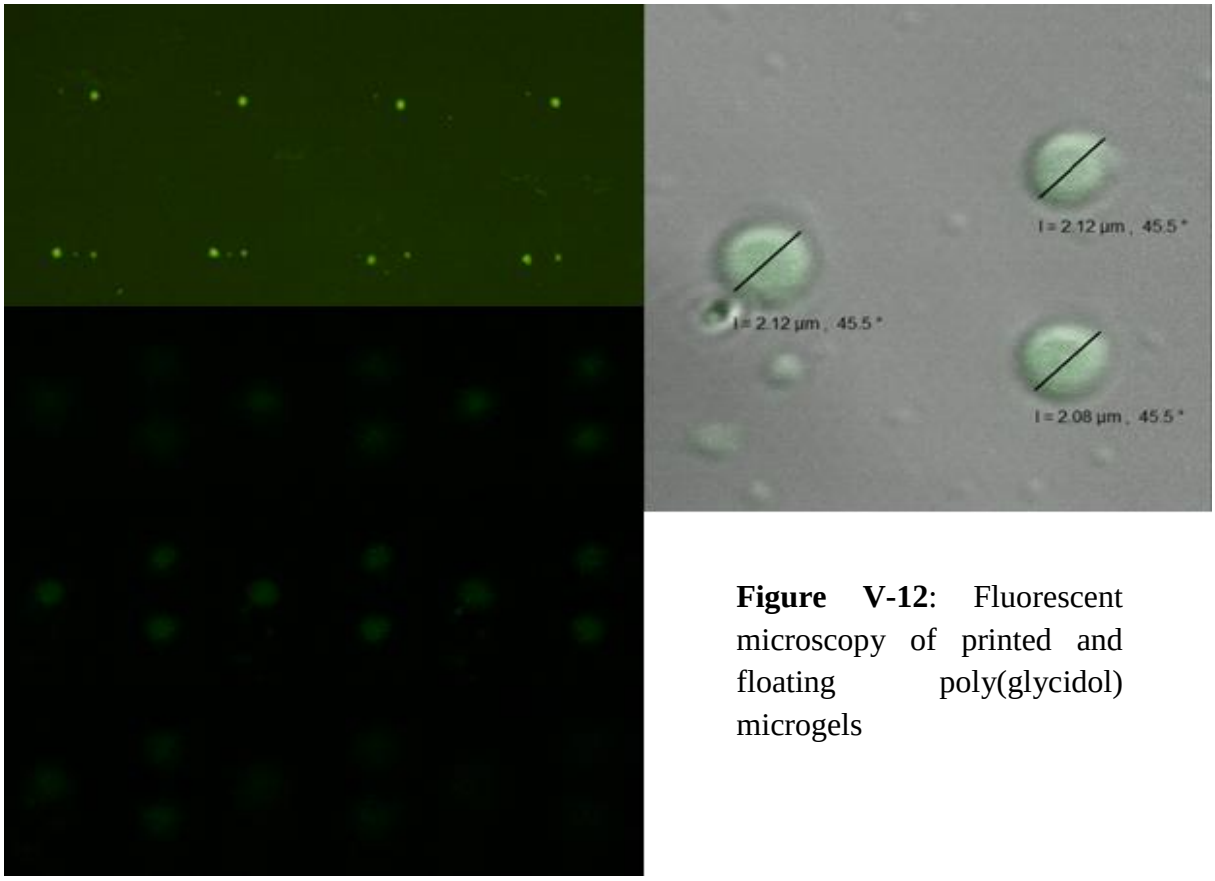

Figure V-12: Fluorescent microscopy of printed and floating poly(glycidol) microgels

possible due to mixing of the two hydrophilic systems, so Teflon sheets were utilized as a printing surface. The printed particles were visualized using fluorescent microscopy, and after gelation, were washed from the Teflon surface and studied with confocal microscopy. The resulting gel structures were much smaller at an average size of around 2µm. However, the particles maintained the high homogeneity seen in the larger structures as well as the nicely spherical morphology. Furthermore, the drastic decrease in size led to particle structures approaching the 1µm size range that is capable of utilization as a vaccine platform, and since the particles are entirely poly(glycidol) they are very soft, another desirous quality in vaccines.

Control of Microgel Size: Influence of Mass/Volume Percent

The ability to tune the hydrophilicity of the hydrogel system is advantageous, but it is also desirable to be able to direct the size of the particles that are being formed so that the system can

be optimized for various forms of delivery. It was hypothesized that a decrease in the weight percent of the polymer solution, thus decreasing the amount of polymer in each printed drop, would lead to a decrease in the size of the printed polymer structures. To investigate this proposition poly(carbonate)/poly(glycidol) hydrogel precursors were printed as before with the mass percent of the ink being decreased by 20%. The resulting particles looked similar upon printing, but once washed from the surface an interesting change was observed. The particles formed with the lower weight percent solution were decreased in size by almost the same amount as the decrease in weight percent, with particles an average size of around 7.75μm. The ability to tune the size of the printed hydrogels with such an easily manipulated parameter is an exciting discovery that opens the door to the formation of even more particle sizes than have been created thus far.

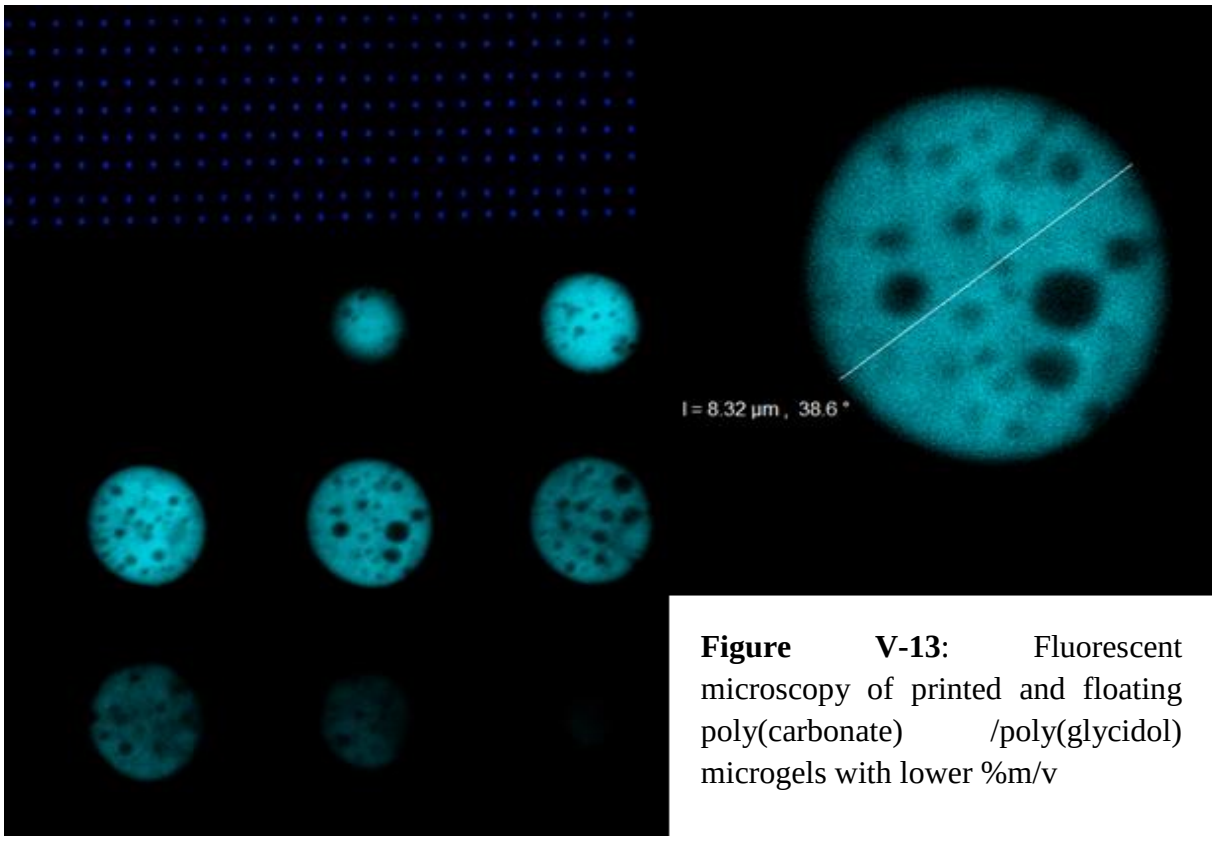

Figure V-13: Fluorescent microscopy of printed and floating poly(carbonate) /poly(glycidol) microgels with lower %m/v

Utilization of AFM to Determine Mechanical Properties of Microparticles

In order to determine if any change in the mechanical properties of the hydrogel structures occurs due to the small size of the printed microgel systems, an advanced atomic force microscopy technique was employed. In this type of measurement, an AFM cantilever with known spring constant is used to investigate the different gel systems on a silica surface. Since the spring constant of the cantilever is known, measurements can be directly correlated to the mechanical properties of the printed gel structures.

Conclusion

The discovery of a method for the formation of highly controlled and monodisperse micron-sized particles, with a method that is exceptionally scalable, has been described. Though piezoelectric printing has been employed previously for polymer deposition, and there are methods available for the formation of microparticles, the marriage of particle synthesis with piezoelectric printing is truly novel. These systems are tunable, not only through the incorporation of variable polymer structures, but also with the utilization of varied solution concentration. This work represents the first steps along a path towards the formation of reproducible and scalable microparticle formation capable of incorporating a seemingly endless list of therapeutic cargo.

Experimental

Materials

All reaction solvents used were HPLC quality and purchased form Sigma Aldrich. All NMR solvents were purchased from Cambridge Isotope Laboratories, Inc. and used without further purification. 2,2-bis(hydroxymethyl) propionic acid (Bis-HPA), Amberlyst® 15 Hydrogen Form (A-15), allyl glycidyl ether (AGE), anhydrous Iso-Amyl alcohol (IAOH), 3,6-Dioxa-1,8-octanedithiol, nile red, coumarin 30, and 2,2-dimethoxy-2-phenylacetophenone (DMPA) were

purchased from Sigma Aldrich and used without further purification. Glycdiol (GLY) was purchased from Sigma Aldrich and vacuum distilled prior to use. Thiol PEG Thiol (HS-PEG-SH) was purchased from Nanocs and used without further purification. 2,2'-Azobis[2-(2-imidazolin-2-yl)propane]dihydrochloride (VA-044) was purchased from Wako chemicals and used without further purification. Tin(II) trifluoromethane sulfonate ($Sn(OTf)_2$) was purchased from Strem Chemicals Inc. and used without further purification. Teflon sheets were obtained from ePlastics. Dialysis membranes (Spectra/Por® 7, molecular weight cut-off (MWCO): 1,000 Da) were obtained from Spectrum Laboratories, Inc. 5-methyl-5-allyloxycarbonyl-1,3-dioxane-2-one (MAC), and 5-methyl-5-ethyloxycarbonyl-1,3-dioxane-2-one (MEC) were synthesized according to the literature and recrystallized prior to use. MEC/MAC copolymers were synthesized according to work previously published and dialyzed before use.

Characterization

^{1}H NMR and ^{13}C NMR spectra were obtained from a Bruker AC400 Fourier Transform Spectrometer, with $CDCl_3$/TMS as the solvent. Gel permeation chromatography (GPC) was carried out with a Waters chromatograph system equipped with a Waters 2414 refractive index detector, a Waters 2481 dual λ absorbance detector, a Waters 1525 binary HPLC pump, and four 5 mm Waters columns (300 mm x 7.7 mm), connected in series with increasing pore size (100, 1000, 100,000 and 1,000,000 Å respectively). All runs were performed with dimethylformamide (DMF) or tetrahydrofuran (THF) as the eluent at a flow rate of 1 mL/min.

General Procedure for the synthesis of GLY, AGE copolymers.

A 25 mL round bottom flask, equipped with stir bar, was capped with a rubber septum and flame dried under nitrogen. $Sn(OTf)_2$ (5.2mg; 12.48μmol; 0.4 eq) was then added to round bottom flask and the reaction vessel was then immediately purged with nitrogen again prior to the addition of

IAOH (43.7mg 495.6µmol; 17.4 eq) via microsyringe. The initiator-catalyst mixture was then allowed to stir at room temperature for 30 minutes before lowering the reaction vessel into an ice water bath. After the reaction vessel had been cooled for 5 minutes the AGE monomer (834mg; 7.31mmol; 250 eq) was added dropwise to the stirring reaction. The GLY monomer (2.17g; 29.24mmol; 1000eq) was added dropwise in 4 separate aliquots, allowing 5 minute breaks between each aliquot, to ensure the exothermic reaction did not overheat and decompose. After stirring was completely impeded (~14 hours) the crude reaction mixture was solubilized in a minimal amount of methanol and precipitated into vigorously stirring ethyl acetate. The precipitation solvent was allowed to settle before carefully decanting the ethyl acetate. The resulting GLY/AGE copolymer was solubilized in methanol, removed to a weighed 6-dram vial, and dried on the rotary evaporator, then under high vacuum, to afford the translucent, viscous product. 1H-NMR (600MHz, MeOD) δ:6.0-5.90 (m, $–OCH_2C\mathit{H}CH_2$), 5.37–5.17 (m, $–OCH_2CHC\mathit{H}_2$) .3.97-3.42 (6H). 13C-NMR (150MHz, MeOD) δ: 136.31, 117.39, 81.37, 79.81, 75.12, 73.88, 72.01-72.94, 70.42-71.17, 64.41, 62.53, 62.06, 27.99, 27.60.

Coating of Glass Substrates with Poly(glycidol)

The ability to remove the printed hydrogels from the chosen substrate proved difficult. Due to the small size of the printed particles, favorable surface interactions between the gels and surface hindered the facile removal of the products. For this reason it was decided that the glass substrates would be coated with poly(glycidol) which afforded a hydrophilic surface that could be easily removed by simple water rinsing. This method also yields a surface with favorable hydrophilic/hydrophobic interactions between the poly(glycidol) and poly(methyl-ethyl-co-methyl-allyl-carbonate) printing solution, which allows for an increase in the printing density on each surface as the printed poly(carbonate) polymer remains static on the hydrophilic surface.

General Procedure for Formation of Hydrogel Printing Solution in DMSO (Samples 1 and 2)

3,6-Dioxa-1,8-octanedithiol (0.5eq. per alkene) was added via micro syringe to a solution of the allyl functionalized polymer (100mg total mass) and 2,2-dimethoxy-2-phenylacetophenone (DMPA, 0.2eq. per alkene) in DMSO with the desired fluorescent dye. After thorough mixing with the tip of a syringe, and allowing to rest to ensure no air bubbles were present, the prepared printing solution was loaded into a Dimatix printing cartridge using a blunt tip needle. The printing cartridge was then loaded into the Dimatix materials printer. Printing substrates were then placed on the printing platen before printing was begun. After printing of the particles, the printed microdots were irradiated with long wave UV light (365nm) for 5 minutes to induce gelation. After gelation had occurred the substrates were imaged using fluorescent microscopy to visualize the printed region before being rinsed with water to dissolve the poly(glycidol) and liberate the microdots from the surface. The microdots were then imaged using confocal microscopy to investigate their sizes.

General Procedure for Formation of Hydrogel Printing Solution in Water (Sample 3)

HS-PEG-SH (0.5eq. per alkene) was added to a solution of the allyl functionalized polymer (100mg total mass) in water and mixed well with the tip of a needle until completely solubilized in a 1-dram vial. 2,2'-Azobis[2-(2-imidazolin-2-yl)propane]dihydrochloride (VA-044, 0.2eq. per alkene) was then added to the printing solution along with the thiolated fluorescent dye. The solution was again mixed with the tip of a needle and allowed to rest to ensure no air bubbles were present before the prepared printing solution was loaded into a Dimatix printing cartridge using a blunt tip needle. The printing cartridge was then loaded into the Dimatix materials printer. Teflon strips were then placed on the printing platen before printing was begun. After printing of the

particles the printed microdots were irradiated with long wave UV light (365nm) for 5 minutes to induce gelation. After gelation had occurred, the substrates were imaged using fluorescent microscopy to visualize the printed region before being rinsed with water to liberate the microdots from the surface. The microdots were then imaged using confocal microscopy to investigate their sizes.

General Procedure for Formation of Bulk Hydrogel Samples in DMSO (Samples 1 and 2)

3,6-Dioxa-1,8-octanedithiol (0.5eq. per alkene) was added via micro syringe to a solution of the allyl functionalized polymer (100mg total mass) and 2,2-dimethoxy-2-phenylacetophenone (DMPA, 0.2eq. per alkene) in DMSO with the desired fluorescent dye in a 1-dram vial (See Figure V-14). After thorough mixing with the tip of a syringe, and allowing the solution to rest to ensure no air bubbles were present, the solution was irradiated with long wave UV light (365nm) for 5 minutes to induce gelation. The gels were then rinsed sequentially with 3mL aliquots of water, methanol, methylene chloride, methanol and finally water again to remove any unreacted starting materials. The gels were then submerged in water and frozen before being lyophilized to afford the dry hydrogel product.

General Procedure for Formation of Bulk Hydrogel Samples in Water (Sample 3)

HS-PEG-SH (0.5eq. per alkene) was added to a solution of the allyl functionalized polymer (100mg total mass) in water and mixed well with the tip of a needle until completely solubilized in a 1-dram vial. 2,2'-Azobis[2-(2-imidazolin-2-yl)propane]dihydrochloride (VA-044, 0.2eq. per alkene) was then added to the printing solution along with the thiolated fluorescent dye (See Figure V-14). The solution was again mixed with the tip of a needle and allowed to rest to ensure no air bubbles were present before being irradiated with long wave UV light (365nm) for 5 minutes to induce gelation. The gels were then rinsed sequentially with 3mL aliquots of water, methanol,

ethylene chloride, methanol and finally water again to remove any unreacted starting materials. The gels were then submerged in water and frozen before being lyophilized to afford the dry hydrogel product.

Sample	Poly(carbonate)	Poly(glycidol)	Solvent	Fluorescent Dye
1	100mg	0mg	200µL	Nile Red
2	70mg	30mg	400µL	Coumarin 20
2b	70mg	30mg	500µL	Coumarin 20
3	0mg	100mg	1000µL	Thiolated Dye

Figure V-14: Dilution of printing solutions for microgel formation.

Fluoroscopy Measurements.

Fluoroscopy images were obtained using two separate microscopes. For the printed samples still on the substrates, a Nikon AZ 100 M microscope with halogen lamp was used to image the freshly printed gels before and after gelation. Once the gels had been removed from the substrates, and suspended in water, the individual gels were imaged using a Zeiss LSM 510 Inverted Confocal Microscope.

References

1. Anselmo, A., and Mitragotri, S. (2014) An overview of clinical and commercial impact of drug delivery systems, *Journal of Controlled Release 190*, 15-28.

2. Stevens, D., Rahalkar, A., Spears, B., Gilmore, K., Douglas, E., Muthukumar, M., and Harth, E. (2015) Semibranched polyglycidols as "fillers" in polycarbonate hydrogels to tune hydrophobic drug release, *Polymer Chemistry 6*, 1096-1102.

3. Ndong, J., Stevens, D., Vignaux, G., Uppuganti, S., Perrien, D., Yang, X., Nyman, J., Harth, E., and Elefteriou, F. (2015) Combined MEK Inhibition and BMP2 Treatment Promotes Osteoblast Differentiation and Bone Healing in Nf1(Osx)(-/-) Mice (vol 30, pg 55, 2015), *Journal of Bone and Mineral Research 30*, 1118-1118.

4. Kim, I., Byeon, H., Kim, T., Lee, E., Oh, K., Shin, B., Lee, K., and Youn, Y. (2012) Doxorubicin-loaded highly porous large PLGA microparticles as a sustained-release inhalation system for the treatment of metastatic lung cancer, *Biomaterials 33*, 5574-5583.

5. Dhanda, D., Tyagi, P., Mirvish, S., and Kompella, U. (2013) Supercritical fluid technology based large porous celecoxib-PLGA microparticles do not induce pulmonary fibrosis and sustain drug delivery and efficacy for several weeks following a single dose, *Journal of Controlled Release 168*, 239-250.

6. Elkharraz, K., Faisant, N., Guse, C., Siepmann, F., Arica-Yegin, B., Oger, J., Gust, R., Goepferich, A., Benoit, J., and Siepmann, J. (2006) Paclitaxel-loaded microparticles and implants for the treatment of brain cancer: Preparation and physicochemical characterization, *International Journal of Pharmaceutics 314*, 127-136.

7. Ungaro, F., Bianca, R., Giovino, C., Miro, A., Sorrentino, R., Quaglia, F., and La Rotonda, M. (2009) Insulin-loaded PLGA/cyclodextrin large porous particles with improved aerosolization properties: In vivo deposition and hypoglycaemic activity after delivery to rat lungs, *Journal of Controlled Release 135*, 25-34.

8. Hu, C., Feng, H., and Zhu, C. (2012) Preparation and characterization of rifampicin-PLGA microspheres/sodium alginate in situ gel combination delivery system, *Colloids and Surfaces B-Biointerfaces 95*, 162-169.

9. Shibuya, K., Nagao, D., Ishii, H., and Konna, M. (2014) Advanced soap-free emulsion polymerization for highly pure, micron-sized, monodisperse polymer particles, *Polymer 55*, 535-539.

10. Telford, A., Pham, B., Neto, C., and Hawkett, B. (2013) Micron-sized polystyrene particles by surfactant-free emulsion polymerization in air: Synthesis and mechanism, *Journal of Polymer Science Part a-Polymer Chemistry 51*, 3997-4002.

11. Buyukserin, F., Camli, S., Yavuz, M., and Budak, G. (2011) Novel antifouling oligo(ethylene glycol) methacrylate particles via surfactant-free emulsion polymerization, *Journal of Colloid and Interface Science 355*, 76-80.

12. Trotta, M., Cavalli, R., Carlotti, M., Battaglia, L., and Debernardi, F. (2005) Solid lipid micro-particles carrying insulin formed by solvent-in-water emulsion-diffusion technique, *International Journal of Pharmaceutics 288*, 281-288.

13. Riess, G., and Labbe, C. (2004) Block copolymers in emulsion and dispersion polymerization, *Macromolecular Rapid Communications 25*, 401-435.

14. Visaveliya, N., and Kohler, J. (2015) Simultaneous size and color tuning of polymer microparticles in a single-step microfluidic synthesis: particles for fluorescence labeling, *Journal of Materials Chemistry C 3*, 844-853.

15. Shiba, K., and Ogawa, M. (2009) Microfluidic syntheses of well-defined sub-micron nanoporous titania spherical particles, *Chemical Communications*, 6851-6853.

16. Bippus, L., Jaber, M., and Lebeau, B. (2009) Laponite and hybrid surfactant/laponite particles processed as spheres by spray-drying, *New Journal of Chemistry 33*, 1116-1126.

17. Castrejon-Pita, J., Baxter, W., Morgan, J., Temple, S., Martin, G., and Hutchings, I. (2013) FUTURE, OPPORTUNITIES AND CHALLENGES OF INKJET TECHNOLOGIES, *Atomization and Sprays 23*, 541-565.

18. Childers, E., Wang, M., Becker, M., Fisher, J., and Dean, D. (2015) 3D printing of resorbable poly(propylene fumarate) tissue engineering scaffolds, *Mrs Bulletin 40*, 119-126.

19. Cox, S., Thornby, J., Gibbons, G., Williams, M., and Mallick, K. (2015) 3D printing of porous hydroxyapatite scaffolds intended for use in bone tissue engineering applications, *Materials Science & Engineering C-Materials For Biological Applications 47*, 237-247.

20. O'Brien, C., Holmes, B., Faucett, S., and Zhang, L. (2015) Three-Dimensional Printing of Nanomaterial Scaffolds for Complex Tissue Regeneration, *Tissue Engineering Part B-Reviews 21*, 103-114.

21. Trachtenberg, J., Mountziaris, P., Miller, J., Wettergreen, M., Kasper, F., and Mikos, A. (2014) Open-source three-dimensional printing of biodegradable polymer scaffolds for tissue engineering, *Journal of Biomedical Materials Research Part a 102*, 4326-4335.

22. Lee, B., Yun, Y., Choi, J., Choi, Y., Kim, J., and Cho, Y. (2012) Fabrication of drug-loaded polymer microparticles with arbitrary geometries using a piezoelectric inkjet printing system, *International Journal of Pharmaceutics 427*, 305-310.

23. Scoutaris, N., Alexander, M., Gellert, P., and Roberts, C. (2011) Inkjet printing as a novel medicine formulation technique, *Journal of Controlled Release 156*, 179-185.

24. Alomari, M., Mohamed, F., Basit, A., and Gaisford, S. (2014) Personalised dosing: Printing a dose of one's own medicine, *International Journal of Pharmaceutics*.